Concawe
Environmental Science for European Fuel Manufacturing

Report

Report no. 8/26

Impact of Sea Shipping Emissions on Future Urban Air Quality in Major European Ports: A 2030 Scenario Analysis

ISBN 978-2-87567-216-2

Impact of Sea Shipping Emissions on Future Urban Air Quality in Major European Ports: A 2030 Scenario Analysis

Prepared by: Jessie Zhang (TNO), Elisa Majamäki (FMI), Marya el Malki (TNO), Andreas Pseftogkas (TNO), Marilena Karyampa (TNO), Jukka-Pekka Jalkanen (FMI), Jeroen Kuenen (TNO), Blaise Kelly (TNO), Janot Tokaya (TNO), and Peter Coenen (TNO)

Under the supervision of: T. Megaritis (Concawe Science Associate)

At the request of:

Concawe Air Quality Management Group (AQMG)

Thanks for their contribution to:

Members of AQMG

Concawe/FuelsEurope Secretariat Members

Brussels
July 2026

KEYWORDS

air quality; shipping; atmospheric modelling; emission inventories; emission scenarios; emissions

INTERNET

This report is available as an Adobe pdf file on the Concawe website (www.concawe.eu).

CONTENTS

SUMMARY

As land-based air pollutant emissions are projected to decline due to sectoral air quality and climate policies, sea shipping emissions under a "business-as-usual" scenario become increasingly important in explaining elevated concentrations of air pollutants. The intended decarbonisation of shipping though alternative fuels will further affect future air pollution from the sector. This study assesses how sea shipping, under a number of hypothetical sensitivity scenarios, would affect air pollutant emissions and air quality in Europe compared to other sectors, with a focus on four selected European seaport areas.

Sea shipping emissions were calculated using the Ship Traffic Emission Assessment Model (STEAM), combined with land-based emissions from the CAMS-REG inventory, and used as inputs to the LOTOS-EUROS chemistry transport model. The analysis domain covers mainland Europe and its surrounding sea corridors, with particular focus on Rotterdam (The Netherlands), Antwerp (Belgium), Marseille (France) and Piraeus in Athens (Greece).

A base case scenario for 2023 was defined (as the most recent year with complete and reliable data at the time of the study), with three sensitivity scenarios for 2030 developed for comparison. These are hypothetical scenarios and do not represent agreed upon or decided legislation. The "2030 BAU" scenario reflects the future situation under current and agreed policies until 2030, including emission control areas (ECA) in the Baltic Sea, North Sea, Mediterranean and Norwegian Sea. The "2030 LNG" scenario increases liquefied natural gas (LNG) energy share to 20% (compared to 11-12% in BAU 2030). The "2030 all-EU ECA" scenario assumes a hypothetical EU-wide sulphur and nitrogen emission control area (SECA and NECA) extending 200 nautical miles from the coastline, excluding the Canary Islands and the Azores. The extent and form of future ECAs remains uncertain and this scenario should be interpreted accordingly.

The air pollutants included in the assessment of the shipping and non-shipping emissions are oxides of nitrogen (NO_x), sulphur oxides (SO_x), particulate matter (PM_{10} and $PM_{2.5}$), ammonia (NH_3), carbon monoxide (CO), volatile organic compounds (VOC), and non-methane VOC (NMVOC). The air quality impact assessment focusses on the source apportionment results of PM (PM_{10} and $PM_{2.5}$), nitrogen dioxide (NO_2) and sulphur dioxide (SO_2) that are the key pollutants in assessing current European air quality standards. This report presents primarily the assessment of NO_2 (and PM), while other pollutants are presented in the accompanying Appendix.

The sensitivity scenarios assessed in this study reflect hypothetical stricter regulations, improved energy efficiency, and the adoption of alternative fuels. Shipping NO_x emissions are projected to decrease by 13-19% by 2030 relative to 2023, representing a shipping share of 24-26% of total NO_x emissions in 2030. NH_3 emissions are projected to increase significantly due to the wider use of SCR and alternative fuels (such as LNG and methanol), however they remain a small contributor compared to land-based sources (<1%).

The hypothetical expansion of ECAs and uptake of alternative fuels will also alter the spatial emission distribution compared to 2023, with a SECA leading to reductions of 44-56% in SO_x and 24-30% in $PM_{2.5}$ emissions in the Mediterranean, relative to 2023. The shipping share of total SO_x emissions in 2030 is estimated at 2-3%, while that of $PM_{2.5}$ is 1%.

Land-based emissions are projected to decrease substantially by 2030 by 40% for NO_x (2,048 kton), 25% for SO_x (321 kton), and 35% for $PM_{2.5}$ (462 kton), shifting the relative balance between sectors. For NO_x, the sharper decline on land means that shipping's share grows by 2-3% by 2030, while for SO_x and $PM_{2.5}$ the contribution of sea shipping falls by 2-3% and 1% respectively. At the port-city scale, shipping dominates NO_x emissions (approximately 70%) in the 2023 base case in Marseille and Athens (770 kton and 2,890 kton respectively), while it has a smaller but

still significant role in Rotterdam and Antwerp of 25-30% (5,907 kton and 3,780 kton respectively).

The air quality modelling indicates that pollutant concentrations will reduce by 2030 across all scenarios relative to 2023: 22% (1.8 µg/m³) for NO_2, 14% (1.3 µg/m³) for $PM_{2.5}$ and 14% (0.4 µg/m³) for SO_2. Despite these reductions, shipping's relative NO_2 share across the European domain increases by approximately 5% compared to 2023, as land-based sectoral emissions reduce more. Differences between the 2030 scenarios are modest overall, but the LNG scenario generally lowers concentrations, while the all-EU ECA scenario results in additional NO_2 and $PM_{2.5}$ improvements along the Atlantic and the English Channel-Gibraltar corridors. NO_2 shipping concentrations are expected to decrease in the 2030 BAU scenario by 25% (3 µg/m³) over the North Sea and Baltic Sea, and by 18% (2 µg/m³) along the Mediterranean coasts compared to 2023. Along the EU waterways, the 2030 LNG scenario results in a larger reduction for NO_2 with 23% (0.51 µg/m³), compared to 17% under the all-EU ECA scenario, whereas the latter is more efficient in reducing SO_2 concentrations with reductions of up 60% (0.11 µg/m³). For $PM_{2.5}$, both scenarios result in a similar reduction of 32% (0.11 µg/m³).

In the four port-cities, reductions in NO_2 concentrations are predicted across all 2030 scenarios. Traffic dominates in the Mediterranean cities (road traffic contributes approximately 60% (21 µg/m³) in Athens and 55% (7 µg/m³) in Marseille), while shipping is the largest NO_2 source in the BENELUX cities, contributing about 50% of urban NO_2 across all scenarios. Shipping's relative share increases in all port-cities by 2030 despite decreasing absolute concentrations; e.g., shipping's NO_2 share rises by 8% in Athens and by 6% in Marseille. Shipping contributes 13% (Rotterdam), 10% (Antwerp), and 4% (Athens/Marseille) to $PM_{2.5}$ in 2023, with its share decreasing slightly (by up to 1.5%) across all seaport cities in 2030 as industrial and stationary combustion sources become more prominent.

NO_2 exceedances of the EU daily limit (50 µg/m³) in 2030 are only predicted in Athens (port and city) and in Rotterdam (port). When comparing against the non-binding WHO guideline (25 µg/m³), used here for indicative purposes, exceedances are predicted at all four port-cities, with shipping as the main contributor in Rotterdam and Antwerp, and road traffic as the main contributor in Athens and Marseille. For $PM_{2.5}$ exceedances, road traffic and industry are the main contributors compared to shipping in all four port-cities.

Overall, while absolute sea shipping contributions decrease across all scenarios, shipping's relative share grows in all four port-cities, as other sectors reduce faster. These findings highlight shipping as an important sector for future emission reduction strategies, and serve as a foundation for further refinement through improved emission inventories, higher spatial resolution, the inclusion of emerging pollutants, the integration of monitoring data and extended scenario horizons to 2050.

1. INTRODUCTION

As land-based air pollutant emissions are declining due to dedicated sectoral Air Quality (AQ) and climate policies, the emissions from shipping under a "business-as-usual" (BAU) scenario become even more important in explaining elevated concentrations of air pollutants. As a result of the intended decarbonisation of shipping, alternative fuels will partly replace the current fossil fuels which will therefore affect future emissions of air pollutants from sea shipping.

1.1. AIM

The aim of this study is to examine how sea shipping, under a number of selected sensitivity scenarios would affect air pollutant emissions and their resulting impacts on future air quality in Europe and major seaports by 2030, compared to other sectors.

1.2. BACKGROUND

It is well known that elevated concentrations of air pollutants can lead to adverse effects on both human health and ecosystems. Epidemiological studies have shown that the exposure to pollutants, such as fine particulate matter ($PM_{2.5}$) and nitrogen dioxide (NO_2), is linked to cardiovascular and respiratory diseases, leading to increased hospital admissions and premature deaths (Beelen et al., 2014). Additionally, emissions of particulate matter (PM) and gases alter the atmospheric radiation balance, contributing to climate forcing (Takemura et al., 2005). Protecting human health has therefore been one of the primary drivers to reduce air pollution originating from various anthropogenic and natural sources. In particular for sea shipping, regional and global regulations, including Emission Control Areas (ECA) for sulphur oxides (SOx) (SECA), the EU Sulphur Directive, China's Domestic ECA and ultimately the global 2020 sulphur cap, have been justified by their benefits to air quality and human health.

Nitrogen oxides (NOx) are primarily formed during the combustion process due to the high temperatures and the naturally abundant nitrogen in the atmosphere. PM or aerosols are particles suspended in air which originated from both natural sources, like sea salt, and anthropogenic sources, either directly emitted or formed through secondary atmospheric reactions. While NOx emissions are less detrimental to human health than SOx and PM, they contribute significantly to environmental degradation through nitrogen deposition on soils and water bodies, which leads to eutrophication, biodiversity loss, algae blooms and overall ecosystem damage (Stevens et al., 2018). Similarly, SOx emissions intensify environmental stress by contributing to the acidification of terrestrial and marine ecosystems.

Over the past decades, legislation has been introduced to reduce emissions of these harmful pollutants. In the Netherlands, sea shipping-related air pollution has been shown to represent a growing share compared to other source sectors (Denier van der Gon et al., 2022; Jonson et al., 2015). Since 2020, the International Maritime Organization (IMO) has capped the sulphur content of maritime fuels at 0.5% under the International Convention for the Prevention of Pollution from Ships (MARPOL) Annex VI. Additionally, several SECAs and emission control areas for nitrogen compounds (NECA) have been established to further mitigate sea shipping emissions. In 2023, the IMO adopted its Strategy on the Reduction of GHG Emissions from Ships (MEPC.377(80)), setting a target of reaching net-zero emissions from sea shipping by 2050. These regulatory measures are accelerating the sector's transition to alternative fuels such as methane, methanol, ammonia and hydrogen. The use of

electricity is also increasing, especially at ports, with all trans-European transport network (TEN-T) ports expected to supply shore power for container and passenger ships by 2030. These changes will also alter the emission of air pollutants from sea shipping and, consequently, the sector's impact on air quality.

Emissions are not the only factor that influence the atmospheric pollutant concentrations. Chemical reactions and meteorological conditions like precipitation, solar radiation, wind speed, temperature and relative humidity, also play an important role in the levels of surface air pollution resulting from emissions. Hence, air quality modelling is typically used to predict the impact of the combined effects of all these impacts.

1.3. APPROACH

In this study, insights are gained on sea shipping emissions and the resulting impact on air pollutant concentrations across Europe and at four key seaports (i.e. Antwerp, Marseille, Piraeus in Athens, and Rotterdam) under a sensitivity analysis that includes different shipping fuel scenarios and hypothetical regulatory developments. Ship emission data is produced with the Finnish Meteorological Institute's (FMI) Ship Traffic Emission Assessment Model (STEAM). STEAM uses ship activity data and technical descriptions of the global fleet to model the instantaneous power load, fuel consumption and emissions of each vessel, considering the unique features of a ship. It also considers the ambient conditions ships operate in (Majamäki et al., 2025). Further, the contribution of shipping emissions to air quality is assessed using the chemical transport model (CTM) LOTOS-EUROS. This model computes air quality by taking into account the emissions of pollutants, transport and chemistry in the atmosphere using meteorological data, land use and orographic information.

To support this modelling, harmonised emission datasets are applied across the study domain, ensuring consistency between international shipping and other sectors. For shipping, gridded emissions at 6×6 km2 resolution are developed for 2030 with the STEAM model, based on fleet and fuel projections and assumptions from the DNV Maritime Forecast to 2030. Land-based emissions are derived from country-reported emissions and extrapolated to 2030 using sectoral trends from the 3rd Clean Air Outlook (Klimont et al., 2022).

Alongside total air pollutant concentrations, understanding the sectoral contributions to these concentrations is equally relevant. In general, source apportionment (SA) is applied both in the modelling and monitoring of air pollution. Various techniques exist to specify the sources that may cause the air pollution of interest. These techniques make it possible to estimate how much of an atmospheric concentration originates from a specific source (e.g. traffic, industry, etc.).

The "labelling" source apportionment approach has been used in this study. In this approach the chemical tracers receive a label based on the emission source. These labelled chemical pollutants are traced throughout the model to determine and quantify the contribution of various sources to the surface concentration at any region or location.

1.4. OUTLINE

The methodology used in the study is described in Chapter 2. This chapter provides details on the calculation of the shipping and land-based emissions and the simulations of the atmospheric concentrations.

Chapter 3 presents the results of the study and discussion. The model provides labelled atmospheric concentrations over the simulation domains. Using the simulation results, the contributions of various sectors (including sea shipping) to the air quality in port-cities are computed.

Chapter 4 provides the conclusions from this study.

This report should be read in conjunction with the Appendix, which includes additional details on the emissions and modelling results of this study.

2. METHODOLOGY

This chapter provides a detailed description of the emissions and modelling approaches. Firstly, the assessment scenarios, study area and assessed pollutants are defined. Secondly, the model and calculations for deriving the shipping emissions are discussed, and then the method for the land-based emissions and the merging of the two datasets. Lastly, the atmospheric chemical transport model, its capabilities, inputs and simulation setup are described, followed by the method for evaluating the model results.

2.1. SCOPE AND CONTEXT OF THE STUDY

2.1.1. Assessment scenarios

The following assessment scenarios have been used in this study:

- Base case 2023;
- Business-as-usual (BAU) 2030;
- Increased uptake of liquefied natural gas (LNG) 2030; and
- All-EU ECA for sulphur and nitrogen emissions 2030.

The **"2023 base case"** scenario provides the basis of the 'current' situation. The year 2023 was selected as it was the most recent year with complete and reliable data available at the time of the study.

The **"2030 BAU"** scenario provides the future situation under current and foreseen legislation and regulations. It is based on the low growth transport scenario as defined in the 2020 DNV Maritime Forecast report (DNV-GL, 2020) and uses the EMERGE D1.4 report definitions for the development of ship energy efficiency. It includes agreed policies until 2030, including SOx and NOx ECAs. The ECAs included in this scenario are the existing ones for the Baltic Sea and the North Sea, and future planned ones for the Mediterranean (i.e. SECA in 2025) and the Norwegian Sea (i.e. SECA in March 2027 and NECA for ships contracted to be constructed on or after 1 March 2026). Shore power is also included for container and passenger vessels in all ports according to information from the European Alternative Fuels Observatory (EAFO) (EAFO, 2021). There are also 52 ports in the TEN-T list which do not yet offer shore power but are required to do so by 2030. These have also been included as having shore power available from 1 January 2030. The fuel split within this scenario is linked to the DNV estimates of newbuild LNG vessels. It has been estimated that by 2030 the LNG share will be 11-12% of total energy, i.e. double the 2023 value (further detailed in section 3.2.3). Methanol is assumed to account for 6.3% of energy used by shipping.

The **"2030 LNG"** scenario increases the LNG energy share to 20% (compared to 11-12% in the BAU 2030 scenario). Assumptions concerning fleet development, regulations and shore power remain the same as in the 2030 BAU scenario. All RoRo-passenger vessels (roll-on/roll-off), RoRo cargo ships, gas tankers and passenger ships use LNG as fuel in addition to the existing LNG-fuelled vessels. Methanol usage has been assumed the same level as in the 2030 BAU scenario.

The **"2030 all-EU ECA"** scenario assumes an EU-wide SECA and NECA which extends 200 nautical miles from the coastline, excluding the Canary Islands and the Azores (see Figure 1). Assumptions concerning fleet development, fuel mix and shore

power are the same as in the 2030 BAU scenario. In this scenario, the current scrubber fleet has been included and it has been assumed that no new scrubbers will be installed. It has also been assumed that compliance with NOx reduction requirements will be with selective catalytic reduction (SCR) or LNG.

The assessment scenarios should be seen as sensitivity cases that are included to support interpretation of the modelling results and to explore how alternative assumptions on fuel uptake or regulatory developments may influence future air pollutant concentrations from shipping. The “2030 BAU” and “2030 LNG” scenarios build on DNV maritime outlooks, which represent plausible pathways of the sector’s development rather than a definitive projection of the future. In addition, the “all-EU ECA” scenario is included purely as a hypothetical sensitivity case to illustrate potential impacts and does not represent any policy expectation or agreed legislative initiative.

Figure 1 *Existing and decided ECAs (dark colour) and hypothetical new ECA (white colour) in Europe assumed in the 2030 all-EU ECA scenario*

Background maps data: Google, Landsat Copernicus/IBCAO/U.S. Geological Survey

2.1.2. Study area

The study area encompasses mainland Europe and its surrounding sea corridors, as defined by the all-EU ECA 2030 scenario. The spatial extent of the modelling domain is presented in section 2.4.3 of this report. Particular focus has also been given to four key seaports which serve as focal points for the assessment: Rotterdam (The Netherlands), Antwerp (Belgium), Marseille (France) and Piraeus in Athens (Greece).

The port of **Rotterdam** is the 10th largest port in the world and the largest port in Europe based on throughput volume for 2023 (13.447 million TEU) (World Shipping Council, 2023). It serves as a major hub for containers, liquid and dry bulk. The port stretches westward from the city towards the North Sea, forming an extensive industrial corridor. The main residential areas of Rotterdam lie to the east and southeast of the port.

The port of **Antwerp** is the second largest in Europe, with a throughput volume of 12.515 million TEU in 2023. It handles a wide range of cargo, including containers and liquid bulk, and is a key hub for industrial logistics and maritime trade. It is located at the river Scheldt and serves as a connection between Hamburg and Le Havre in maritime traffic. The main city of Antwerp lies just east of the port, with most residential zones concentrated in the city centre and southern districts. The northern and western areas near the port are more industrial.

The port of **Marseille** (Port of Marseille-Fos), located on the Mediterranean coast, had a throughput volume of 1.331 million TEU in 2023. It is the largest seaport of France and a major logistic hub in the Mediterranean, located at the crossroads of major global maritime trade routes and serving as a critical gateway for trade between Europe, North Africa, Middle East and Asia. It supports a mix of container, bulk, RoRo and cruise traffic. The port is divided into two main areas: the historic Vieux-Port near the city centre and the industrial For-sur-Mer complex to the west. Most residential areas of Marseille are to the north and east of the old port.

The port of Piraeus, located about 10 km southwest of **Athens**, is one of the busiest ports in the Mediterranean with a throughput volume of 5.1 million TEU in 2023. It serves as a hub for containers, passenger ferries and cruise vessels. Its strategic location at the crossroads of Europe, Africa and Asia constitutes a vital maritime gateway for trade between these regions, serving as a connecting point between the Gibraltar – Suez and Gibraltar – Black Sea maritime trade routes. The main city of Athens extends to the northeast of the port, but there are also residential areas around the port itself, to the north and northeast. For clarity and consistency, this port-city will be referred to as Athens in this report.

2.1.3. Assessed pollutants

The following pollutants have been included in the assessment of the shipping and non-shipping emissions: NOx, SOx, particulate matter (PM_{10} and $PM_{2.5}$), ammonia (NH_3), carbon monoxide (CO), volatile organic compounds (VOC), non-methane VOC (NMVOC).

The air quality assessment focusses on the source apportionment results of PM (PM_{10} and $PM_{2.5}$), NO_2 and SO_2 that are the key pollutants in assessing current European air quality standards.

This report focusses primarily on the assessment of NO_2 (and PM), while other pollutants are presented in the Appendix.

2.2. SEA SHIPPING EMISSIONS

2.2.1. STEAM emission model

Ship emission data has been produced with the STEAM model. The main inputs to this are speed and location information in global Automatic Identification System (AIS) data, and technical description of the global fleet in the S&P Global database.

Using this information, STEAM calculates the engine power load, fuel consumption, and emissions from ships visible in the AIS data. A more detailed description of the model can be found in Jalkanen et al. (2009, 2012, 2021) and Johansson et al. (2017). Emission factors of conventional marine fuels in STEAM are described in Grigoriadis et al. (2021) and emission factors of alternative fuels are described in the following chapters of this document.

2.2.1.1. Model version used in this study

This study used model version STEAM5.0. The main improvement compared to earlier versions is an introduction of the possibility of modelling each voyage of a ship individually so that a direct comparison between EU MRV reporting and modelled emissions is possible. This enables more detailed and comprehensive validation of the model.

Additionally, auxiliary machinery fuel consumption has been revised, and very low sulphur fuel oil (VLSFO) has been included in the model. In previous versions, all ships operating in ECAs have been assumed to use distillate fuels or a scrubber. Also, the AIS data processing and filtering has been updated to ensure better coverage of shipping activity, especially near the coastline. Scenario tools have also been revised and STEAM5.0 has the capability to model usage of ammonia and methanol.

Concerning the model output, emissions of gaseous pollutants are generally higher (5-20%) with STEAM5.0 than with the earlier version (STEAM4.3). This is mostly because of changes in the modelling of auxiliary machinery. Emissions of NH_3 are an exception as they are lower with STEAM5.0 due to a revised logic behind SCR usage. Emissions of PM are higher, especially emissions of elemental and organic carbon (EC and OC), and this is mainly due to the introduction of VLSFO in the modelling.

2.2.1.2. Spatial and temporal information

Shipping emissions were generated for the European domain [latitude: 30.0, 72.0; longitude: -30.0, 60.0]. The spatial resolution was 0.05° x 0.1° (lat, lon) and the temporal resolution 24 hours.

2.2.2. Fleet development

All future scenarios have the same assumptions concerning the development of cargo volumes transported by shipping. The base case emission inventory was created with the global AIS dataset from the year 2023. The future scenarios were developed using 2023 AIS data as the base case by applying growth rates. Growth rates were taken from the DNV-GL (2020) low growth scenario. Growth rates for different ship types are given in Table 1 and annual transport work by different vessel types in 2023 and 2030 are shown in Figure 2.

The energy efficiency of ships is assumed to increase by 5% from 2023 to 2030. Following DNV-GL (2020), it is assumed that container ships increase in size with 30%, gas tankers with 40%, and bulk ships with 10% from 2020 to 2050, while other ship types remain with the same average size. The increase of ship size from 2020 to 2050 is assumed to be linear.

Table 1 *Ship type specific annual growth rates from 2023 to 2030 following suggestions by DNV-GL (2020)*

Ship type	Annual change in trade
Tankers	- 0.6%
Bulk carriers	+ 1.3%
Container ships	+ 2.5%
Gas tankers	+ 7.5%
Other cargo ships	+ 1.3%
Non-cargo ships	+ 2.6%

Figure 2 *Annual transport work (in tonne km) by shipping in base case 2023 and future 2030 scenarios*

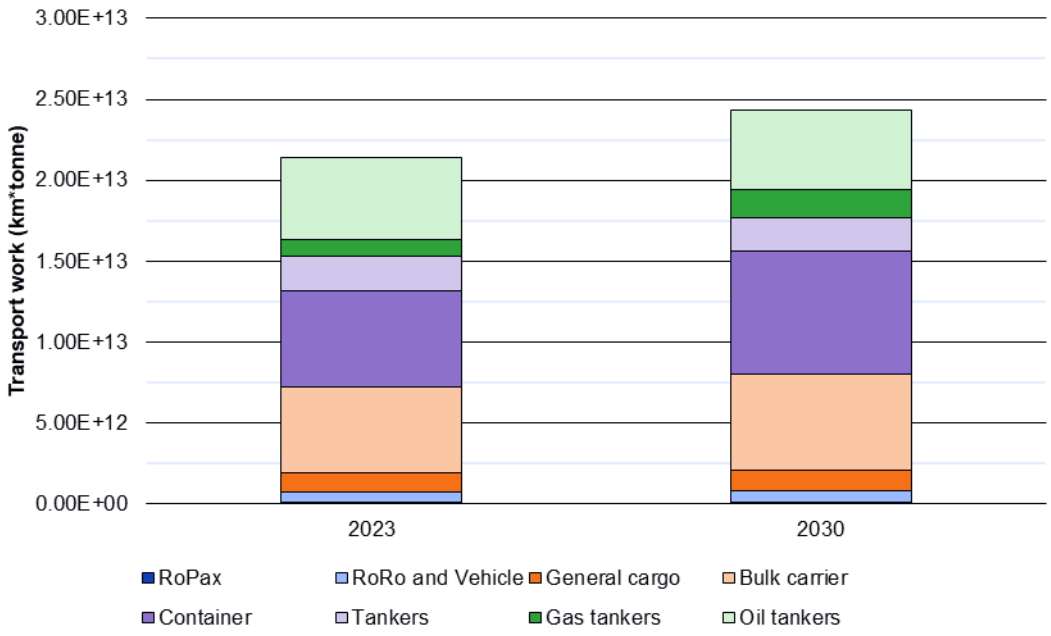

2.2.3. Energy sources

The fuel mix in 2023 has been based on real ship activity in AIS data assuming that ships use the most economically viable fuel technically possible, while following rules concerning the fuel sulphur content. Ships using LNG as fuel were identified from the engine description in the ship technical database. The type of each LNG engine was then further identified, as the type affects the emissions of NOx and methane slip. Future scenarios follow similar logic, however, to simulate the adoption of alternative fuels, some ship types have been assigned to use a specific fuel (further details are presented in the Appendix, section A1 Table 1).

Two different fuel mixes have been considered. In the 2030 BAU and the 2030 all-EU ECA scenarios, the LNG uptake was increased to 11.3% of energy used by shipping (from 4.4% in 2023) by assigning all RoRo-passenger ships to use LNG as fuel in

addition to the existing LNG-fuelled ships. These ship types tend to operate on regular routes and thus, they are probable candidates for early adoption of new types of fuels. Methanol was assumed to be used by vehicle carriers and general cargo ships accounting for 6.3% of energy used by shipping. In the 2030 LNG scenario, the LNG uptake was increased to 19.3% of energy used by shipping. This was done by assigning all RoRo-passenger ships, RoRo cargo ships, gas tankers, and passenger ships to use LNG as fuel in addition to the existing LNG fuelled ships. Methanol usage was assumed to be on the same level as in the other fuel scenario. The fuel mixes in 2023 and the future scenarios are shown in Figure 3.

Figure 3 *Energy sources in 2023 base case and future 2030 scenarios*

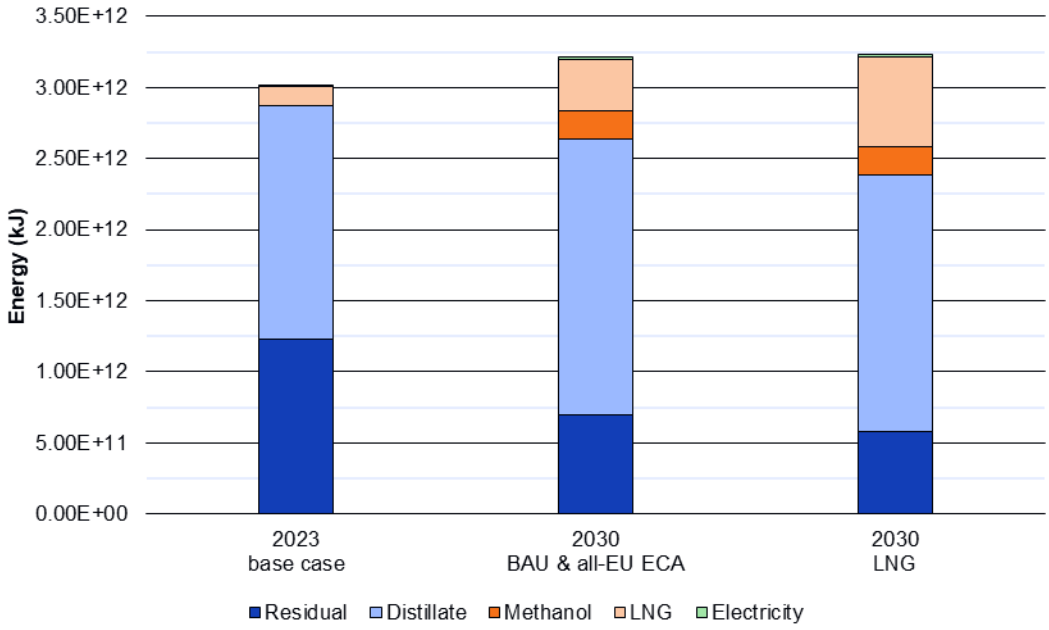

Existing shore power installations were collected from maritime port infrastructure data from the European Alternative Fuels Observatory (EAFO). In 2023, ships which have the capability to use shore power according to the technical database were assumed to connect at any terminal providing shore power. In the 2030 scenarios, all TEN-T ports have been assumed to offer shore power for containerships and passenger vessels. The estimated contribution of shore power to the total energy sources of shipping remains small; 0.04% in the 2023 base case and 0.68% in the 2030 scenarios.

Emission factors of marine engines in 2030 were assumed to be on similar level as in 2023 but improvements in energy efficiency will lower the emissions. Emission factors for methanol engines are based on values reported by Fridell et al. (2021).

2.3. LAND-BASED EMISSIONS

2.3.1. Background on the CAMS-REG emissions inventory

Land-based emissions refer to all anthropogenic sources within the study area originating from land-based activities and inland shipping, excluding international sea shipping. These were derived from the CAMS-REG version 7 (v7) inventory (Kuenen et al., 2022), which provides a harmonized, Europe-wide dataset covering

air pollutants (SOx, NOx, NMVOC, CO, NH_3, PM_{10}, $PM_{2.5}$). The inventory is primarily based on official national submissions to the Centre on Emission Inventories and Projections (CEIP) under the Convention on Long-Range Transboundary Air Pollution (CLRTAP) and to the United Nations Framework Convention on Climate Change (UNFCCC), supplemented by estimates from the Greenhouse Gas - Air Pollution Interactions and Synergies (GAINS) model for non-EU countries (excluding the UK, Switzerland, Norway, and Iceland). Reported data are standardised across approximately 250 sector–fuel categories, with additional quality checks and adjustments to ensure consistency and address reporting gaps.

CAMS-REG is updated annually, with each release linked to the most recent reporting cycle; v7 is based on 2023 submissions. Methodological improvements in v7 (compared to v6) include revised allocations for large point sources, harmonised PM emissions accounting for condensables, and the removal of NMVOC emissions from cultivated crops to avoid double-counting with biogenic sources. A persistent limitation, however, is the two-year delay in national emission reporting, which means that CAMS-REG inventories lag 2-3 years behind real time. To address this, an extrapolation procedure is applied using sector-specific activity data (e.g., electricity generation, fertilizer use) and proxy indicators to estimate recent emission trends. Using this approach, emissions for 2022 and 2023 were derived from v7 extrapolated from the year 2019 to exclude the anomalous COVID-19 years (2020–2021). Some uncertainty remains due to possible fuel-use changes linked to the war in Ukraine and subsequent rise in energy prices. Despite these uncertainties, the extrapolation provides a continuous and up-to-date time series through 2023.

At the time this study was initiated, CAMS-REG v8 was still under development. As its methodology is unchanged and differs only in updated national submissions, a verification exercise was undertaken by comparing the v7 versus v8 data for 2021 and 2022. The comparison showed that the two versions are highly consistent at the EU+ level, with differences below 5%, supporting the use of the extrapolated v7 emissions. Larger differences occur at regional, country, and sectoral levels, and therefore results at finer scales should be interpreted with caution.

To support air quality modelling, CAMS-REG is distributed with complementary products, including country- and sector-specific speciation profiles for PM and NMVOC, and default effective emission heights, allowing direct application in regional and urban-scale models.

2.3.2. Methodology for developing 2030 emission scenarios

From the perspective of land-based emissions, the different 2030 scenarios introduced in section 2.1.1 are identical, since the assessment scenarios only differ with respect to international sea shipping. The scenario development presented here therefore focuses on distinguishing land-based emissions in 2030 from those in 2023. The Clean Air Outlook scenarios developed for the European Commission by the International Institute for Applied Systems Analysis (IIASA) as part of the 3rd Clean Air Outlook (Klimont et al., 2022) form the basis for this work.

These scenarios illustrate the expected impacts of the ‘Fit for 55’ climate and energy package and the Zero Pollution 2030 targets on emissions and air quality. In this study, the Current Legislation (CLE) scenario is applied as the main reference. This scenario reflects all current EU and national legislation on air pollutants, assumes the full implementation of Fit for 55, includes projections from the Price-Induced Market Equilibrium System (PRIMES) energy model and the Common Agricultural Policy Impact (CAPRI) agricultural model implemented in GAINS,

integrates the agricultural part of the revised Industrial Emissions Directive proposal, adopts preliminary assumptions for the Euro 7 emission standard, and introduces the SECA in the Mediterranean Sea.

The emission scenario for this study was developed by first mapping emissions from GAINS sectors and fuels to the detailed sector/fuel combinations used in the CAMS-REG inventory. From these, country-, sector-, and fuel-specific scaling factors were calculated for future years by comparing emissions in those years to 2020 levels. Where data was missing or scaling factors were unrealistically large, gap-filling and capping procedures were applied to ensure consistency. To resolve mismatches between GAINS and CAMS-REG for some sectors, additional scaling factors were derived at the gridded nomenclature for reporting (GNFR) sector level to keep aggregated totals aligned. These factors were then applied to the CAMS-REG 2020 base emissions to generate projections for 2030.

For the 2030 scenarios, an updated speciation of NMVOC and PM emissions was prepared to capture the differences in underlying sectors between 2023 and 2030. The speciation of PM and NMVOC is needed because these pollutants are complex mixtures whose individual components have different chemical and physical properties. Accurately representing these differences is therefore essential for modelling their transformation and impact in the atmosphere (detailed in Section 2.4).

- **NMVOC**: The speciation profile remains the same across all scenarios. For land-based emissions, NMVOC emissions are available for approximately 300 sectors, with speciation calculated at that sectoral level. These are later aggregated to the 15 GNFR sectors. If the distribution of activity or fuel use changes within a sector, the GNFR level split adjusts accordingly through a weighted average.
- **PM**: Unlike NMVOC, PM speciation differs between scenarios. For shipping, FMI provides specific splits for EC and OC, which are calculated at a higher sectoral detail. Non-shipping PM emissions and speciation, however, remain consistent across all scenarios and follow the same 300-sector approach as NMVOC before aggregation to GNFR.

2.3.3. Processing emissions

The land-based emissions for both the 2023 base case and the 2030 scenarios were spatially distributed using the regular CAMS-REG approach (Kuenen et al., 2022) at 0.05°x0.1° (lat-lon) by GNFR sector and for each pollutant, with an additional split of GNFR B_Industry having refineries separated from other industrial emissions. These were then complemented with sea shipping emissions allocated by sea basin from the STEAM model. For 2030, the same land-based emission dataset was combined with each of the three different shipping scenarios. This approach ensures compatibility with, and suitability for, the air quality modelling performed in the following steps of this analysis.

2.4. AIR QUALITY MODELLING

2.4.1. Model description

LOTOS-EUROS (v2.3.003) is a 3D chemistry transport model using the Eulerian approach to simulate air pollution dispersion in the lower troposphere solving the advection-diffusion equation on a regular latitude-longitude-grid with variable resolution over Europe (Manders et al., 2017; Schaap et al., 2008).

LOTO-EUROS v2.3 uses a linear advection scheme (Hooghiemstra, 2006) with horizontal diffusion. The vertical transport, diffusion and stability follow an exposure class approach. The vertical grid is based on the terrain following vertical coordinates along with meteorological input pressure level. The height of the layers on top of the 25 m surface layer is determined by pressure from meteorological input. Twelve model layers are used (with seven stacked boundary layers on top).

Gas-phase chemistry is simulated using the TNO CBM-IV scheme, which is a condensed version of the original scheme (Whitten et al., 1980). Hydrolysis of dinitrogen pentoxide (N_2O_5) is explicitly described following Schaap et al. (2004). LOTOS-EUROS explicitly accounts for cloud chemistry, computing sulphate formation as a function of cloud liquid water content and cloud droplet pH (Banzhaf et al., 2012). For aerosol chemistry, the thermodynamic equilibrium module ISORROPIA2 is used (Fountoukis & Nenes, 2007). Dry Deposition fluxes are calculated using the resistance approach as implemented in the DEPosition of Acidifying Compounds (DEPAC) module (van Zanten et al., 2010). Furthermore, a compensation point approach for NH_3 is included in the dry deposition module (Wichink Kruit et al., 2012), while the wet deposition module accounts for droplet saturation (Banzhaf, 2013).

2.4.2. Source apportionment

TNO has developed a system to track the contribution of emission categories within a LOTOS-EUROS simulation (source apportionment) based on a labelling (or tagging species) technique (Kranenburg et al., 2013). This technique provides conserved mass information about the source contributions to air pollution concentration. Tagging species is therefore different from brute force (another common approach) that applies emission reduction scenarios to derive the impact of sources. Detailed comparisons of all source apportionment methods are described in (Zhang et al., 2025).

The labelling source apportionment technique has been previously used to investigate the origin of PM (episodes) (Banzhaf, 2013; Timmermans et al., 2017, 2022), NO_2 (Pseftogkas et al., 2024) and nitrogen deposition (Curier et al., 2014; Thürkow et al., 2023). Besides the total pollutant concentrations, the contributions of selected sources to these concentrations are calculated. The labelling routine is implemented for primary, inert aerosol tracers as well as for chemically active tracers containing a C, N (reduced and oxidised) or S atom, as these are conserved and traceable.

The source apportionment module for LOTOS-EUROS provides a source attribution valid for current atmospheric conditions as all chemical conversions occur under the same oxidant levels. Further details and validation of this source apportionment module are presented in Kranenburg et al. (2013).

2.4.3. Simulation setup

The model and setup follow the Copernicus Atmospheric Monitoring Service (CAMS) regional ensemble operational forecasts and analyses over Europe. In this context the model is regularly updated and validated using observations from ground and satellite observations. The model performance is also subject to numerous peer-reviewed publications (Schaap et al., 2015; Escudero et al., 2019; Skoulidou et al., 2021; Timmermans et al., 2022). An overview can be found on the model's website: www.lotos-euros.nl.

2.4.3.1. Domains and resolution

The nested sequence of model runs contains simulation over a parent domain across Europe with coarser resolution and three nested domains around the four seaport areas, with higher resolution. The different domains are shown in Figure 4.

The parent domain (15°W, 40°E, 30°N, 70°N) offers a simulation over Europe at a coarse resolution (longitude x latitude: 0.50° x 0.25°, approximately 25 x 25 km2) and provides boundary conditions for the three higher-resolution nested simulations. These nested domains are:

- BENELUX (Belgium, Netherlands, Luxembourg) extending from 1.5°E to 9°W and from 49°N to 54.5°N;
- the French Mediterranean coast (2.5°E, 7.5°E, 41°N, 46°N); and
- the southern coast of Greece (21.5°E, 26.5°E, 34.8°N, 39.8°N).

Each nested domain operates at a finer resolution (longitude x latitude: 0.1 x 0.05, about 6 x 6 km2), with a 1:5 ratio to the parent domain. The nested domains only receive input from the parent domain and do not interact with or influence it.

Figure 4 *Domain of modelling simulation with the blue line indicating the outer domain and red lines indicating the nested domain runs*

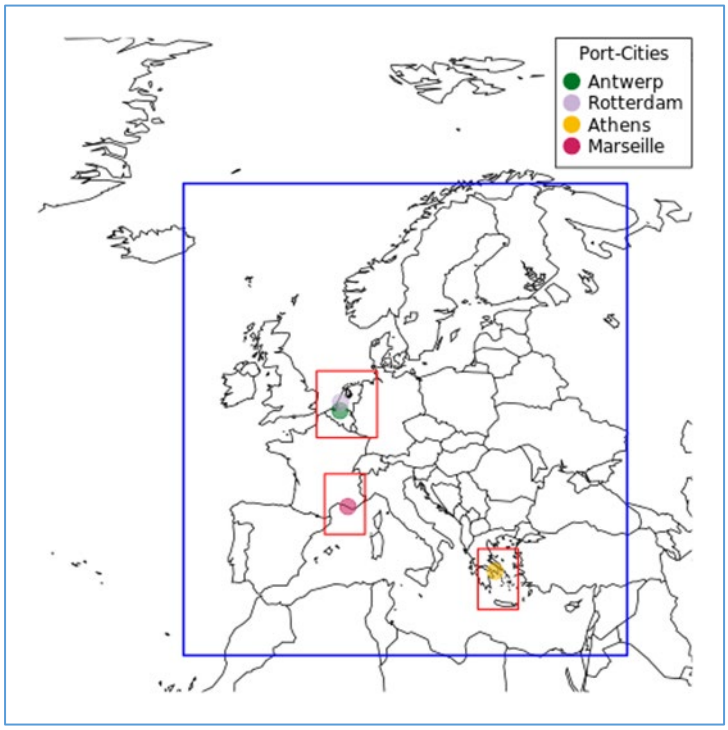

The dots indicate the four seaport areas (Antwerp, Rotterdam, Athens and Marseille).

2.4.3.2. Meteorology and boundary conditions

The LOTOS-EUROS model uses offline meteorology with the European Centre for Medium-Range Weather Forecasts (ECMWF) operational forecast – Integrated Forecasting System (IFS) and atmospheric composition species as boundary condition. IFS provides hourly estimates for a large number of atmospheric, land and oceanic climate variables, that are necessary inputs for calculations of

atmospheric concentrations. IFS data cover the Earth on a 30 km grid and resolve the atmosphere using 137 levels from the surface up to a height of 80 km. Typical inputs required by LOTOS-EUROS are, for example, surface and air temperature, cloud cover, windspeed and direction, precipitation and relative humidity.

2.4.3.3. Spatial and temporal profiles

In LOTOS-EUROS, the temporal variation of the emissions is based on CAMS TEMPO v4.1 (Guevara et al., 2021). The stationary combustion emission (mostly residential combustion) was further scaled with a heating-degree-days factor derived from temperature-based heating demand. The vertical distribution of emissions for point and area sources follow the stack height approach (adapted from Thunis et al. (2008)). For this study, sea shipping area and point sources were adapted based on outputs from the STEAM model (described in section 2.2.1). Emissions from both industrial and power area sources follow the stack height vertical distribution from the height of industrial point sources.

The biogenic emission routine is based on detailed information on tree species over Europe (Köble & Seufert, 2001). The emission algorithm is described in Schaap et al. (2009) and is very similar to the simultaneously developed routine by Steinbrecher et al. (2009). The sea salt emission is described using Mårtensson et al. (2003) for the fine mode and Monahan et al. (1986) for the coarse mode. Desert dust emissions are adapted based on the parameterisation from Marticorena & Bergametti (1995) and Mokhtari et al. (2012). Fire emissions were taken from GFAS-daily v1.2 dataset (Kaiser et al., 2012; Rémy et al., 2017).

2.4.3.4. Labelled sources

Table 2 presents the labels that were applied to label emission sources from different sectors. A special split is made between international shipping and inland shipping. International shipping includes emissions from ships travelling in sea regions, whereas inland shipping describes the emissions occurring on inland waterways. In some cases, significant contributions come from ships travelling on rivers flowing in or near these cities. This is categorised as inland shipping.

These sectors are labelled or tagged for all PM species of fine and coarse bins and include EC, primary organic matter (POM), rest of primary particulate matter (RESTPPM), and secondary inorganic aerosols (SIA): Nitrate (NO_3^-), Ammonium (NH_4^+), and Sulphate (SO_4^{2-}). Five labelled bins are tagged with natural source dominated species, Sodium (Na mass converted to sea salt) and Dust. In this study, the anthropogenically emitted dust was not considered. Besides PM, gas species labelling includes NO_2, NO, NH_3, SO_2 and nitric acid (HNO_3).

For the analysis, the focus has been on NO_2 and $PM_{2.5}$ which are the two key pollutants in current air quality regulations and exceedance events. The main report presents the results for NO_2 and $PM_{2.5}$ where significant, while the Appendix (sections B2 and B3) presents the results for other pollutants.

Table 2 *List of modelled labelled sources and their explanations*

Source sector	Explanation
Shipping	Emissions from inland and sea shipping activities
Public power	Electricity and heat production (power plants)
Other stationary combustion	Other fuel use in buildings and commerce
Fugitives	Fugitive emissions from fuels (oil, gas, coal handling)
Solvents	Use of solvents and products (e.g., paints, cleaning)
Road transport (exhaust)	Exhaust emissions from road transport (including gasoline, diesel and LPG gas)
Road transport (non-exhaust)	Brake wear, tyre wear, road abrasion and evaporation from road transport
Aviation	Emissions from domestic and international aviation
Off-road	Non-road transport & machinery (e.g., tractors, construction, rail)
Waste	Solid waste disposal, wastewater treatment, waste burning
Agricultural	Emissions from livestock, manure and storage
Industry	All industrial combustion sources other than refineries and power generation
Refineries	Fuel combustion in refineries
Natural	Biogenic sources, naturally emitted desert dust, sea salt and wild fire
Boundary	Initial condition and contribution from outside of the parent domain

2.4.4. Presentation of results (city source apportionment)

For each assessed seaport area, a ‘core city area’ and a ‘port area’ were defined for presenting the results. The core city area used for each location was as defined by the Eurostat 2021 Urban Audit database (Eurostat, 2021) (Figure 5). This was used to determine surface concentrations and source apportionment results weighted by the area highlighted in pink on the native model grid to represent the port city. The measurement location used in the results section for the city was also selected from the highlighted urban area. In addition, the Eurostat 2009 Land Cover database (Eurostat, 2013) was used to determine measurement locations within each port area (grey highlight). It should be noted that the ‘city domains’ used in the emissions results are different from the ones used for the modelling – these are presented in the Appendix (section A2 Figure 4 to Figure 7).

Figure 5 *Core City area definition (Urban audit, 2021) and port area from Eurostat land cover (2019)*

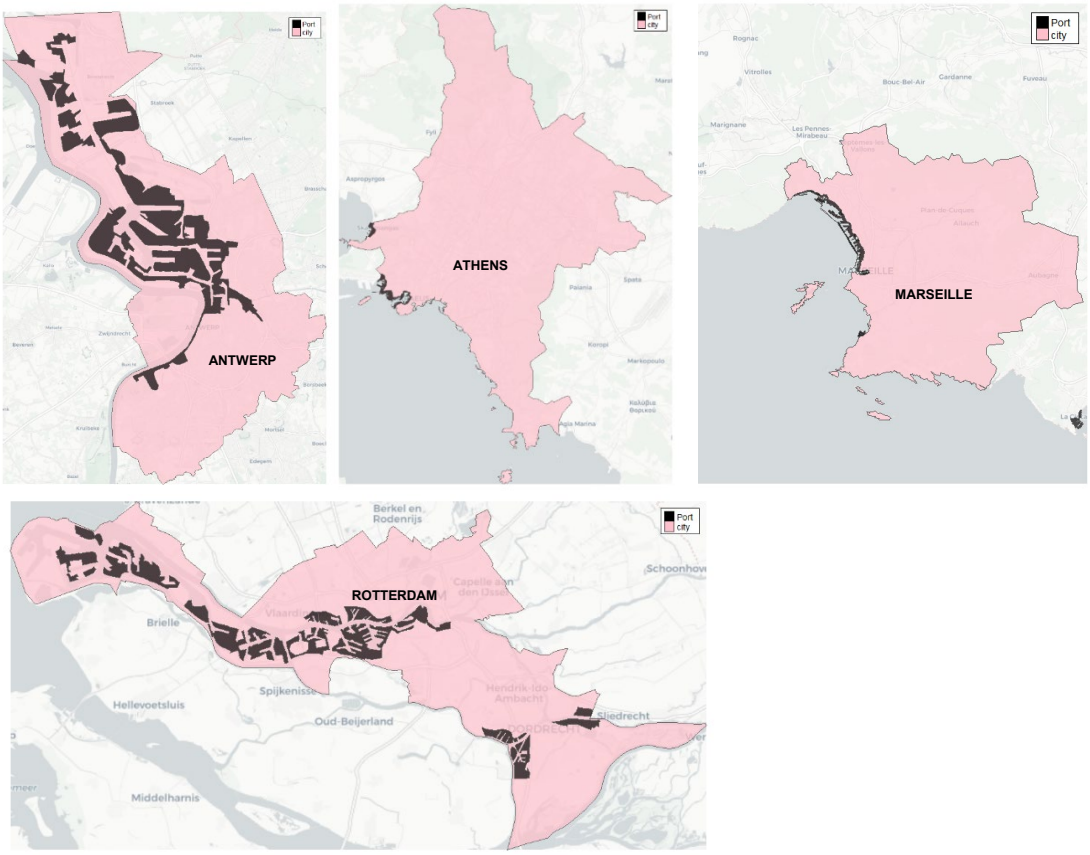

2.4.5. Evaluation of modelled concentrations

The model concentrations have been validated with measurements from the European Environment Agency (EEA) and the Environmental Database for Atmospheric Studies (EBAS). EEA data is collected from national monitoring networks of each member state and includes pollutants such as $PM_{2.5}$, PM_{10}, NO_2, nitric oxide (NO), SO_2 and ozone (O_3) from urban, suburban, background and rural stations. EBAS observations focus on more rigorously quality-assured data in the background and rural sites. They include stations with speciated PM, such as sulphate, nitrate, ammonium and sodium measurements which are key to indicate model performance in terms of chemistry composition and natural sources of particulate matter. Usually, EBAS data take a longer time to be made publicly available when compared to EEA's near-real time dataset.

Regarding the evaluation of the modelled concentrations for the parent domain and year 2023, data from approximately 3,500 EEA stations across Europe was used (Figure 6). Moreover, two EBAS stations, located in Italy (Ispra) and the Netherlands (Cabauw), were also selected for the evaluation of the modelled speciated PM concentrations. Evaluation of the modelled concentrations of the primary species was performed for each separate zoomed-in sub-domain with the corresponding EEA ground-based observations. The validation against the EBAS observations is presented in the Appendix (section B1).

Figure 6 *Location of EEA stations used for the validation of the LOTOS-EUROS parent domain*

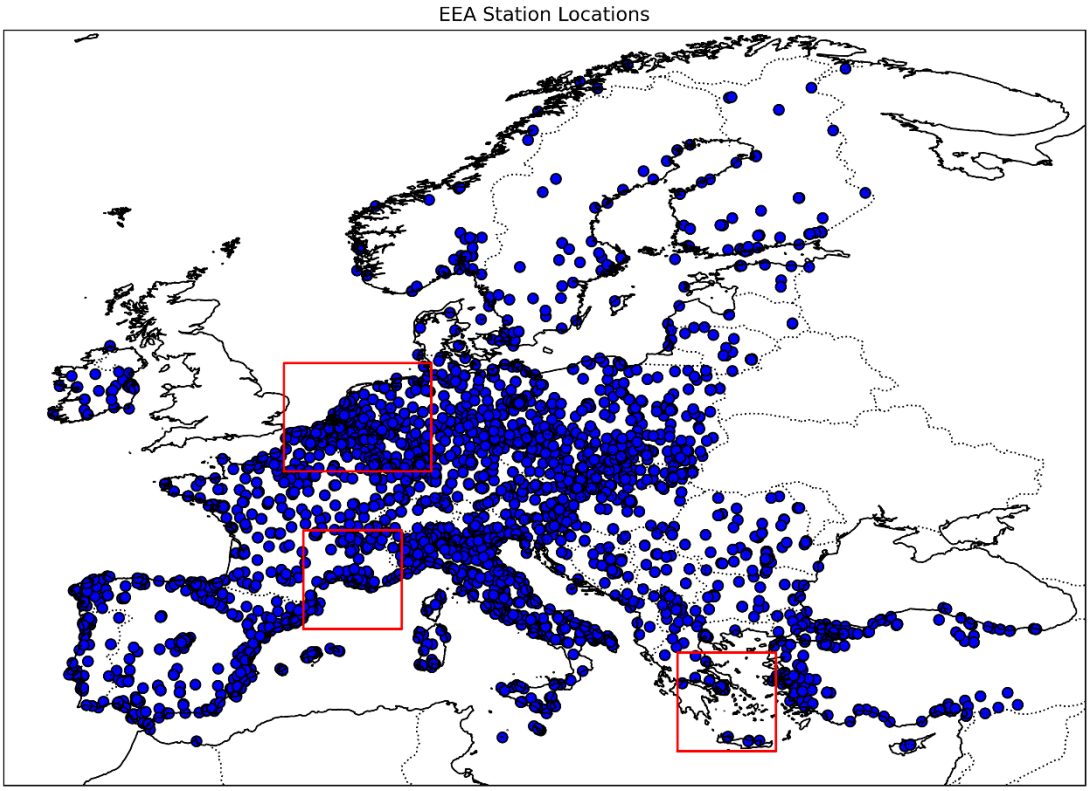

2.5. ASSUMPTIONS

Regulations

In the 2030 BAU and 2030 LNG scenarios, only existing or "decided" regulations are included in the simulations. Therefore, no future regulatory changes beyond those already decided are reflected in this study.

Emission control areas

- The Baltic Sea, North Sea, English Channel, and Norwegian Sea are already ECAs for NOx and SOx, while the Mediterranean Sea is an ECA for SOx. These ECAs are shown with a dark colour in Figure 1.
- In the 2030 all-EU ECA scenario, SOx and NOx ECAs are assumed within 200 nautical miles of the EU coastline (excluding the Canary Islands and the Azores). The start dates assumed for these are:
  - New all-EU SECA: 1 January 2028.
  - New all-EU NECA: applicable to ships built in 2027 onwards.
- There is no agreed legislative initiative regarding new ECAs thus the actual entry dates of new ECAs are uncertain and are only hypothetical for the purposes of the study. While the effects of SECA are immediate, the effects of NECA are delayed since they apply only to newbuild ships.

Global sulphur limit

A 0.5% global sulphur limit in marine fuels is assumed in all simulations, and no consideration is given to any potential future tightening of sulphur limits.

Emission factors and technologies

- Engine emission factors in 2030 are assumed to be at the same level as in 2023.
- New emission control technologies are not considered.
- Installations of scrubbers and SCRs are assumed to remain at 2023 levels.
- SCRs are assumed to be used only inside NECA areas.
- Existing scrubber ban areas (as of 2023) are included in the 2030 simulations.

Fuel scenarios

- Fuels are assigned by ship type, meaning all ships of the same type convert to the defined fuel.
- For LNG ships, slow-speed engines (≤130 rpm) are assumed to be high-pressure dual fuel, and medium- and high-speed engines are assumed to be low-pressure dual fuel.

Shipping traffic (AIS data)

- AIS data from 2023 is used as the baseline.
- Ship traffic is scaled to represent future growth, while the geographical distribution remains the same as in 2023. It is uncertain whether geopolitical issues could significantly shift major trade lanes and/or alternative fuel uptake during the model period and this has not been taken into consideration.

Ship fleet age

The average age of the fleet is assumed constant by incrementally increasing build years with the modelling year.

Effect of NECA start date

- With a 2027 start date, ~4,300 IMO-registered ships are subject to NECA by 2030; with a 2029 start date, only ~2,100 ships. The full potential of NECA is not visible by 2030.
- Simulations were undertaken to test both start year and emissions of NOx and NH_3 from this sensitivity test are shown in the Appendix (section A1 Figure 3).

Extrapolation of recent years (2022–2023)

Emissions were estimated by extrapolating sector-specific activity data and proxy indicators. Abrupt changes in energy use, agriculture and industry may not be fully captured.

Energy crisis and war in Ukraine

The extrapolation assumes potential fuel-use shifts from these events have limited or averaged-out effects in the dataset.

Mapping between GAINS and CAMS-REG categories

GAINS sector–fuel combinations were mapped to more detailed CAMS-REG categories, assuming sectoral integrity and pollutant relevance are preserved despite definitional mismatches.

Dependence on GAINS model

The methodology uses GAINS for non-EU data and scenario scaling.

Clean Air Outlook scenarios

Assumes full and timely implementation of EU policies such as Fit for 55, Euro 7, and the Mediterranean SECA.

2.6. LIMITATIONS OF THE STUDY

The findings presented here are subject to several uncertainties. Shipping emission inventories rely on aggregated traffic data and generalised emission factors, which may underestimate real-world variability in vessel operations and port activity; in some cases, emissions in ports may be significantly underestimated. The spatial resolution of the data also limits the ability to capture localised hotspots, making city-level concentration estimates less precise.

The modelling uses average meteorological conditions and a steady fleet composition, meaning that local outcomes may diverge under different weather patterns or technology adoption rates. Moreover, the scenario analysis was restricted to 2030; extending the horizon to 2050 could reveal more pronounced impacts of hypothetical regulatory measures such as SECA and NECA, as well as the long-term implications of different fuel and technology transitions.

These limitations highlight where improvements in methods, data, and pollutant coverage could have the most significant effect. Addressing them would not only refine emission estimates but also strengthen the relevance of results.

3. RESULTS AND DISCUSSION

3.1. EMISSIONS IN EUROPE

This section outlines the annual emissions originating from both sea shipping and land-based sources across the scenarios introduced in section 2.1.1. The analysis considers how emissions vary under the different scenarios, allowing for a comparison of their potential impacts on overall emission levels.

Key highlights
• NOx emissions from shipping are projected to decrease 13-19% by 2030 (compared to 2023), due to stricter regulations, improved energy efficiency, and the adoption of alternative fuels. • NH_3 emissions from shipping are projected to increase significantly by 2030 (compared to 2023), due to the wider use of SCR and alternative fuels, such as LNG and methanol. However, they still remain a small contributor to total emissions compared to other sources. • The expansion of emission control areas (NECA/SECA) and the uptake of alternative fuels will alter the spatial distribution of emissions, with the Mediterranean SECA leading to significant reductions in SOx (44-56%) and $PM_{2.5}$ emissions (24-30%). • Land-based emissions are projected to decrease substantially by 2030, with reductions of ~40% for NOx and ~35% for $PM_{2.5}$, while NH_3 remains largely unchanged. • Port cities show strong variation by 2030, with sea shipping contributing ~70% of NOx in Marseille and Athens, and 25-30% in Rotterdam and Antwerp, reflecting the persistent or growing contribution of land-based sectors, such as inland shipping and industrial activity.

3.1.1. Sea shipping emissions

This section presents the total annual shipping emissions in the European domain for NOx, NH_3, $PM_{2.5}$ and SOx. Annual emissions of CO and NMVOCs, as well as emissions of all pollutants for each different sea region are presented in the Appendix (section A1).

Figure 7 presents the total emissions of NOx and NH_3 from shipping in the European domain for the four assessment scenarios. Emissions of NOx are expected to decrease in all future scenarios in comparison with the 2023 base case where NOx shipping emissions are predicted to be 3,885 kt. Under the 2030 BAU scenario, NOx shipping emissions are predicted to be 3,391 kt (13% reduction compared to 2023 base case), while under the 2030 LNG and 2030 all-EU ECA scenarios, NOx shipping emissions are predicted to reduce further, by 19% (3,165 kt) and 14% (3,356 kt) respectively. These emission reductions are due to more ships being applicable to NECA regulations, the increase in energy efficiency of ships, and changes in the fuel mix of shipping.

Emissions of NH_3 are expected to increase in all future scenarios in comparison to the 2023 base case across the domain. The estimated increase in NH_3 emissions across the domain is from 49 t in 2023 to 163 t in the 2030 BAU and 2030 LNG scenarios, and 243 t in the 2030 all-EU ECA scenario. All modelled NH_3 emissions from shipping are from usage of SCR units and this is very visible in the 2030 all-EU ECA scenario where the establishment of new NECA also increases the usage of SCRs. Thus, as the number of tier III ships with SCR is increasing, NH_3 emissions are also increasing. However, NH_3 emissions from shipping are still relatively low in comparison to other sources (see section 3.1.3 and Figure 12).

Figure 7 *Total emissions of NOx (kt) and NH_3 (t) from shipping in the European domain in the 2023 and 2030 assessment scenarios*

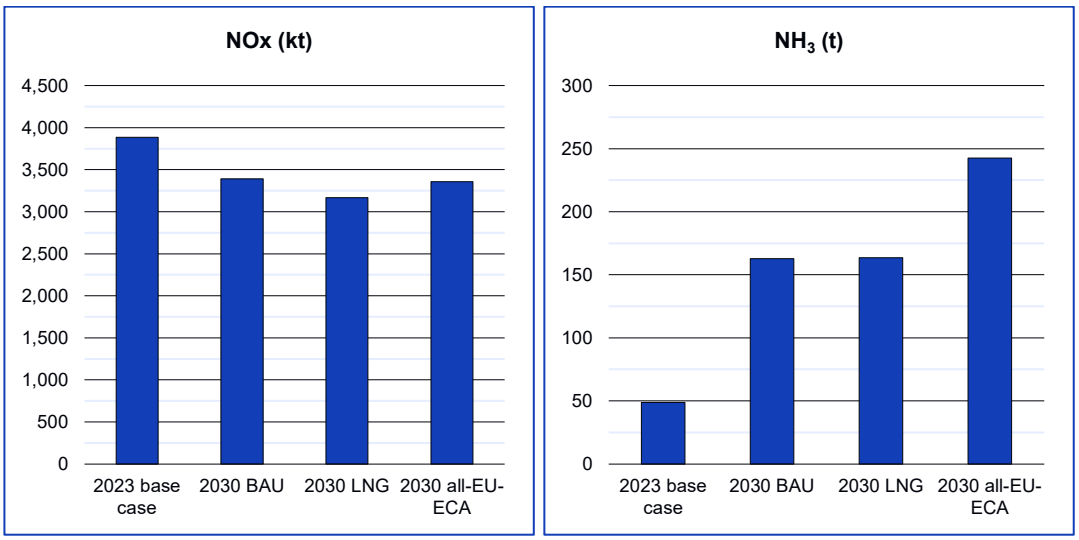

Figure 8 presents the total emissions of $PM_{2.5}$ and SOx from shipping in the European domain for the four assessment scenarios. Emissions of $PM_{2.5}$ and SOx are projected to decrease in the future in comparison with the 2023 base case scenario. The estimated reduction in $PM_{2.5}$ emissions across the domain is 24% (22 kt) in the 2030 BAU, and 30% (28 kt) in the 2030 LNG and all-EU ECA scenarios. The estimated reduction is SOx emissions across the domain is 44% (171 kt) in the 2030 BAU, 48% (187 kt) in the 2030 LNG, and 56% (218 kt) in the 2030 all-EU ECA scenarios.

The Mediterranean Sea is a SECA from 2025 onwards and this is predicted to reduce emissions of SOx and $PM_{2.5}$. Additionally, the increase in consumption of methanol and methane as fuel will lower these emissions. In the all-EU SECA scenario, SOx emissions are predicted to decrease by over 20% in comparison to the 2030 BAU scenario.

Figure 8 *Total emissions of $PM_{2.5}$ (kt) and SOx (kt) from shipping in the European domain in the 2023 and 2030 assessment scenarios*

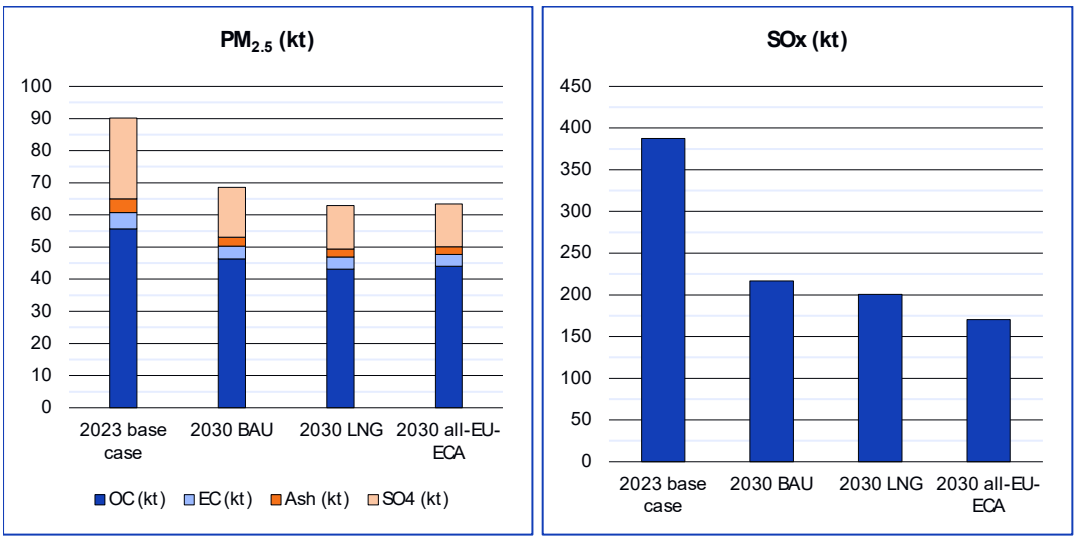

Figure 9 shows the geographical distribution of SOx emissions in the 2023 base case and the 2030 all-EU ECA scenarios. The effect of a hypothetical new SECA, as well as existing SECAs, is clearly visible. The borders of the SECA are highlighted because ships are assumed to change fuels immediately when entering the SECA.

Figure 9 *Annual emissions of SOx (kg) in the 2023 base case scenario (left) and the 2030 all-EU ECA scenario (right)*

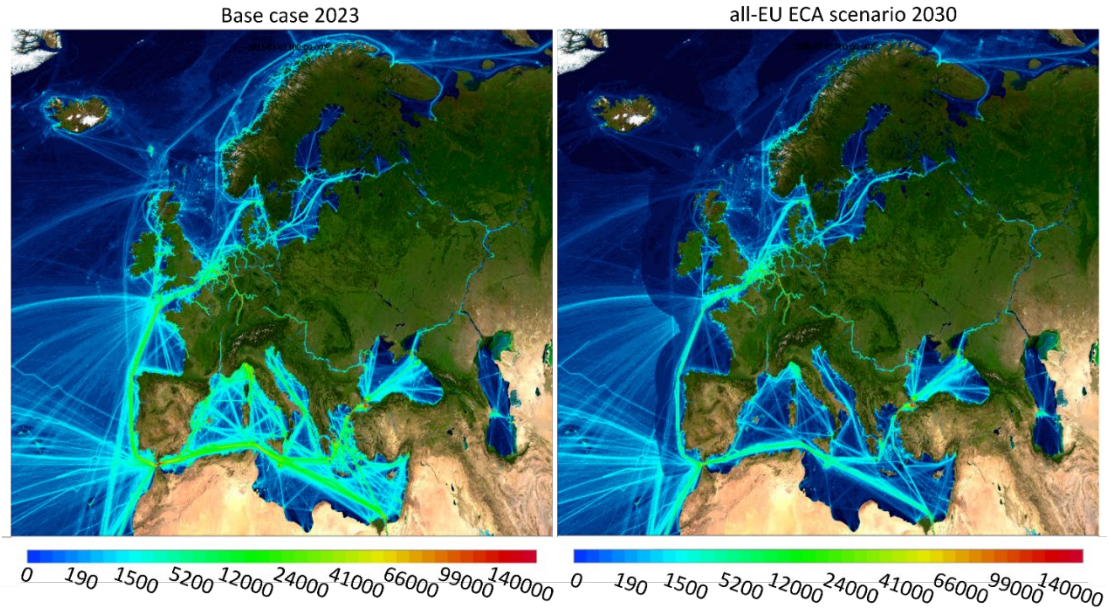

3.1.2. Land-based emissions

This section examines land-based emissions and their evolution from the 2023 baseline to the 2030 scenarios. Additional details are also presented in the Appendix (section A2).

Figure 10 illustrates the total emissions from land-based sources within the EU+ borders (EU27 countries plus Norway, Switzerland, Iceland and the UK) under the 2023 and 2030 assessment scenarios for the main pollutants. This focus reflects the more pronounced policy-driven emission reductions in the EU+ compared to the rest of the domain. For 2030, the scenarios produce identical outcomes, since the only differences among them concern sea shipping and not land-based emissions.

It can be seen that overall emissions decline substantially, with particularly pronounced reductions for NOx of 2,048 kton (~40%) and $PM_{2.5}$ of 462 kton (~35%), while NH_3 shows only minimal changes. To further disentangle the drivers behind these reductions, the sectoral composition of land-based emissions is examined in the following analysis.

Figure 10 *Total emissions from land-based sources in the EU+ region across assessment scenarios*

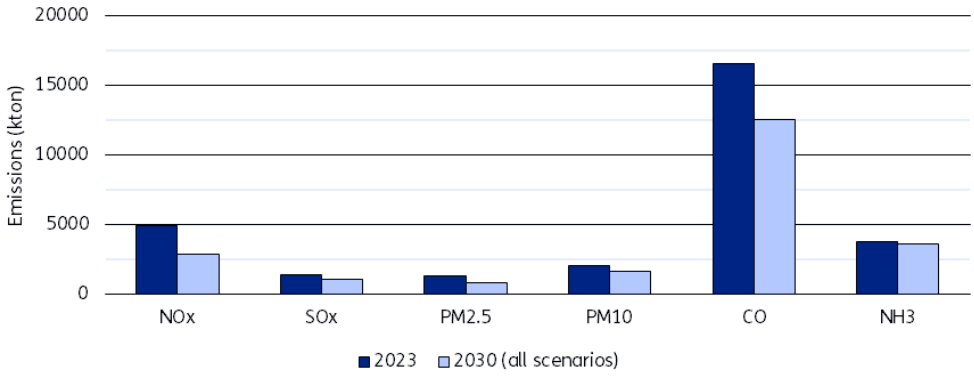

For NOx emissions, the largest reduction between 2023 and 2030 is observed in the road transport exhaust sector, with an anticipated reduction of 1,319 kton (~60%), as seen in Figure 11. This outcome is consistent with the effects of stricter EU legislation, which include improved engine design but most importantly the widespread deployment of advanced after-treatment systems. Noticeable decreases are also evident in the off-road, other stationary combustion, and public power generation sectors.

Figure 11 *Sectoral composition of NOx land-based emissions in the EU+ region across assessment scenarios*

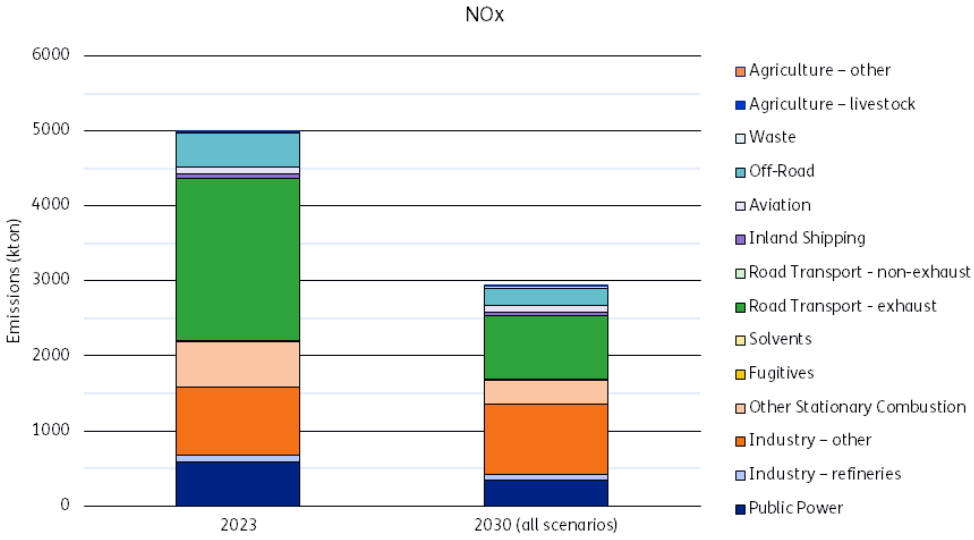

In contrast, the main drivers of reductions in $PM_{2.5}$ and SOx emissions in the EU+ region are found in the other stationary combustion sector, with decreases of 428 kton (~50%) and 214 kton (~70%) respectively. These reductions align with assumptions on stricter regulatory measures, the adoption of cleaner appliances, and potential shifts toward cleaner energy alternatives. For all the pollutants discussed, an increase is observed in the industry-other sector, particularly for SOx, which rises by 79 kton (~15%). Further details on these pollutants are provided in the Appendix (section A2).

3.1.3. Combined (anthropogenic) emissions

This section considers emissions from both land-based and sea shipping sources to assess the relative contribution of sea shipping to overall emissions across the study domain and the different assessment scenarios. Detailed tables for all pollutants can be found in the Appendix (section A2).

Figure 12 and Figure 13 illustrate the growing importance of sea shipping as a contributor to NOx emissions in the 2030 scenarios compared with the 2023 baseline. NOx emissions from sea shipping (labelled as 'Sea' in Figure 13) decrease across all scenarios, between 2,906 kton and 3,131 kton (20%-25%). This is driven by the extension of NECA regulations, improvements in ship energy efficiency and shifts in the fuel mix (particularly in the LNG scenario). However, the reductions in land-based emissions are marginally higher resulting in an increase of shipping share to total NOx emissions (~2-3%) under the 2030 BAU and all-EU ECA scenarios.

For SOx, the relative share from sea shipping declines in the 2030 scenarios, most notably in the 2030 all-EU ECA case. However, it should be noted that sea shipping was already a minor contributor to total SOx emissions, and this decline represents a reduction in its relative contribution from around 5% to 2–3% across all scenarios.

Figure 12 *Relative contribution (%) of sea shipping to total emissions in the European domain across all assessment scenarios for NOx, SOx, $PM_{2.5}$, PM_{10}, CO and NH_3*

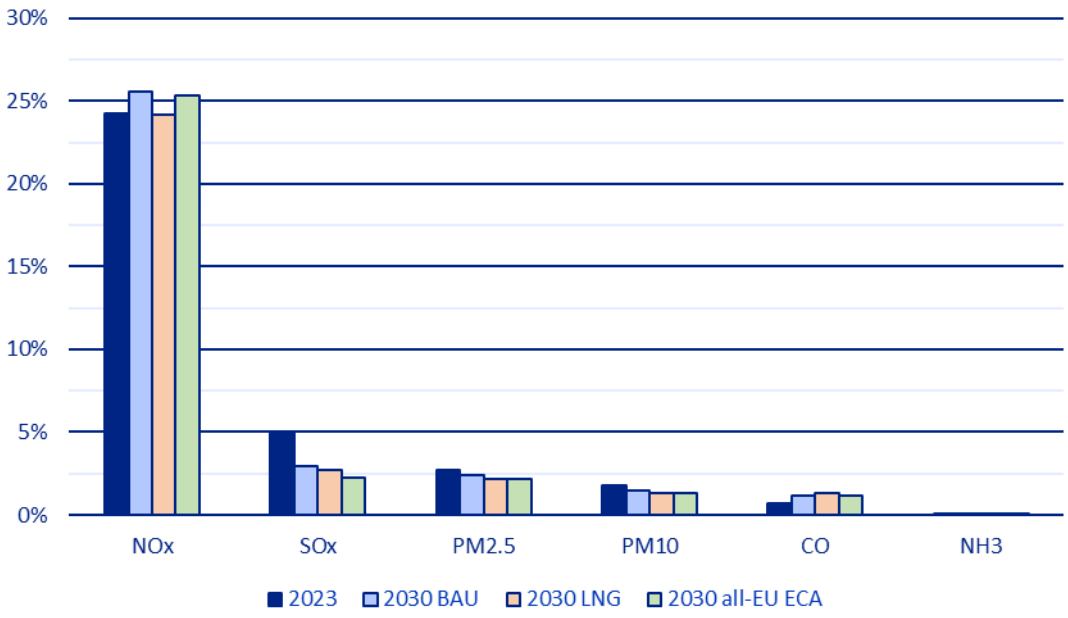

The relative importance of sea shipping appears different when land-based emissions are disaggregated by region. Figure 13 distinguishes between EU+ countries, mostly subject to EU air quality policies, non-EU European countries, and countries outside the European continent but included in the study domain. For NOx, the EU+ region is the largest contributor of land-based emissions compared to other regions in 2023. But by 2030, it becomes the lowest contributor due to the increasing relative importance of emissions from non-EU and non-EU+ regions, with stricter EU+ policies captured in the extrapolation to 2030. For SOx, by contrast, non-European regions play the largest role, while for $PM_{2.5}$, it is the non-EU

European countries that dominate emissions. These regional differences highlight the uneven distribution of emission sources across the study domain.

Figure 13 *Relative importance of sea shipping and emissions breakdown by region for NOx, SOx and $PM_{2.5}$ across assessment scenarios*

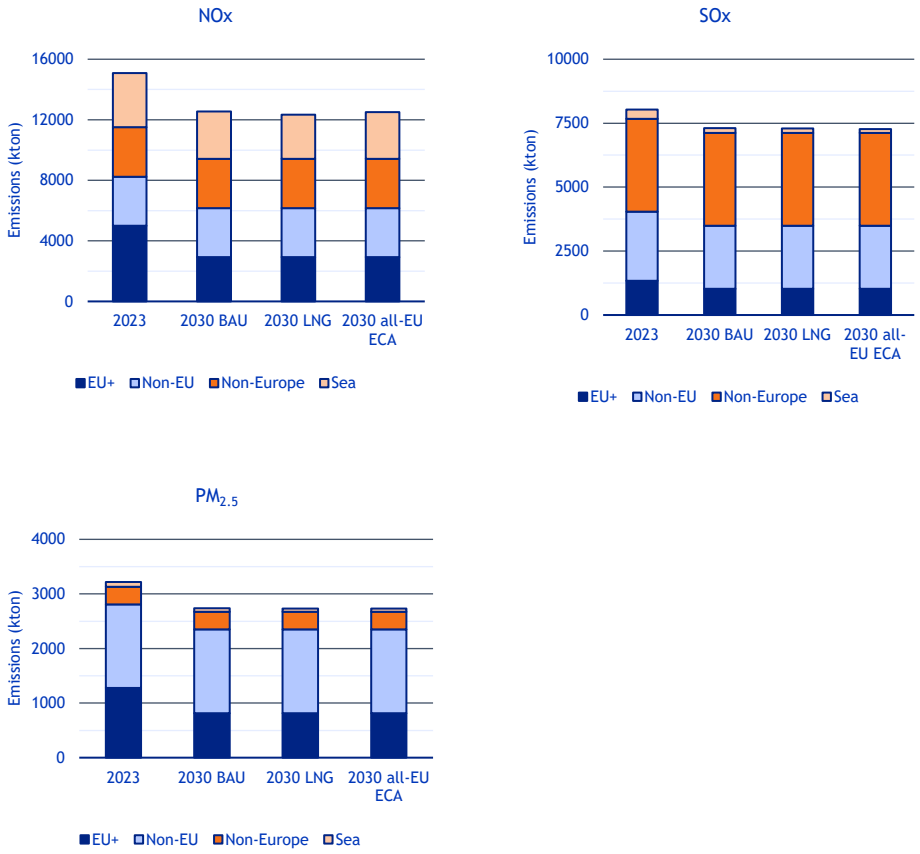

The analysis regarding the emissions focusses also on the four major port cities of interest: Rotterdam, Antwerp, Athens (Piraeus), and Marseille. The extent used around each port area for the calculation of emissions is provided in the Appendix (section A2 Figure 4 to Figure 7). As shown in Figure 14, total NOx emissions are predicted to decrease by 12% to 50% in 2030 compared to 2023 across all cities and scenarios. In terms of sectoral contributions, the relative importance of sea shipping varies considerably across these locations and is projected to shift by 2030.

Across all scenarios, the contribution of sea shipping decreases in Antwerp (~18%), while it increases slightly in Rotterdam (~2%) and more significantly in Marseille (~11%) and Athens (~15%). By 2030, sea shipping accounts for around 70% of total NOx emissions in Marseille (~770 kton) and Athens (~2,890 kton), whereas the share is lower, but still considerable, in Rotterdam (~25%, ~5,907 kton) and Antwerp (~30%, ~3,780 kton). These changes are driven largely by reductions in land-based emissions, particularly from road transport exhaust in both Rotterdam and Antwerp, and from public power generation in Athens, which further amplify the relative dominance of sea shipping in the emissions profile of Marseille and Athens.

In contrast, the contribution of sea shipping in Rotterdam and Antwerp is smaller but still considerable. This is partly explained by the presence of significant other

activities, including refineries, industrial operations, and in the case of Antwerp, public power generation, which increases in 2030. In addition, both ports are closely linked to extensive inland waterway networks, with Rotterdam in particular, having notable emissions from inland shipping. These emissions are not counted as sea shipping but are attributed at the national level. Differences between the assessment scenarios are generally small across all ports, although the 2030 LNG scenario consistently results in the lowest NOx emissions from sea shipping (up to 3% for all assessed ports except Marseille 9%).

Figure 14 *Sectoral contribution to NOx emissions in the European domain in the four ports and their cities across assessment scenarios*

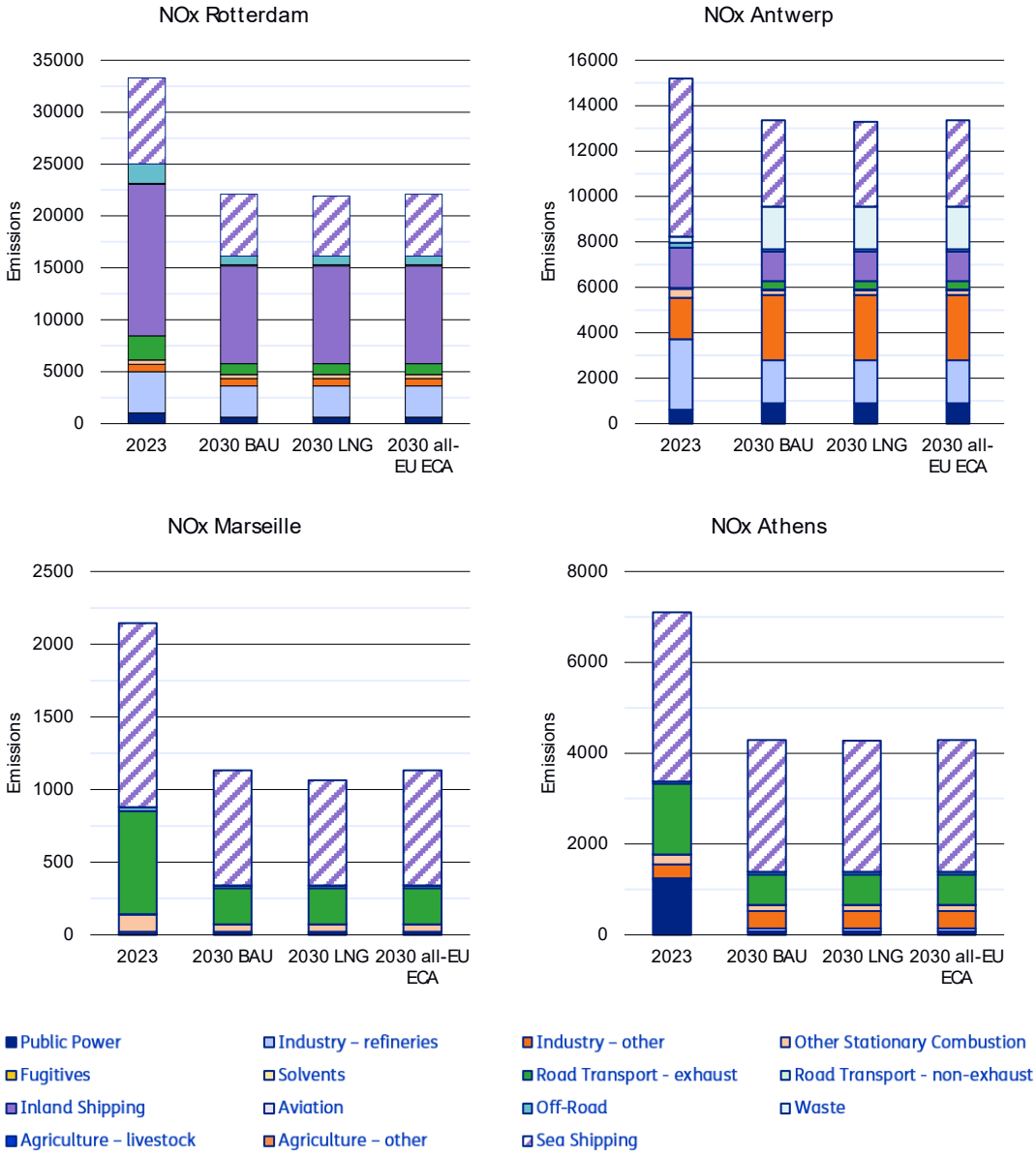

As shown in Figure 15, the relative contribution of sea shipping to SOx emissions is only dominant in Marseille (~ 75%), while in absolute terms the emissions from shipping are comparable across Antwerp, Rotterdam and Athens (ranging between

270 kton and 292 kton in 2023), with Marseille lower at 94 kton. This difference can be partly explained by the choice of the spatial domain: for Antwerp and Rotterdam, for example, the defined port domains extend further inland, likely capturing a larger share of industrial sources and resulting in a more pronounced contribution from land-based emissions. In 2030, refinery activities alone account for nearly 75% of SOx in Rotterdam and around 55% in Antwerp. Other sectors, including fugitives and industry other, also contribute significantly. Unlike better regulated sectors with cleaner alternatives, such as public power generation in Athens where emissions decline, several industrial subsectors show slower reductions or even slight increases in SOx emissions between 2023 and 2030.

Figure 15 *Sectoral contribution to SOx emissions in the European domain in the four ports and their cities across assessment scenarios*

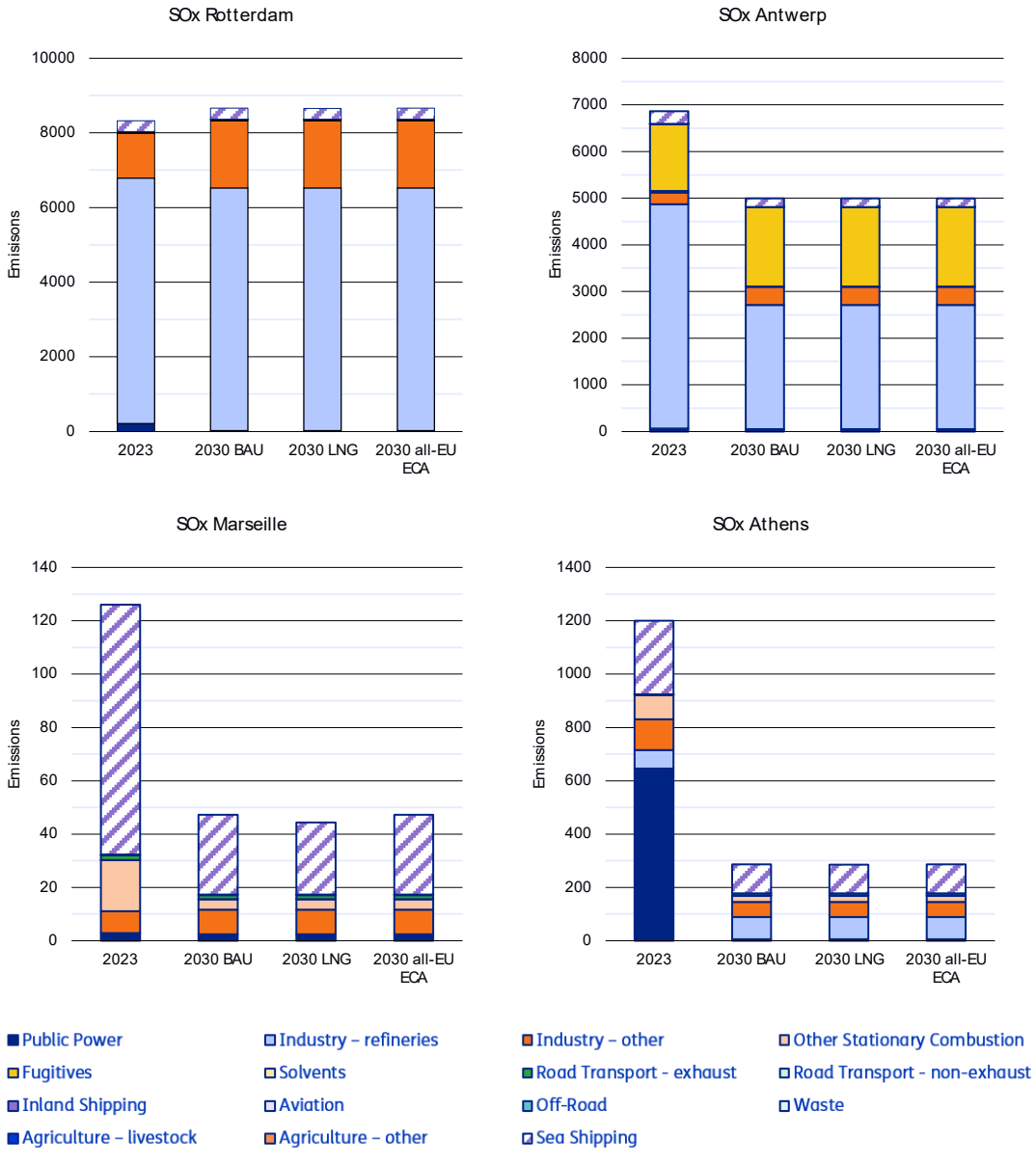

3.2. MODEL VALIDATION

This section presents the LOTOS-EUROS model performance for NO_2 and $PM_{2.5}$ concentrations across Europe and at the four seaport areas. Background/rural stations from the EBAS dataset have been used, as well as urban stations from the EEA dataset. The validation against the EBAS dataset for PM subspecies is presented in the Appendix (section B1).

Key highlights
• Comparison against the EEA observation stations shows an overall strong performance of the model (R^2 > 0.7 for most regions; RMSE 3–7 µg/m³). • The model slightly underestimates NO_2 concentrations in late spring–early summer and slightly overestimates concentrations in late autumn–winter, most likely linked to boundary layer mixing and NOx lifetime representation. • The model captures reasonably the $PM_{2.5}$ daily variability (R^2 ≈ 0.6), though summer PM is underestimated. • The validation shows that the model tends to underestimate $PM_{2.5}$ and PM_{10} concentrations in the Mediterranean cities (Marseille and Athens) (MNB 30–40%), particularly in summer and early autumn, most likely due to under-representation of local sources such as residential wood burning and dust. • The validation of the seaport areas shows consistent seasonal patterns, with overestimation of NO_2 concentrations in Antwerp and Rotterdam, good representation of the seasonal variability in Athens and Marseille, and shipping contributions peaking in summer and road traffic dominating winter NO_2.

3.2.1. Validation against EEA stations

An initial evaluation of the model performance is shown in the scatter plot of Figure 16 for the parent and the nested domains. Comparisons between the daily averaged measured and modelled NO_2 (top) and $PM_{2.5}$ (bottom) surface concentrations across all stations are provided with different colours for each region.

The model performs reasonably well for all instances and species. Specifically, the coefficient of determination (R^2) between the daily average modelled and the observed concentrations across all stations is strong (R^2 > 0.7) for all regions whereas the root mean squared error (RMSE) ranges between 3 and 7 µg/m³. As expected, the EU parent domain (grey) shows the highest RMSE and discrepancies with the observed NO_2 surface concentrations (mean normalised bias (MNB) approximately -44%) due to the coarse resolution in the configuration of the simulations. Comparisons between the modelled surface concentrations and the in-situ measurements in the BENELUX (red) and the Mediterranean/Greece (green) domains show the lowest discrepancies (MNB of approximately -10% and -13% respectively), while the Mediterranean/France (purple) domain displays, overall, a moderate performance (MNB approximately -32%).

Regarding PM concentrations, the BENELUX region shows the lowest discrepancies (MNB between 10% and 20% and R^2 ~0.7), whereas the Mediterranean sub-domains show similar deviations from the observations (MNB between 30% and 40% for $PM_{2.5}$). Modelled PM concentrations in the Mediterranean/France domain show a better co-variability with the observations (R^2 ~0.7 and RMSE ~3 µg/m³) compared to the Mediterranean/Greek sub-domain (R^2 ~0.5 and RMSE ~7 µg/m³). This might be attributed to the under-representation of localised emission sources such as residential wood burning and fine dust particles, which are prevalent in Mediterranean coastal areas.

Overall, LOTOS-EUROS underestimates both the fine (2.5 µm) and especially the coarse (10 µm) PM concentrations. This underestimation is more prominent during

summer and early fall seasons (Appendix, section B1 Figure 12), partially due to lacking secondary organic matter processes in this model version, as the Volatility Basis Set (VBS) framework was not used in these runs. Nevertheless, the increased spatial resolution of the simulations has a considerable effect on the performance of the model, providing more localised details on various emission sources and better adjusting to topography complexities, since all simulations use identical emission and time profiles. A comprehensive validation analysis for the European domain, the nested domains, and the selected city/port areas is presented in the Appendix (section B1).

Figure 16 *Scatter plot of the daily averaged EEA ground-based measurements and the LOTOS-EUROS modelled surface concentrations for NO_2 (top) and $PM_{2.5}$ (bottom) across all stations for the EU (grey circles), the BENELUX (red squares), the Mediterranean/France (purple triangles) and the Mediterranean/Greece (green diamonds) domains*

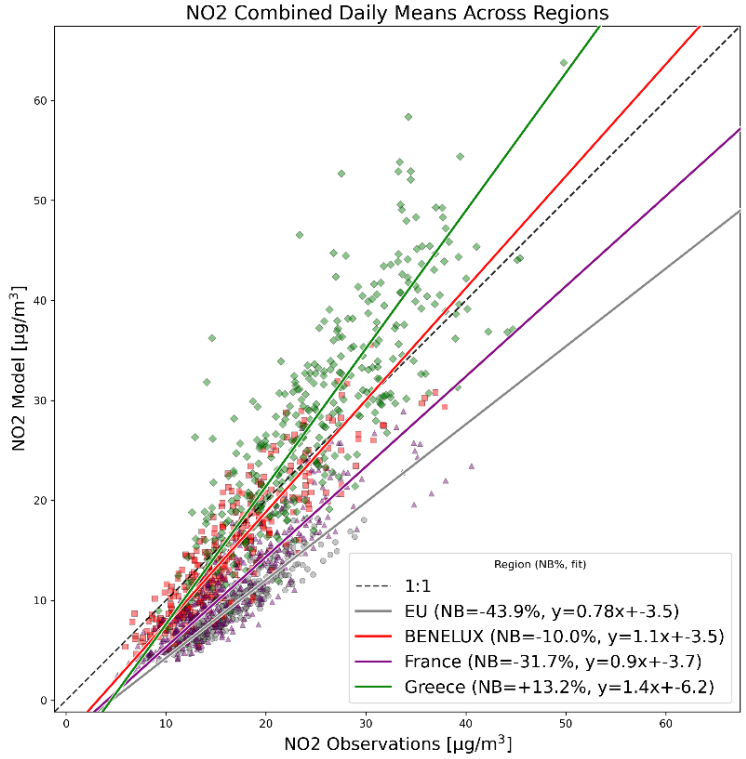

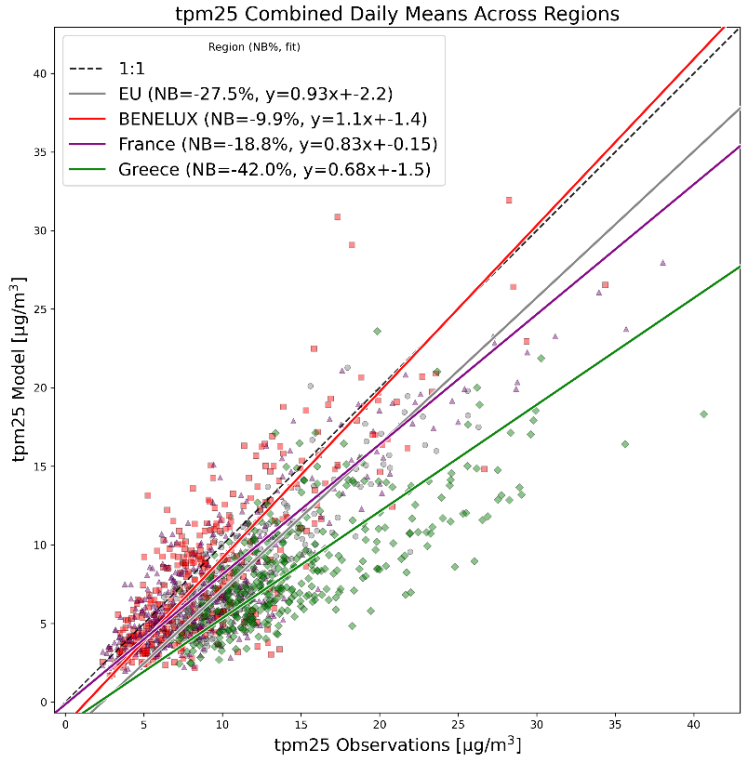

3.2.1.1. Antwerp port and city validation

Figure 17 presents the monthly time series of observed and modelled NO_2 concentrations at the port area (BELAL01 station, left) and the city centre (BETR817 station, right). The monthly time series in the city centre station BETR817 confirms the seasonal variation on non-shipping activities. The model captures most seasonal variability well, except for an underestimation of $PM_{2.5}$ concentrations from May to July, as stated in the validation section and detailed in the Appendix (section B1 Figure 20 and Figure 22). Both the model and observations agree that February sees the highest NO_2 (and $PM_{2.5}$) concentrations, during which shipping plays a secondary role since road traffic is the main contributor. Whereas, during summer, a higher relative contribution of shipping was due to lower activities in road traffic and stationary combustion, as residential heating demand naturally declines.

At the port observation station BELAL01, the model overestimated NO_2 and performed similarly with $PM_{2.5}$. The model suggested a much higher contribution of shipping in NO_2 in the port area, but observations of total NO_2 suggested that shipping and also other sectors are overestimated.

Figure 17 *Monthly NO_2 source apportionment results in Antwerp at the observation sites of BELAL01 (port) [left] and BETR817 (city centre) [right]*

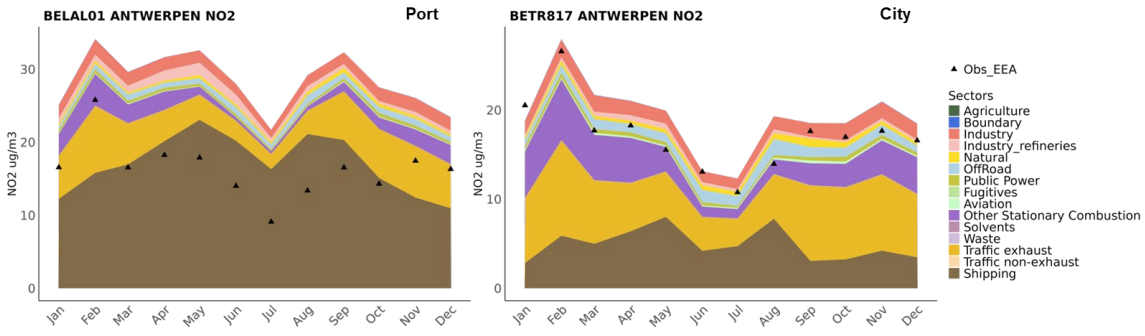

The colours are the 2023 base case results for all sectors that add up to the total surface concentration. The triangle points are the monthly averaged EEA observation data.

3.2.1.2. Rotterdam port and city validation

Figure 18 presents the monthly time series of observed and modelled NO_2 concentrations at the port area (NL00496 station, left) and the city centre (NL00494 station, right). The modelled NO_2 tends to be overestimated in the city while PM is underestimated, especially during winter and summer (Appendix, section B1 Figure 24 and Figure 26). The model matches better in the port station than in the urban station. As expected, shipping contributes more to NO_2 in the port area, while in the urban area, road traffic starts to play a larger role. The highest NO_2 pollution is expected in February and September. However, the sea shipping contribution starts to rise early in July.

This seasonal pattern of shipping from source apportionment results differs between Rotterdam (one peak in September) and Antwerp, where shipping peaks in both May and August. Since the measurement stations suggested that June and July are 'clean' in terms of NO_2, it is highly likely that shipping emissions in summer have been overestimated, as the model is mainly driven by a high shipping contribution. In addition, the port station has a higher shipping contribution of NO_2 than $PM_{2.5}$ (Appendix, section B2 Figure 47). For PM, the differences are small between the port and the city.

Figure 18 *Monthly NO_2 source apportionment results in Rotterdam at the observation sites of NL00496 (port) [left] and NL00494 (city centre) [right]*

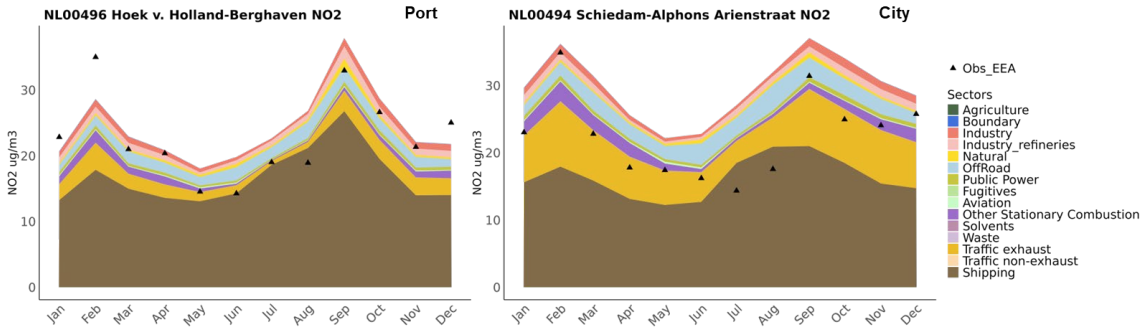

The colours are the 2023 base case results for all sectors that add up to the surface concentration. The triangle points are the monthly averaged EEA observation data.

3.2.1.3. Athens port and city validation

Figure 19 presents the monthly time series of observed and modelled NO_2 concentrations at the port area (GR0030A station, left) and the city centre (GR0003A station, right). In the port of Athens, the model slightly underestimates the ground-based measurements but captures well the seasonal variability. Shipping is the main contributor in the port, peaking in July (~30 µg/m^3 and a relative contribution higher than 50%), when shipping activities are enhanced due to increased passenger vessels traffic. Concentrations are lower during the winter months when road traffic contribution rises.

In the city centre of Athens, road traffic is the dominant contributor, accounting for more than half of the total NO_2 concentrations. Shipping NO_2 levels demonstrate a major drop compared to the port. Shipping shows a seasonal variability, with higher concentrations during the cold periods of the year and lower in warm periods, due to stronger photolysis in summer. The model performs reasonably well in the city centre site, with slight overestimation of the measured concentrations.

Figure 19 *Monthly NO_2 source apportionment results in Athens at the observation sites of GR0030A (port) [left] and GR003A (city centre) [right]*

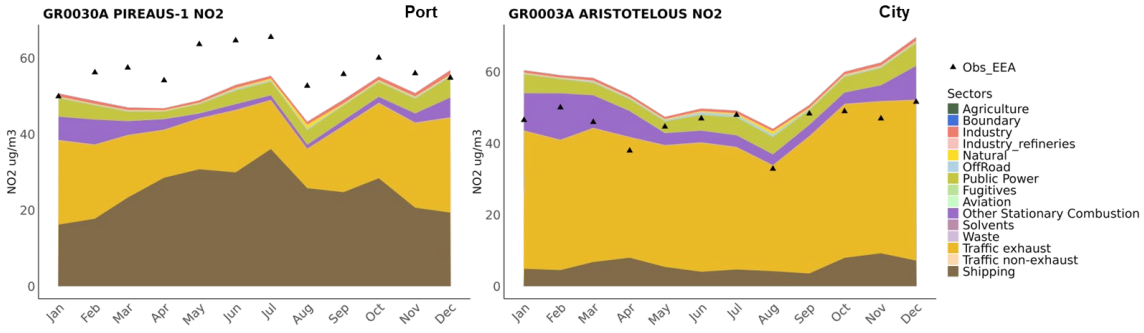

The colours are the 2023 base case results for all sectors that add up to the surface concentration. The triangle points are the monthly averaged EEA observation data.

3.2.1.4. Marseille port and city validation

Figure 20 presents the monthly time series of observed and modelled NO_2 concentrations at the port of Marseille (FR03043 station, left) near the city centre and Port-de-Bouc (FR02008 station, right). It can be observed that the model follows the variability of the measurements but slightly underestimates the observations. Road traffic exhaust emissions contribute the most to NO_2 concentrations followed by shipping emissions. NO_2 concentrations attributed to sea shipping peak in the summer and fall in the winter, showing the same variability with the relative contribution.

In the Port-de-Bouc site, NO_2 concentrations mainly stem from industrial activities, while shipping is the second strongest contributor. The concentrations here display a similar variability as in the port of Marseille, peaking in summer and dropping in winter.

Figure 20 *Monthly NO_2 source apportionment results in Marseille at the observation sites of FR03043 (Port of Marseille-Fos) [left] and FR02008 (Port-De-Bouc) [right]*

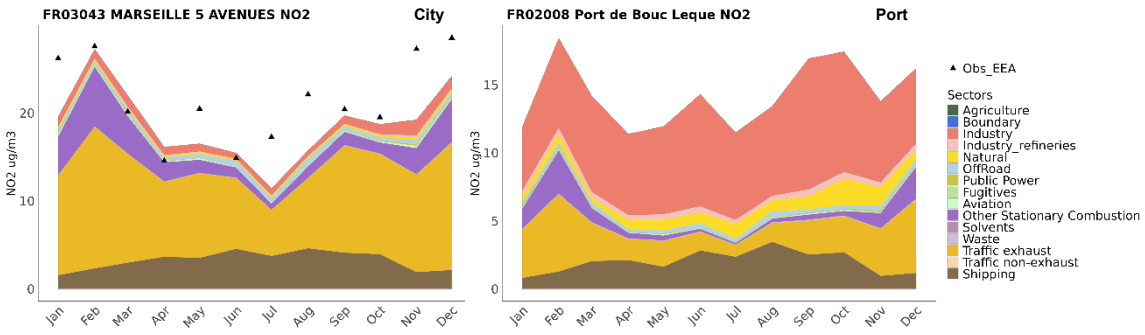

The colours are the 2023 base case results for all sectors that add up to the surface concentration. The triangle points are the monthly averaged EEA observation data. Note that there are no observations for Port-De-Bouc [right].

3.3. AIR POLLUTANT CONCENTRATIONS OVER EUROPE

This section provides an overview of the modelled air pollutant concentrations across Europe (section 3.3.1) and the contribution of sea shipping emissions to air quality in Europe (section 3.3.2), along with comparison between the assessment scenarios.

Key highlights
• Air pollutant concentrations are projected to decrease across the full European domain by 2030, with average reductions of ~22% (1.8 µg/m^3) for NO_2, ~14% (1.3 µg/m^3) for $PM_{2.5}$ and ~14% (0.4 µg/m^3) for SO_2 relative to 2023. • The 2030 assessment scenarios show strong reductions in shipping-related pollution, especially along major European shipping lanes and coastal cities. Despite this, the relative shipping share across the European domain increases by ~5% for NO_2 compared to 2023, as land-based emissions decline more rapidly. • Shipping is a small contributor (~5%) to both $PM_{2.5}$ and SO_2 in 2023 across the full domain, falling to around 2% in 2030 as stronger regulations take effect. • Along the EU waterways, the 2030 LNG scenario results in a larger reduction for NO_2 with 23% (0.51 µg/m^3), compared to 17% under the all-EU ECA scenario, whereas the latter is more efficient in reducing SO_2 concentrations with reductions of up 60% (0.11 µg/m^3). For $PM_{2.5}$, both scenarios result in a similar reduction of ~ 32% (~ 0.11 µg/m^3). • NO_2 concentrations attributed to shipping are predicted to decrease in the 2030 BAU scenario by ~25% over the North Sea and Baltic Sea, and by ~18% along the Mediterranean coasts compared to 2023. • Differences between the 2030 scenarios are modest overall, but the LNG scenario generally lowers concentrations, while the all-EU ECA scenario results in additional NO_2 and $PM_{2.5}$ improvements along the Atlantic and the English Channel-Gibraltar corridors.

3.3.1. Total modelled concentrations across Europe

Figure 21 presents the total modelled concentrations of NO_2, SO_2 and $PM_{2.5}$ for the 2023 base case scenario and the absolute differences against the 2030 BAU scenario. NO_2 concentrations are, overall, higher over metropolitan cities (e.g., Madrid, Paris, Milan, Athens, Istanbul) and are located close to the source since NO_2 is short-lived in the lower troposphere. The main sources of NOx emissions are road transport and shipping, accounting for approximately 50% over the whole European domain (Appendix, section A2 Table 10).

SO_2 concentrations are more prominent in eastern Europe originating mostly from industrial activities (smelters) and fossil fuel combustion (coal-fired power plants). $PM_{2.5}$ concentrations are higher over central and eastern Europe, with significant hotspots over the Po Valley (Italy) and the Balkans.

$PM_{2.5}$ sources vary based on the location and the season of the year. Most prominent anthropogenic sources are residential heating and industrial activities (~30%) (Appendix, section B2 Figure 39). Naturally formed particles also show a strong contribution over the European domain (~25%).

Concentrations of pollutants are overall lower in the 2030 BAU scenario over continental Europe. On an average across the whole European domain, the estimated reductions compared to the 2023 base case are ~22% (1.8 µg/m^3) for NO_2, ~14% (0.4 µg/m^3) for SO_2 and ~14% (1.3 µg/m^3) for $PM_{2.5}$, with larger reductions observed over areas with higher concentrations.

Figure 21 *Predicted annual average total surface concentrations of NO_2 (top), SO_2 (middle) and $PM_{2.5}$ (bottom) across the parent European domain for the 2023 base case scenario (left) and absolute concentration differences between the 2030 BAU and 2023 base case scenarios (right)*

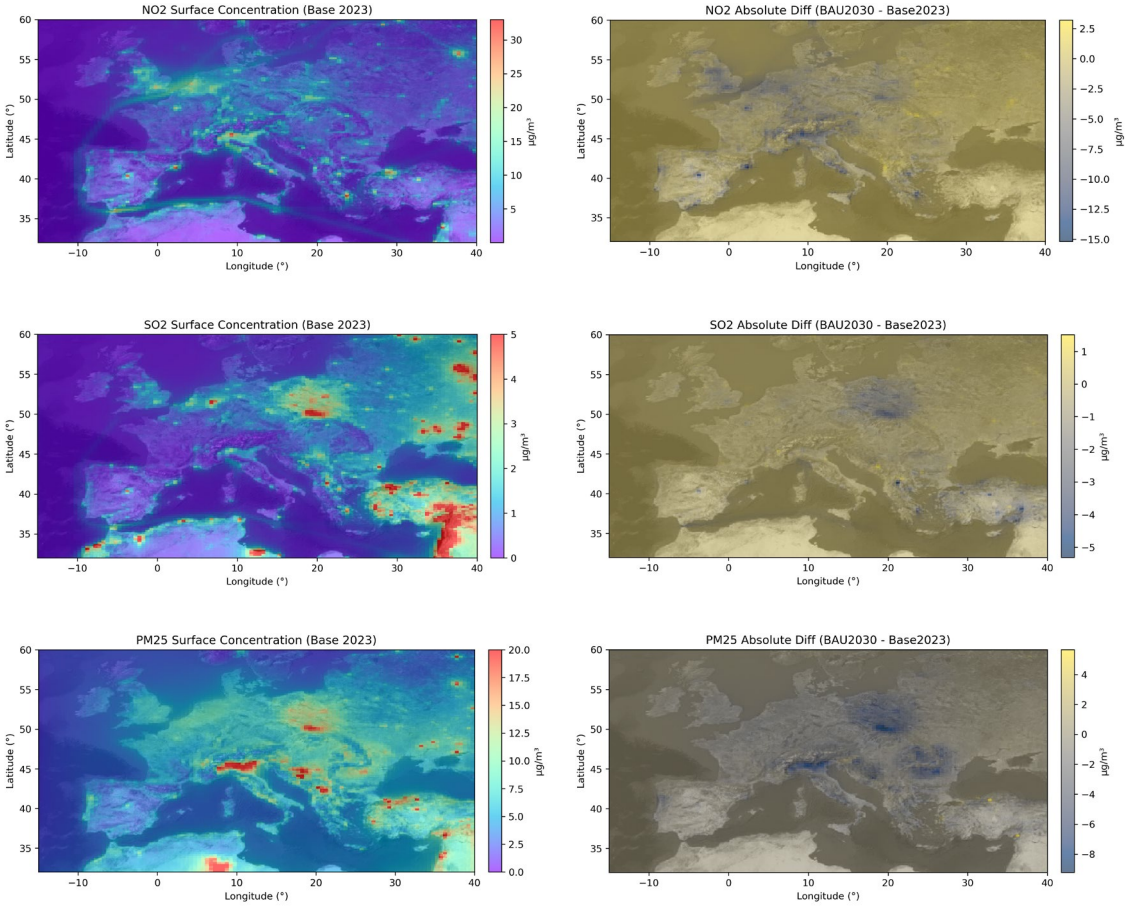

Figure 22 shows the relative share of the aggregated sectors on NO_2 concentrations across the parent European domain. For all scenarios, road traffic exhaust and sea shipping emissions are the largest contributors, accounting for around 50% of NO_2 concentrations in Europe. The share of the traffic sector drops in all 2030 scenarios (from ~28% in 2023 to ~23%), whereas the shipping share shows a slight increase of ~5% in all future scenarios. Despite the reduction of NO_2 absolute levels originating from shipping activities, the slight increase in the relative share is mainly attributed to the reduced contribution of other sectors (e.g., traffic exhaust and stationary combustion). Regarding $PM_{2.5}$ and SO_2, shipping is a small contributor (~5%) in the base case scenario and reduces further (to ~2%) in the future scenarios (further details are presented in the Appendix, section B2 Figure 39 and Figure 40).

Figure 22 *Annual relative contribution of the aggregated sectors on NO_2 concentrations over Europe for the 2023 base case and 2030 future scenarios*

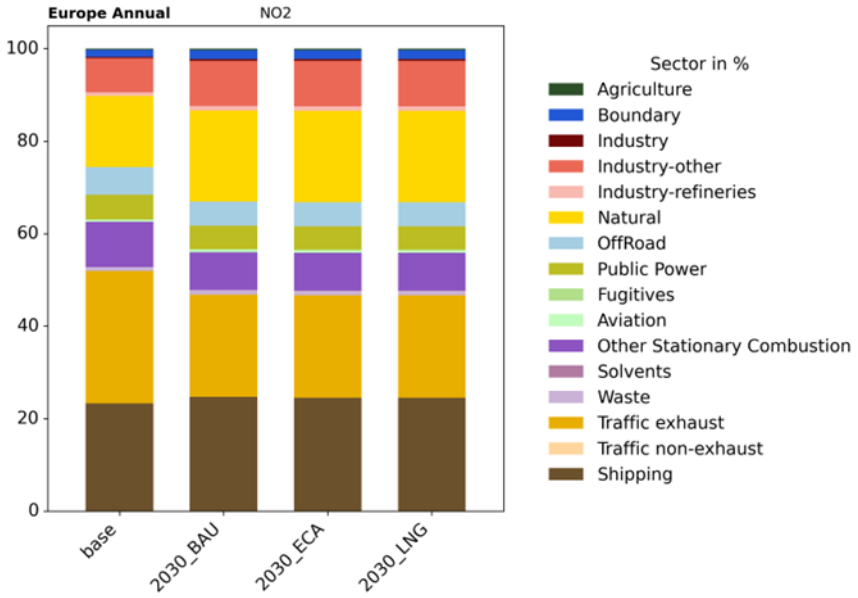

3.3.2. Contribution of shipping emissions to air quality in Europe

Figure 23 shows the predicted annual average surface concentrations originating from the shipping sector for the 2023 base case scenario and the absolute differences between the 2023 base case and 2030 BAU scenarios across the European domain. Similar comparisons between the 2023 base case and the 2030 all-EU ECA and 2030 LNG scenarios are presented in the Appendix (section B2 Figure 36 to Figure 38).

NO_2 shipping concentrations are expected to decrease under the 2030 BAU scenario by approximately 3 µg/m^3 (~25%) over the shipping lanes in the North Sea and the Baltic Sea, and by approximately 2 µg/m^3 (~18%) in the Gibraltar Strait and the European coasts of the Mediterranean Sea, staying in line with the emission trends. This can be attributed mainly to the enforcement of the NECA regulations and the increase in the energy efficiency of ships.

Modelled SO_2 shipping concentrations are also projected to decrease by up to 1.5 µg/m^3 under the 2030 BAU scenario over prominent shipping lanes and coastal port areas (Marseille, Genoa, Athens) in the Mediterranean Sea after its designation as an ECA in early 2025.

$PM_{2.5}$ concentrations are expected to drop by approximately 0.5 µg/m^3 in the 2030 BAU scenario compared to the 2023 base case scenario in the Mediterranean waterways, mainly since its designation as a SECA will lead to limited formation of sulphate aerosols. $PM_{2.5}$ shipping concentrations are estimated to decrease by approximately 0.2 µg/m^3 over the North Sea indicating that NECA regulations might also have an impact in reducing NOx emissions and subsequently negatively affecting the formation of secondary PM (nitrate particles). These estimates reflect the discrepancies on annual levels. The magnitude of the reductions may also differ largely depending on the season of the year.

Overall, the existing and foreseen regulations in the 2030 BAU scenario will lead to reductions of pollutant concentrations originating from shipping activities with a stronger impact in the Mediterranean Sea.

Figure 23 *Predicted annual average shipping surface concentrations of NO_2 (top), SO_2 (middle) and $PM_{2.5}$ (bottom) across the parent European domain for the 2023 base case (left) and absolute concentration differences between the 2030 BAU and the 2023 base case scenarios (right)*

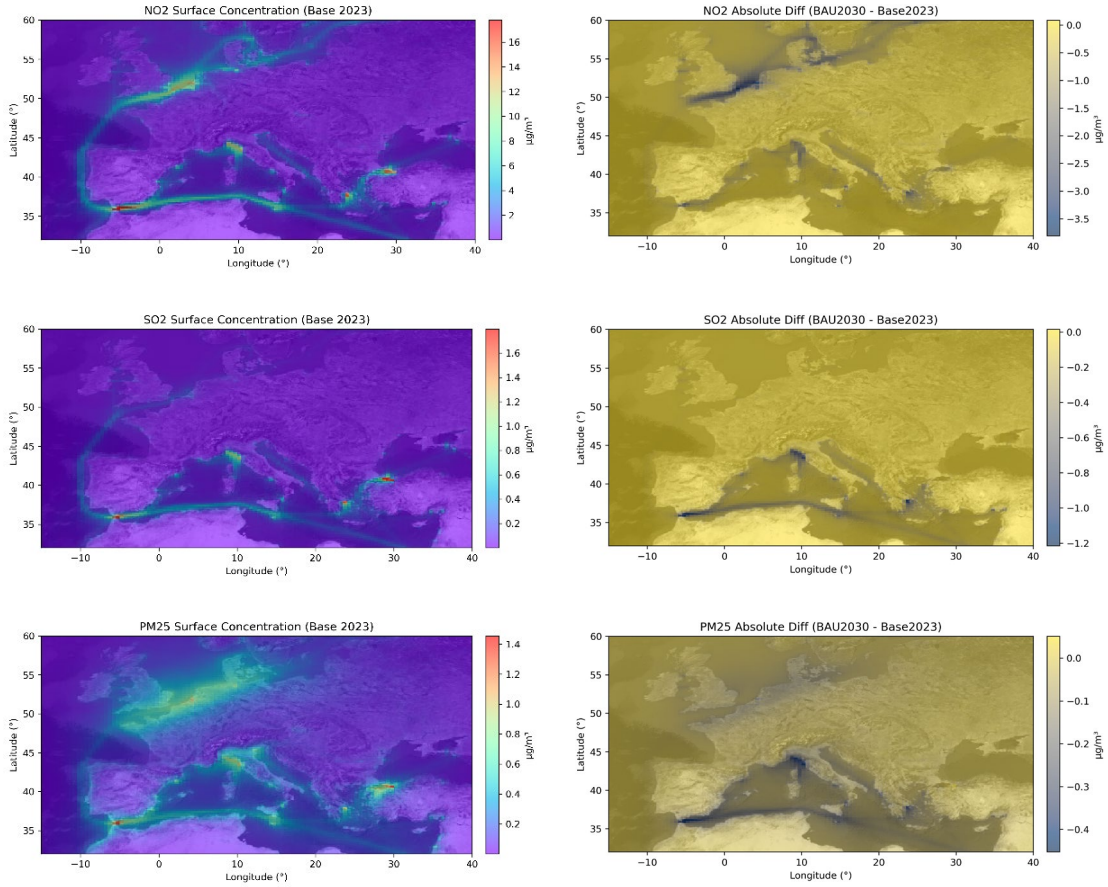

Figure 24 presents the differences between the three future scenarios for the NO_2 and $PM_{2.5}$ surface concentrations resulting from the shipping activity in the EU waterways. Firstly, as expected, both NO_2 and $PM_{2.5}$ concentrations are lower in the 2030 all-EU ECA scenario along the Atlantic European coastlines (top row) which are not included in the 2030 BAU scenario. Secondly, the 2030 LNG scenario shows lower concentrations for both NO_2 and $PM_{2.5}$ (by an average of 1.1 µg/m^3 for NO_2 and 0.06 µg/m^3 for $PM_{2.5}$) over the main shipping lanes and coastal areas compared to the 2030 BAU scenario (middle row), indicating that the increased LNG energy share will slightly improve air quality in coastal areas.

Differences in terms of absolute concentrations are higher for NO_2 (~1.5 µg/m^3) and lower for $PM_{2.5}$ (~0.05 µg/m^3), similar to the Mediterranean waterways between the 2030 LNG and the 2030 all-EU ECA scenario (bottom row). However, the 2030 LNG scenario shows slightly higher shipping concentrations (~0.1 µg/m^3) for both NO_2 and $PM_{2.5}$ over the English Channel – Gibraltar shipping lane, an area designated as an ECA in the 2030 all-EU ECA scenario but not in the 2030 LNG scenario. Nevertheless, the impact remains negligible.

Figure 24 *Predicted differences in NO_2 (left) and $PM_{2.5}$ (right) annual average surface concentrations originating from the shipping sector between the 2030 all-EU ECA and 2030 BAU scenarios (top), the 2030 LNG and 2030 BAU scenarios (middle) and the 2030 LNG and 2030 all-EU ECA scenarios (bottom)*

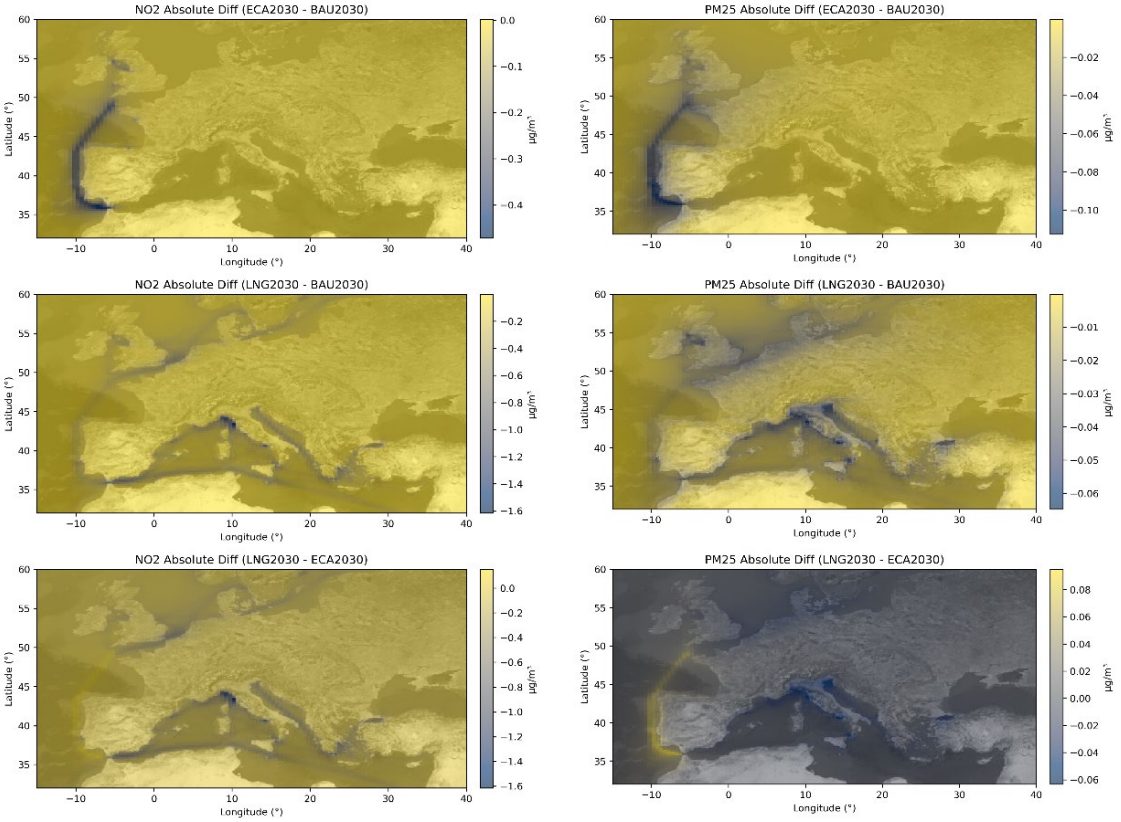

Table 3 shows the absolute and relative differences of the annual mean surface concentrations attributed to the shipping sector for NO_2, $PM_{2.5}$ and SO_2 between the 2023 base case and the 2030 assessment scenarios over the whole European domain and the EU waterways. Regarding NO_2 surface concentrations attributed to shipping activities, all 2030 scenarios are predicted to have similar impact resulting in reductions in European waterways that range between ~0.4 µg/m^3 (16-17%) in the 2030 BAU and 2030 all-EU ECA scenarios and ~0.5 µg/m^3 (23%) in the 2030 LNG scenario.

SO_2 and $PM_{2.5}$ concentrations show similar reductions across all future scenarios, with the reductions under the 2030 all-EU ECA scenario being slightly higher. The 2030 all-EU ECA scenario projects the highest reduction of 0.11 µg/m^3 (60%) in SO_2 concentrations over EU waterways, slightly above the 2030 BAU and 2030 LNG scenarios, which show reductions of 41% and 45% respectively. Finally, $PM_{2.5}$ concentrations are also projected to decrease comparably across scenarios, by 32% in the 2030 LNG and 2030 all-EU ECA scenarios (~0.1 µg/m^3) and by 27% (0.09 µg/m^3) in the 2030 BAU scenario compared to the 2023 base case.

Table 3 *Annual average absolute and relative differences between the 2030 scenarios and the 2023 base case for NO_2, SO_2 and $PM_{2.5}$ across the whole EU domain and the EU waterways*

Pollutant and scenario	Full domain		Waterways	
NO_2	Absolute difference ($\mu g/m^3$)	Relative difference	Absolute difference ($\mu g/m^3$)	Relative difference
2030 BAU	-1.77	-22 %	-0.37	-16 %
2030 LNG	-1.85	-23 %	-0.51	-23 %
2030 all-EU ECA	-1.78	-23 %	-0.39	-17 %
SO_2	Absolute difference ($\mu g/m^3$)	Relative difference	Absolute difference ($\mu g/m^3$)	Relative difference
2030 BAU	-0.35	-13 %	-0.08	-41 %
2030 LNG	-0.35	-14 %	-0.09	-45 %
2030 all-EU ECA	-0.35	-14 %	-0.11	-60 %
$PM_{2.5}$	Absolute difference ($\mu g/m^3$)	Relative difference	Absolute difference ($\mu g/m^3$)	Relative difference
2030 BAU	-1.34	-14 %	-0.09	-27 %
2030 LNG	-1.36	-14 %	-0.11	-32 %
2030 all-EU ECA	-1.35	-14 %	-0.10	-32 %

3.4. CONTRIBUTION OF SHIPPING EMISSIONS ON AIR QUALITY FOR EACH SEA PORT AREA

This section presents the results for each seaport area (port and nearest city). An overview of the results is first presented for NO_2 and $PM_{2.5}$ concentrations. The detailed results for NO_2 concentrations for each location are presented subsequently, while the detailed results for $PM_{2.5}$ and SO_2 concentrations are presented in the Appendix (sections B2 and B3).

3.4.1. Overview of all port cities

Key highlights
• Reductions in NO_2 concentrations are predicted at all four port cities by 2030, however annual average concentrations in Athens remain above the upcoming EU 20 µg/m³ limit. • Mediterranean cities (Athens, Marseille) and BENELUX cities (Antwerp, Rotterdam) show distinct source patterns: traffic dominates in the Mediterranean cities, while shipping is the largest NO_2 source in the BENELUX cities, contributing about 50% of urban NO_2 across all scenarios. • Shipping's relative share increases in all cities by 2030, despite of decreasing absolute concentrations, because other sectors fall faster; e.g., shipping's NO_2 share rises by 8% in Athens and by 6% in Marseille. Even though NO_2 shipping share increases by less than 5% in the BENELUX cities, shipping remains a dominant source contributing around 50% to total concentrations. • Reductions in $PM_{2.5}$ concentrations are predicted at all four port cities by 2030, driven mainly by declines in non-shipping anthropogenic emissions. • Shipping plays a relatively small role in $PM_{2.5}$ compared to NO_2, contributing ~13% (Rotterdam), 10% (Antwerp), and ~4% (Athens/Marseille) in 2023, with its share decreasing slightly (by up to 1.5%) across all cities in 2030 as industrial and stationary combustion sources become more prominent.

3.4.1.1. NO_2 concentrations

By 2030, all projected scenarios for annual average NO_2 surface concentrations in Antwerp, Rotterdam, Athens and Marseille indicate notable improvements in urban air quality. Figure 25 shows the predicted NO_2 concentrations for each area broken down by each source sector for the four assessment scenarios (2023 base case and 2030 BAU, 2030 LNG and 2030 all-EU ECA).

In the 2030 BAU scenario, the road traffic contribution to NO_2 levels is anticipated to reduce by more than half, with other non-shipping sectors also show reductions. While NO_2 concentrations in all four port cities currently remain within the current annual NO_2 regulatory limit of 40 µg/m³, the projections suggest that, by 2030, NO_2 concentrations on average over Athens will exceed the more stringent limit of 20 µg/m³ set under the revised ambient air quality directive (AAQD) (EU Directive 2024/2881).

The four port cities evaluated can be grouped to Mediterranean cities (Athens and Marseille), and BENELUX cities (Antwerp and Rotterdam), as each group shows similar source apportionment results. For all cities evaluated, predicted future NO_2 concentrations are similar across the scenarios assessed, with the 2030 LNG scenario showing marginally lower levels than the others.

In Athens and Marseille, road traffic exhaust is the dominant contributor to NO_2 levels in all scenarios, though its share decreases considerably (by 8% and 15% respectively) from 2023 to 2030 BAU. Stationary combustion and shipping play secondary roles, with the contribution of shipping being more pronounced in the 2030 scenarios (compared to the 2023 base case), as its relative share increases by 8% in Athens and by 6% in Marseille. In addition, Athens is the only city that has a significant contribution (10%) from power generation in 2023 which is projected to be completely phased out in 2030 (~1%).

In Rotterdam and Antwerp, the sectoral apportionment shifts noticeably. Here, shipping is the largest source of NO_2 contributing to approximately half of the total city centre concentration across all scenarios. Industrial emissions also play a significant role, especially in Antwerp. The road traffic share is predicted to reduce by 6% in Rotterdam and by 10% in Antwerp from 2023 to 2030, while the share of industrial NO_2 concentrations is projected to increase by 3% in Rotterdam and by 8% in Antwerp from 2023 to 2030.

Unlike the emissions, where the shipping contribution decreases in Antwerp and Rotterdam in the 2030 future scenarios, the shipping contribution to surface NO_2 concentrations in the urban areas increase. This is because there is a non-linear relationship between relative emission reduction and its actual contribution to air quality. On the other hand, the modelled results agree with the emission results on the 2030 LNG scenario resulting in the lowest contribution to the NOx species.

Figure 25 *Annual averaged source/sector apportionment of NO_2 surface concentrations in µg/m^3 for all assessment scenarios in Athens (Athina), Marseille, Antwerp (Antwerpen) and Rotterdam*

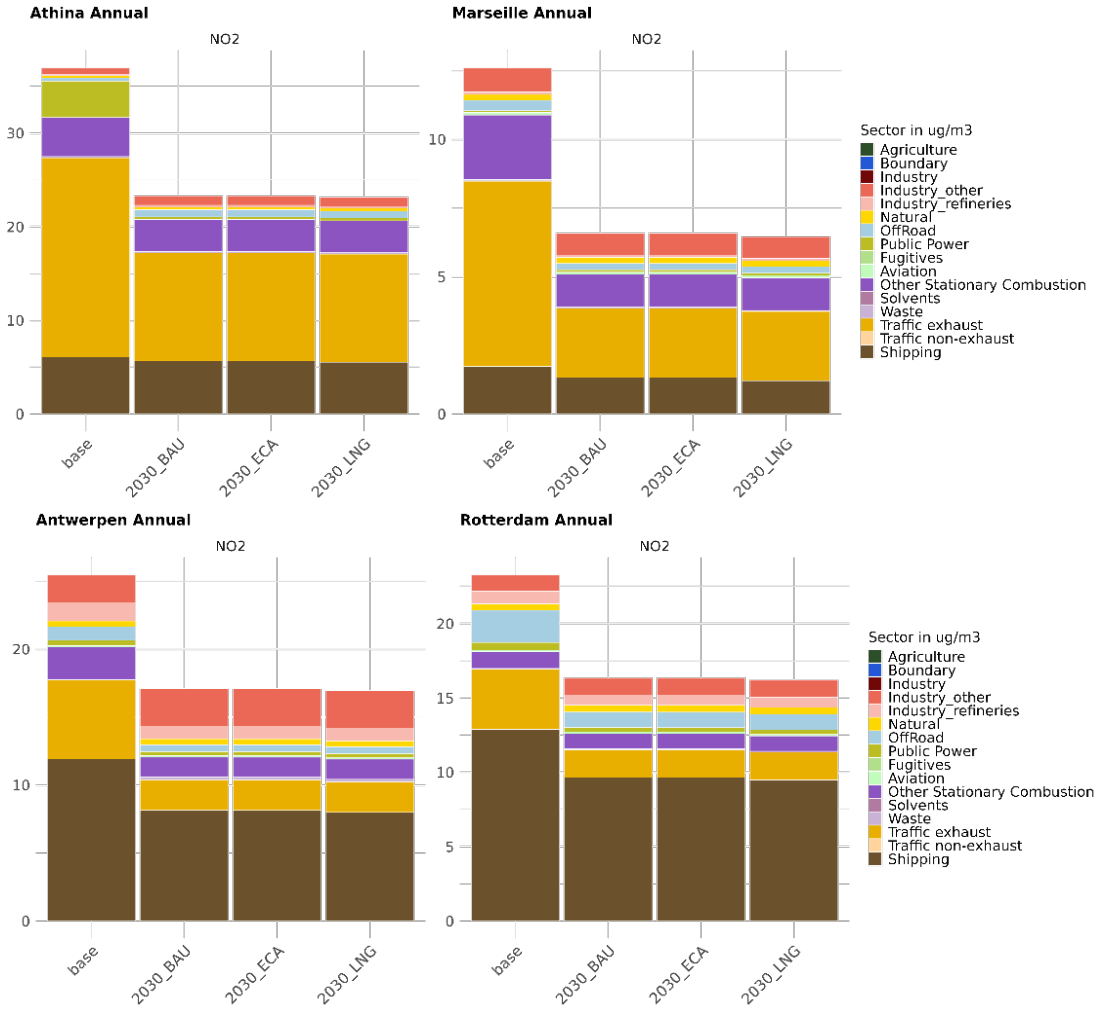

3.4.1.2. $PM_{2.5}$ concentrations

By 2030, all projected scenarios for annual average $PM_{2.5}$ surface concentrations in Athens, Marseille, Rotterdam, and Antwerp indicate notable improvements in urban air quality. Figure 26 shows the predicted $PM_{2.5}$ concentrations for each area broken down by each source sector for the four assessment scenarios (2023 base case, 2030 BAU, 2030 LNG and 2030 all-EU ECA).

The predicted improvement in $PM_{2.5}$ concentrations in 2030 is driven largely by reductions in emissions from both shipping and non-shipping sectors. Aerosols presented in cities have a wider range of sources. Firstly, we assume that natural sources stay the same since there are unlikely to be drastic changes in this short

time scale with sea salt and dust emissions due to their dependency in meteorology and climate. However, with reductions in anthropogenic sources, natural sources play an increasingly important role in urban air quality and potential exceedances. Secondly, road traffic which was one of the dominant contributors to NO_2 in Athens and Marseille, is also a considerable source of $PM_{2.5}$ in these cities. However, residential/stationary combustion, industry and shipping each also maintain a significant share.

In Rotterdam and Antwerp, while shipping dominates the NO_2 apportionment accounting for around half of NO_2 concentrations, it contributes 13% and 10% respectively to $PM_{2.5}$ concentrations in the 2023 base case. In Athens and Marseille, shipping contributes less to total $PM_{2.5}$ (~4% for both cities). In 2030, the relative share of sea shipping to total $PM_{2.5}$ concentrations reduces slightly (by up to 1.5%) across all four cities compared to the 2023 base case (Figure 26). Furthermore, contributions from industrial activities become more prominent in BENELUX cities.

The interaction between emitted gases from sectors such as agriculture, industry, and shipping contribute to the formation of fine aerosols. Agricultural activities-induced NH_3 emissions interact with NOx and SOx (from road traffic, shipping, and industry) to drive the formation of SIA (ammonium nitrate and ammonium sulphate aerosols). This process is particularly relevant in port cities like Antwerp and Rotterdam with major agricultural activities in combination with port, industry and road traffic. Therefore, the composition of aerosols in these cities could provide more insights on the source apportionment.

Figure 26 *Annual averaged source/sector apportionment of $PM_{2.5}$ surface concentrations in µg/m³ for all assessment scenarios in Athens (Athina), Marseille, Antwerp (Antwerpen) and Rotterdam*

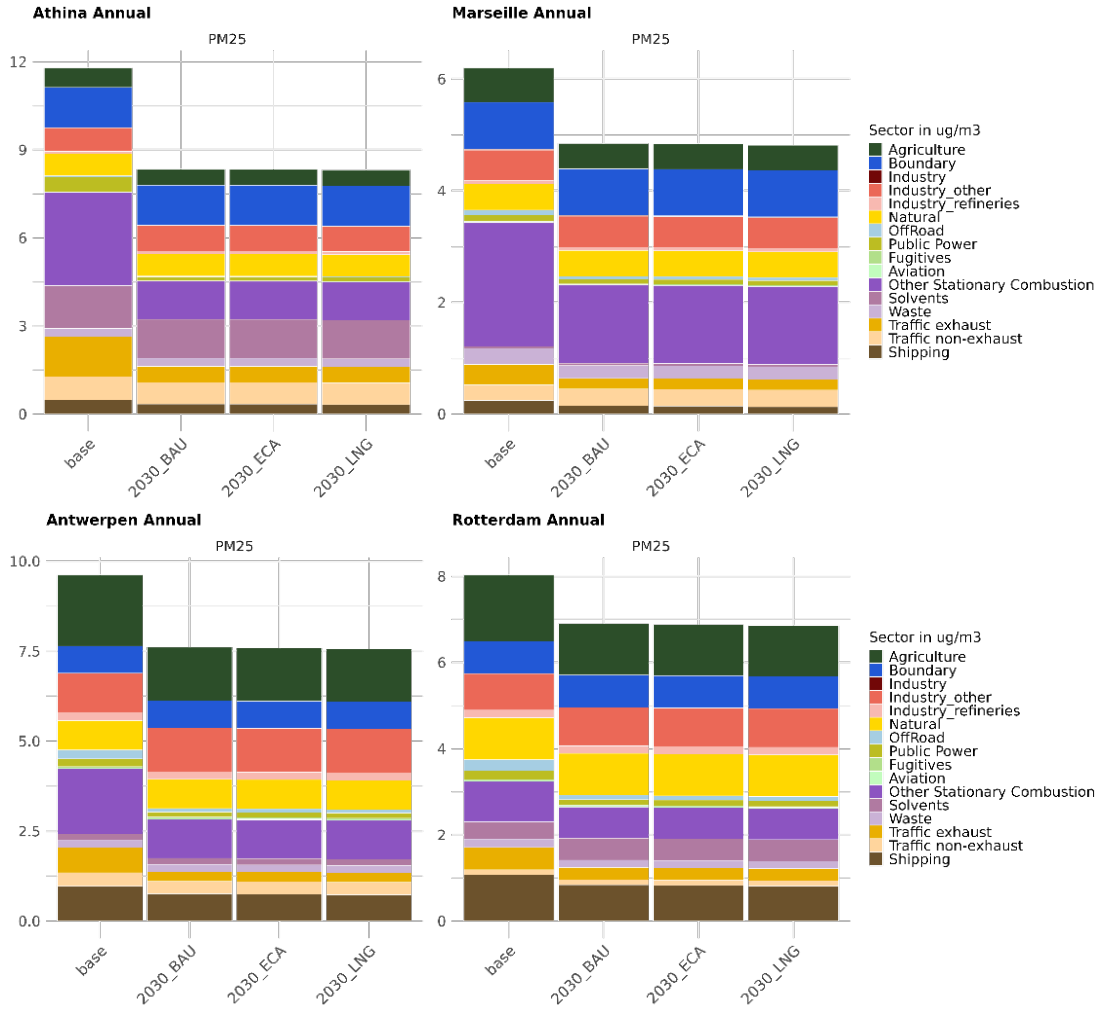

3.4.1.3. PM composition

The PM composition is projected to change from 2023 to 2030 due to various reduction measures in anthropogenic emissions. Due to the small changes in PM composition from shipping, all 2030 shipping scenarios show the same composition of aerosols, therefore only the 2023 base case and 2030 BAU scenarios are shown in the following graphs. Figure 27 presents the PM composition in percentages for the 2023 base case versus the 2030 BAU scenarios for the four seaport urban areas (Athens, Marseille, Antwerp and Rotterdam).

For all four ports and cities evaluated, there are less anthropogenic-related PM species (non-dust and sea salt) in the 2030 composition than in 2023. All cities are projected to have a reduced contribution from nitrate and organic matters and increased influence from Rest of Primary PM (RESTPPM), which includes all other primary PM excluding POM and EC. In this study, the natural PM emissions are identical for both the 2023 and 2030 scenarios due to the fixed meteorological conditions. Dust in the model is treated as inert and sea salt has only limited reaction with SIA, therefore natural PM concentrations stay the same. As a result of

the projected reduction of anthropogenic emissions, the natural PM concentrations will be increasingly important from a composition point of view.

In the Mediterranean cities, Athens and Marseille, contributions from Saharan dust intrusion are significant and will contribute to about 1/5 of PM_{10} composition in 2030 due to the decline of other anthropogenic sources, followed by sea salt. They add to approximately 40% in total PM, accounting for natural emissions. In Athens, all primary species (EC, POM, RESTPPM) account for approximately 45% of the PM_{10} composition in both assessment years, while in Marseille their contribution is slightly lower (approximately 35%). Secondary inorganic aerosols follow, contributing to about 20-30% in both 2023 and 2030.

In the BENELUX port cities, Antwerp and Rotterdam, SIA account for about 40% of all PM in both 2023 and 2030. This suggests that any effort in reduction of PM from both shipping and non-shipping sectors will experience a non-linear effect due to the chemistry from concentrations compared to emissions. Although these cities are far from a desert, they share significantly higher sea salt contribution and therefore the total natural contribution is approximately 45%, which is similar to the Mediterranean cities. Lastly, the primary pollutants here contribute less than SIA and natural sources.

Figure 27 *PM_{10} composition in percentage of 2023 base case versus the composition of the 2030 scenarios in the cities of Athens (Athina), Marseille, Antwerp (Antwerpen) and Rotterdam*

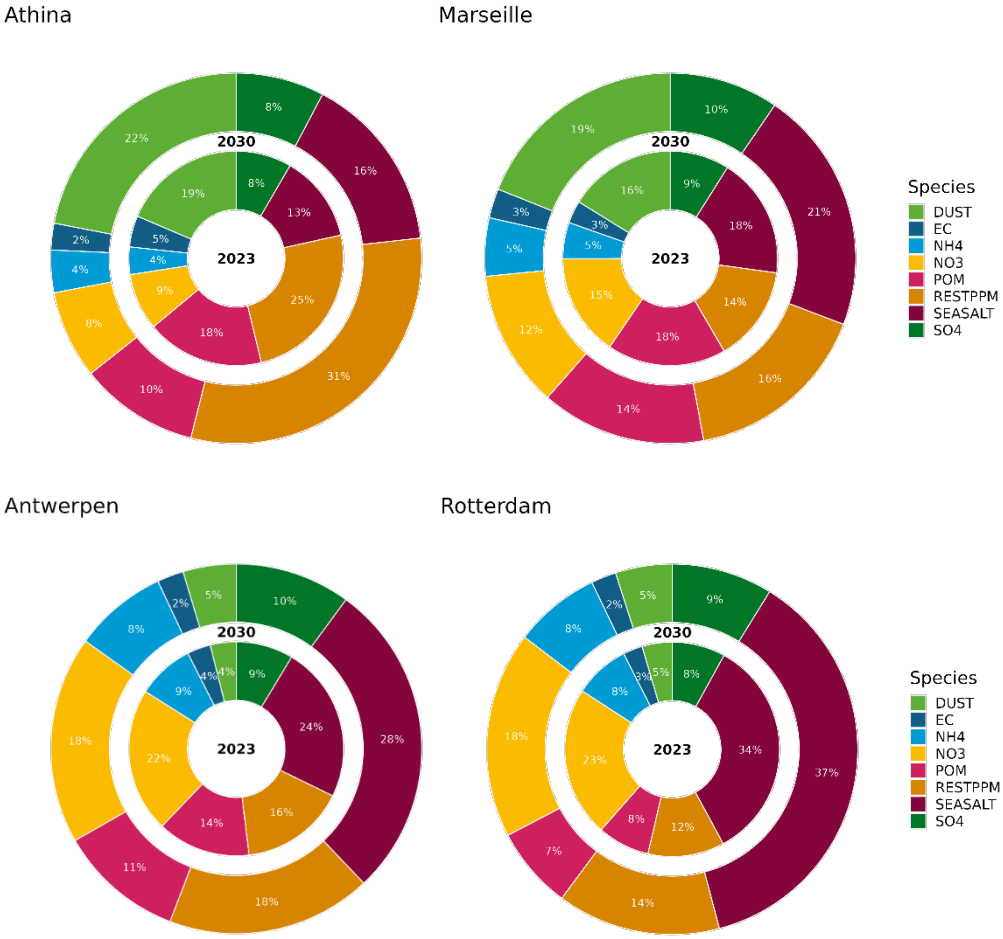

3.4.2. Antwerp

Key highlights
• Shipping remains a major source of NO_2 concentrations in Antwerp, contributing up to 20 µg/m³ (≈80%) in the port in 2023, with reductions of up to 5 µg/m³ under the 2030 BAU scenario. • Differences between the 2030 sensitivity scenarios in Antwerp are small, with shipping remaining a major contributor to urban air quality: ~47–48% of NO_2 and ~10% of $PM_{2.5}$ in the city core across all scenarios, and only minor additional reductions under the LNG scenario. • Seasonal variation in Antwerp remains consistent between 2023 and 2030, with increases in shipping's relative share for NO_2 and $PM_{2.5}$ in the summer. • While no exceedances of the EU NO_2 daily limit (50 µg/m³) are predicted in Antwerp in 2030, when comparing to the WHO guideline (25 µg/m³) exceedances are predicted at both the port and city centre observation stations. The main contributors to these are shipping for NO_2, and industry for $PM_{2.5}$ in 2030.

Figure 28 shows the modelled NO_2 concentrations and the relevant shipping contribution in Antwerp in the 2023 base case simulation, together with the relevant results under the projected 2030 BAU scenario and associated differences. The city core (as defined in section 2.4.4 and marked with a white contour on the maps) is used for evaluating the shipping impact averaged across the city. Relevant observation station locations are used for validation and analysis with observed data, i.e. station BELAL01 in the port area and station BETR817 in the city. Overall, the 2023 base case simulation from LOTOS-EUROS accurately captures the daily concentrations of NO_2 compared to the EEA stations in the city (further details are presented in the Appendix, section B1 Figure 20 to Figure 23).

The highest NO_2 concentration (~30 µg/m^3) is predicted along the Scheldt River and in the urban area, where the shipping contribution is up to around 80% (25 µg/m^3) in the 2023 base case, as seen in Figure 28. In the 2030 BAU scenario, the shipping contribution has reduced to below 15 µg/m^3. The net difference of the NO_2 concentrations attributed to shipping emissions from the 2030 BAU to the 2023 base case scenarios is up to -5 µg/m^3 immediately south of the port, while in the city centre it reaches up to -2 µg/m^3.

Minimal differences were observed within the three 2030 scenarios (Figure 29). In the 2030 LNG scenario, NO_2 concentrations are predicted to be lower compared to the 2030 BAU scenario, but this additional reduction doesn't exceed 0.5 µg/m^3. In the 2030 all-EU ECA scenario, the predicted changes in terms of NO_2 concentrations compared to the 2030 BAU scenario are negligible.

A similar trend was also observed on shipping contributions to $PM_{2.5}$ concentrations between 2030 and 2023, where the maximum shipping contributions to total $PM_{2.5}$ were reduced from approximately 1.0 to 0.8 µg/m^3 (Appendix, section B3 Table 23). Unlike NO_2, $PM_{2.5}$ has a smooth concentration gradient between the shipping lane/city centre to background locations. $PM_{2.5}$, as aggregate aerosols species, on average has a longer lifetime, therefore it is less localised in the city centre. Both the 2030 LNG and 2030 all-EU ECA scenarios show consistent small reduction over the whole area.

Figure 28 *Annual averaged total NO_2 surface concentrations [in µg/m^3] and shipping sector share [in %] within the Antwerp city core area (highlighted in white)*

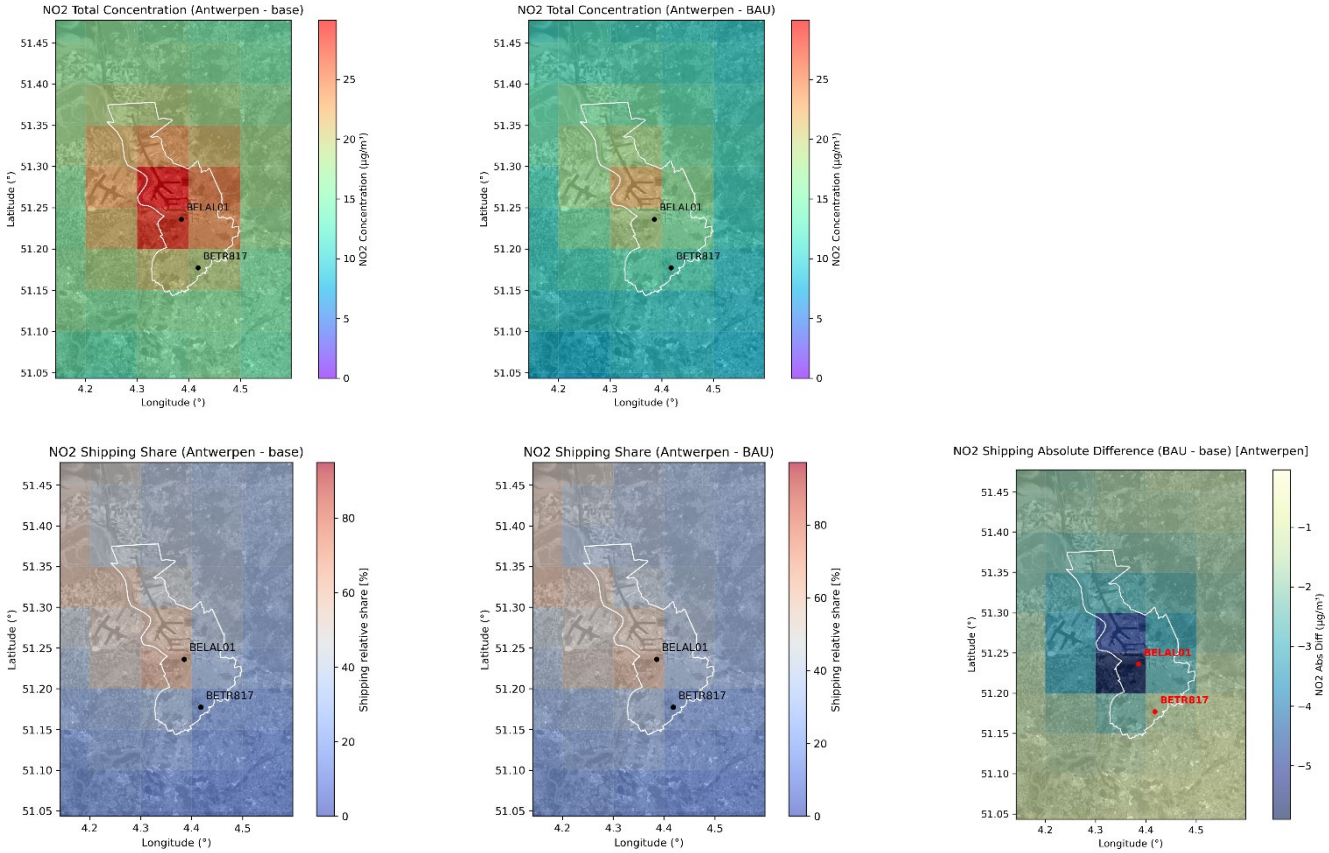

Observation stations are marked as points. The top row shows the total modelled surface concentration in the 2023 base case (left) and 2030 BAU (right) scenarios. The bottom row shows the relative shipping share in the 2023 base case (left), and 2030 BAU (middle) scenarios, and the difference in the NO_2 concentrations attributed to shipping between the 2030 BAU and 2023 base case scenarios.

For the averaged city core of Antwerp, all three 2030 scenarios show limited differences, with the 2030 LNG scenario giving the lowest shipping contribution to NO_2 concentrations (Figure 29). In relative terms for the city core, shipping contributes 47-48% of NO_2 and 10% of $PM_{2.5}$ in the 2030 scenarios.

The relative annual contribution of shipping across the 2030 scenarios and the 2023 base case stays similar in Antwerp for both $PM_{2.5}$ and NO_2 concentrations regardless of scenario selected. Shipping will therefore remain the main contributor to NO_2 concentrations with all scenarios. The monthly relative contribution (Figure 29) shows limited differences in Antwerp city irrespective of the 2030 scenario (the BAU, LNG, and all-EU ECA lines are overlapping in the figure). Seasonal patterns revealed that shipping's share in both NO_2 and $PM_{2.5}$ increases during the summer months despite the relative consistent maritime activities, compared to the 2023 base case. This is due to the reduction of emissions from other sectors that consist of strong seasonality.

Figure 29 *Predicted annual NO_2 surface concentrations attributed to shipping (in $\mu g/m^3$, left) and predicted shipping contribution to monthly NO_2 surface concentrations (right) in Antwerp city*

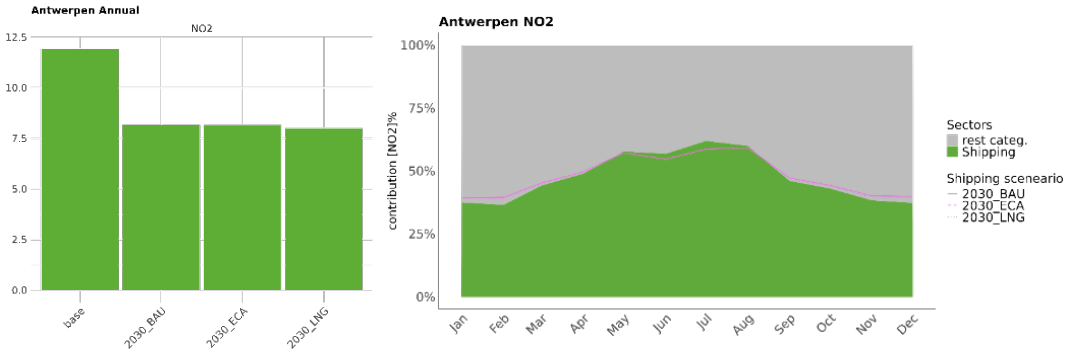

The pink lines are the three different 2030 scenarios of shipping contribution to surface concentration in $\mu g/m^3$.

The annual NO_2 source apportionment results for the two observation sites located in the port (BELAL01) and Antwerp city centre (BETR817) are presented in Figure 30. Similar to the seasonal source apportionment, the port area has significantly higher contribution in both relative and absolute terms from shipping than the city centre. Over 2023 to 2030, the relative share of shipping to total NO_2 concentrations stays at the same level in both port and city.

Figure 30 *Predicted NO_2 annual source apportionment results in Antwerp at observation sites BELAL01 (port) and BETR817 (city centre)*

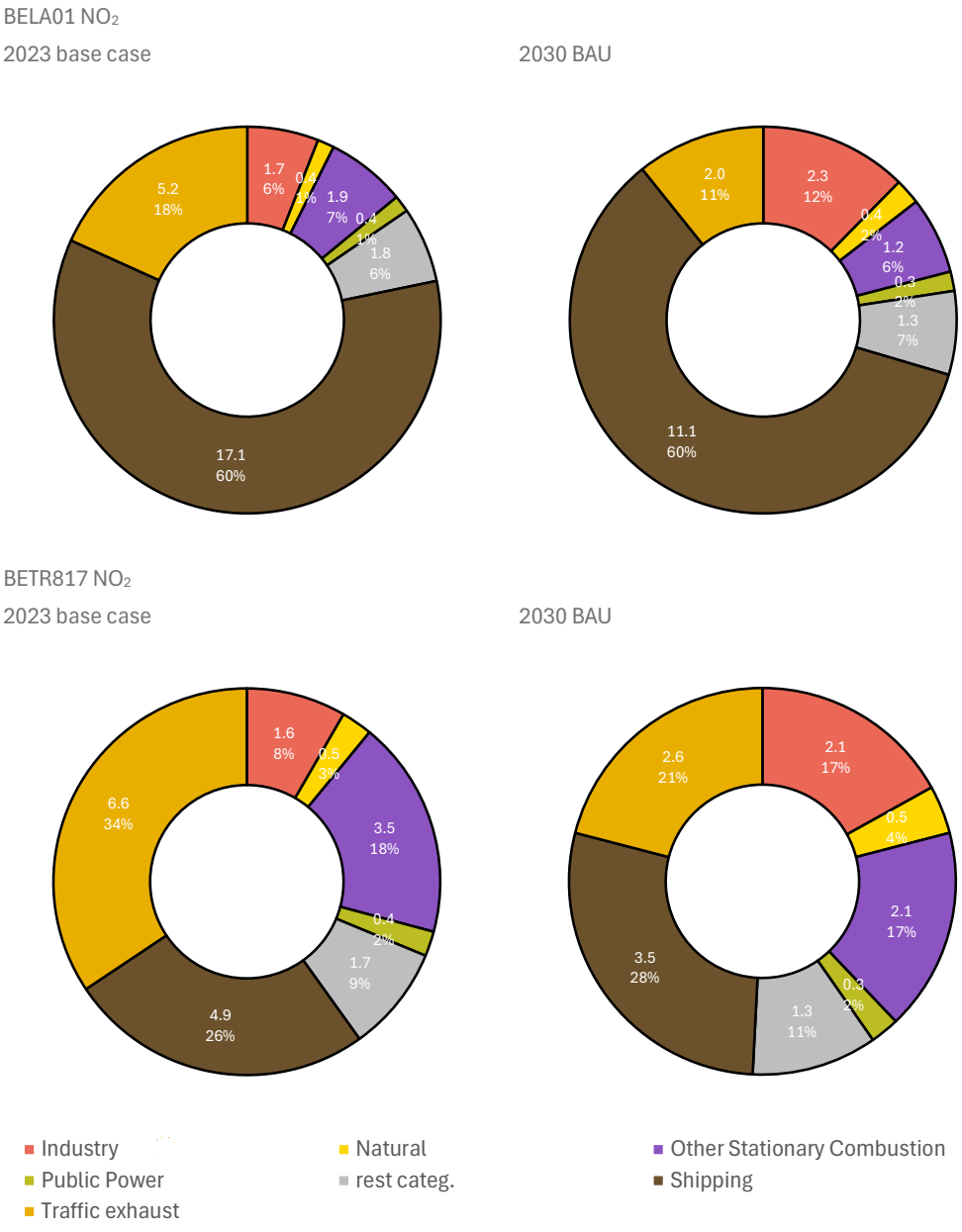

The main contributing sectors are shown here, whereas the remaining sectors are grouped in the "rest categories". The top labels are relative contribution and lower labels are absolute contribution in µg/m^3.

Figure 31 shows the relative contribution of shipping and other sectors to daily surface NO_2 concentrations at the port (BELAL01) and the city centre (BETR817) stations. Due to the overall projected decline of anthropogenic emissions in 2030, no exceedances are anticipated of the current EU daily (24-hour average) limit of 50 µg/m^3. However, when comparing to the WHO guideline of 25 µg/m^3 the port station has almost three months and the city station one month of exceedances in 2030. Shipping still remains a dominant source of NO_2 concentrations in 2030 and therefore still at risk of contributing to an exceedance.

In relation to $PM_{2.5}$ (Appendix, section B2 Figure 44), the exceedance occasion is primarily driven by residential stationary combustion, but in 2030 it is projected to be mostly due to industry. Shipping remains at a similar level across the different concentration levels in $PM_{2.5}$ (as in NO_2). The results from the assessed scenarios indicate a slight reduction of the shipping's contribution. However, the relative differences between these scenarios are limited and do not affect the number of exceedance days for these pollutants.

Figure 31 *Relative contribution to daily surface NO_2 concentrations at 0-25 µg/m³, 25-50 µg/m³, and exceeding 50 µg/m³ (2030 EU NO_2 daily limit) at stations BELAL01 (port) and BETR817 (city)*

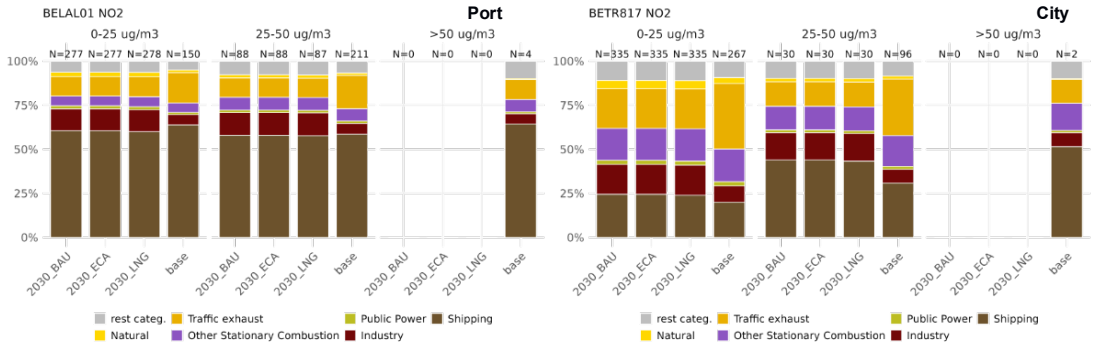

"N" represents the number of days in each scenario within each concentration range.

In summary, despite predicted reduction in absolute concentrations of air pollutants attributed to shipping, the relative influence of shipping remains significant and similar across the assessed scenarios in the port city of Antwerp. Regarding exceedances, current EU AAQD limits for NO_2 do not present compliance issues; however, significant exceedances arise when compared against the non-binding WHO air quality guidelines. For $PM_{2.5}$, results show only a few exceedances of the EU AAQD limit, within the 18 permitted days, yet substantial non-compliance persists relative to the WHO guidelines. The number of days exceeding air quality limits for both NO_2 and $PM_{2.5}$ is unlikely to be substantially altered by the assessed scenarios.

3.4.3. Rotterdam

Key highlights
• Shipping is a major contributor to Rotterdam's air quality in 2023, accounting for ~60% of NO_2 in the city centre and up to 80% in the port, with ~20-25% contribution to $PM_{2.5}$. • By 2030, shipping-related concentrations in Rotterdam decline, with average reductions of ~5 µg/m³ in NO_2 and ~0.4 µg/m³ in $PM_{2.5}$ along the Nieuwe Maas waterway. • Shipping remains a dominant source of urban NO_2 (~58-59%) and $PM_{2.5}$ (~12%) in the city core area. A slight increase in shipping share is estimated for NO_2 (by 3-4%) in 2030 compared to 2023, and a slight reduction for $PM_{2.5}$ (up to 1.5%). Differences between the 2030 scenarios in Rotterdam are small. • Seasonal variation in Rotterdam remains consistent between 2023 and 2030, with increases in shipping's relative share for NO_2 in the summer, peaking at around 70% in July. • No exceedances of the EU NO_2 daily limit (50 µg/m³) are predicted in Rotterdam city centre and only one exceedance at the port in 2030. When comparing to the WHO NO_2 daily limit guideline (25 µg/m³), exceedances are predicted at both the port and city centre observation stations. The main contributors to these are shipping for NO_2, and other sectors such as agriculture for $PM_{2.5}$ in 2030.

Figure 32 shows the modelled NO_2 concentrations and the relevant shipping contribution in Rotterdam in the 2023 base case simulation, together with the relevant results under the projected 2030 BAU scenario and associated differences. The city core area (as defined in section 2.4.4 and marked with a white contour on the maps) is used for evaluating the shipping impact averaged across the city. Relevant observation station locations are used for validation and analysis with observed data, i.e. station NL00496 in the port area and station NL00494 in the city. Overall, the performance of the model for NO_2 and $PM_{2.5}$ is similar as for Antwerp (further details are presented in the Appendix, section B1 Figure 24 to Figure 27).

The highest NO_2 concentration (up to ~30 $\mu g/m^3$) is predicted in the city centre, where the shipping contribution is around 60% (in the 2023 base case). The highest $PM_{2.5}$ concentration (up to 8 $\mu g/m^3$) is also predicted to be found in the city centre, and the associated shipping share is ~20%. The largest shipping contributions are predicted along the coast and the waterway of the Nieuwe Maas. The shipping sector contributes up to 25% of local $PM_{2.5}$ concentration, and up to 80% of NO_2, especially in the port area near the coast.

Rotterdam has a higher shipping contribution to $PM_{2.5}$ compared to Antwerp. The 2030 scenarios have demonstrated an average reduction of about 0.4 $\mu g/m^3$ in $PM_{2.5}$ and 5 $\mu g/m^3$ in NO_2, attributed to shipping, over the grid cells along the Nieuwe Maas waterway. The largest reduction in 2030 for both $PM_{2.5}$ and NO_2 are expected at the western part of the urban area, in Rozenburg and Vlaardingen.

Figure 32 *Annual averaged total NO_2 surface concentrations [in µg/m³] and shipping sector share [in %] within the Rotterdam city core area (highlighted in white)*

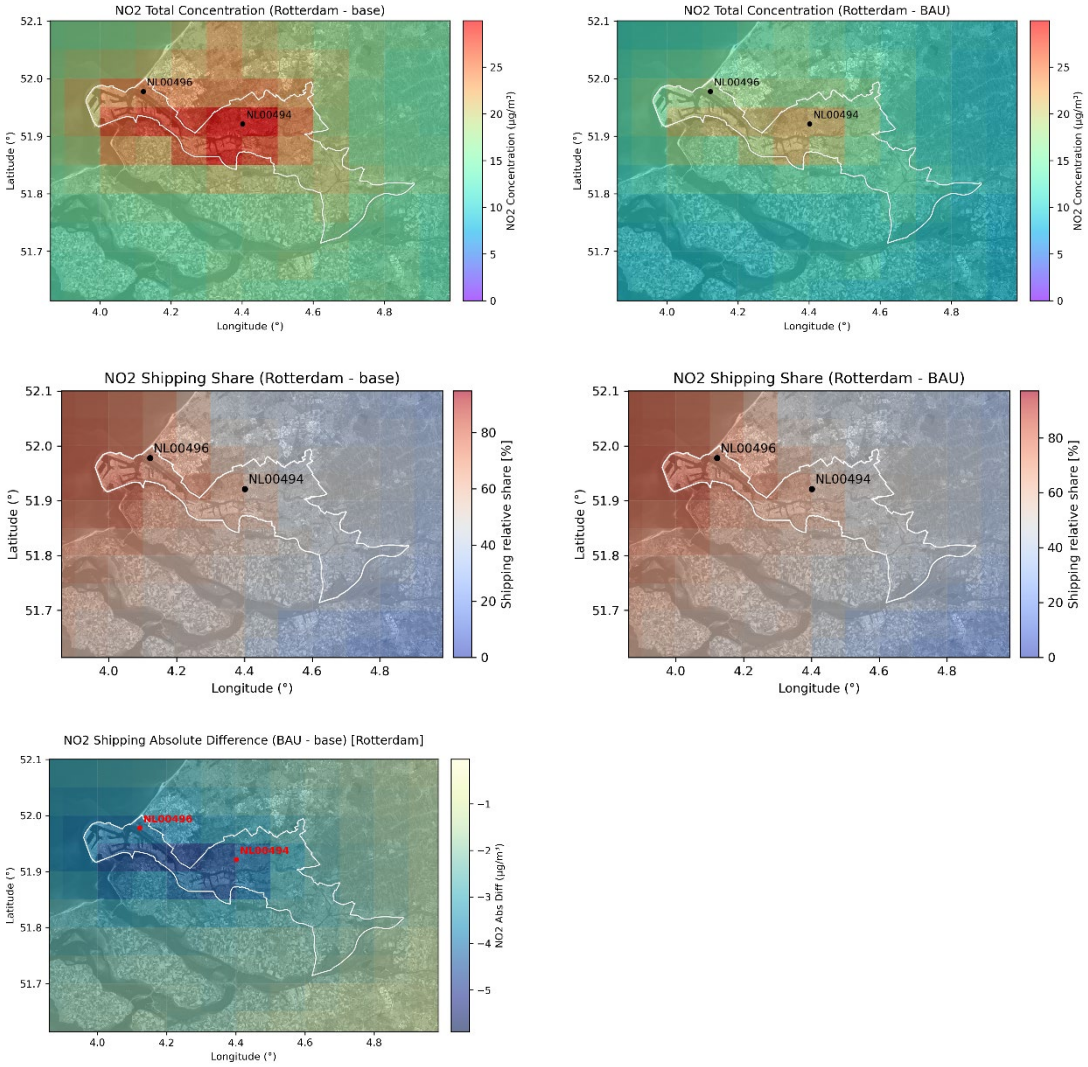

Observation stations marked as points. From top to bottom and left to right: 1) total modelled surface concentration in the 2023 base case and 2030 BAU scenarios; 2) relative shipping share in the 2023 base case and 2030 BAU scenarios; 3) difference in the NO_2 concentrations attributed to shipping between the 2030 BAU and 2023 base case scenarios.

For the city-averaged concentrations in Rotterdam, the predicted relative annual contribution of shipping to both NO_2 and $PM_{2.5}$ in 2030, shows only minor variation across the scenarios (Figure 33 and Appendix, section B3 Table 26 and Table 27). Although the 2030 LNG scenario yields slightly lower shipping-related contributions to both pollutants compared to the other scenarios, the differences are marginal (less than 0.1 µg/m³).

In relative terms for the city core, shipping contributes 58-59% of NO_2 and 12% of $PM_{2.5}$ in the 2030 scenarios. A slight increase in shipping share is estimated for NO_2 (3-4%) in 2030 compared to the 2023 base case, and a slight reduction for $PM_{2.5}$ (up to 1.5%).

Figure 33 also shows the monthly relative contributions (right figure). The 2030 scenarios exhibit a positive offset for NO_2 compared to the 2023 base case. The highest shipping contribution occurs during the summer, especially in July.

Figure 33 *Predicted annual NO_2 surface concentrations attributed to shipping (in $\mu g/m^3$, left) and predicted shipping contribution to monthly NO_2 surface concentrations (right) in Rotterdam city*

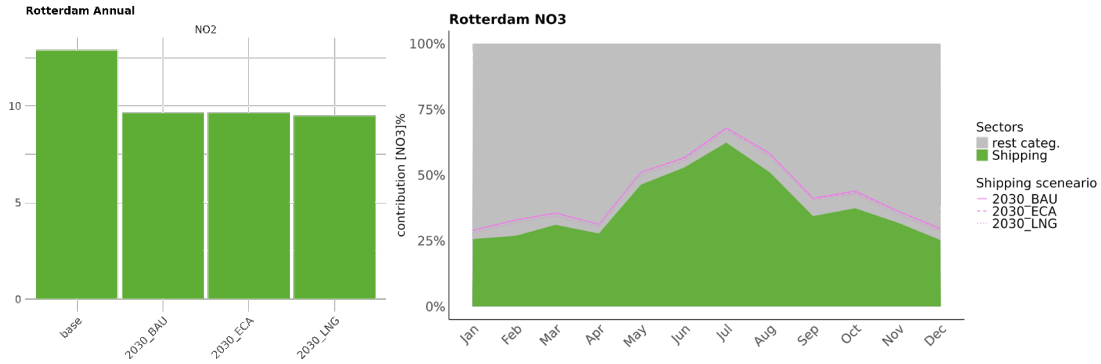

The pink lines are the three different 2030 scenarios of shipping contribution to surface concentration in $\mu g/m^3$.

The annual NO_2 source apportionment results in Rotterdam for the two observation sites located in the port (NL00496) and the city (NL00494) are presented in Figure 34. The results show that shipping is the dominant source for NO_2 in both the port and the city centre. In the city centre, road traffic is also predicted to be a significant source, with lower relative share in 2030 compared to 2023. On the contrary, over 2023 to 2030, the relative share of shipping to total NO_2 concentrations has increased in both the city and port stations.

Figure 34 *Predicted NO_2 annual source apportionment results in Rotterdam at observation sites NL00496 (port) and NL00494 (city centre)*

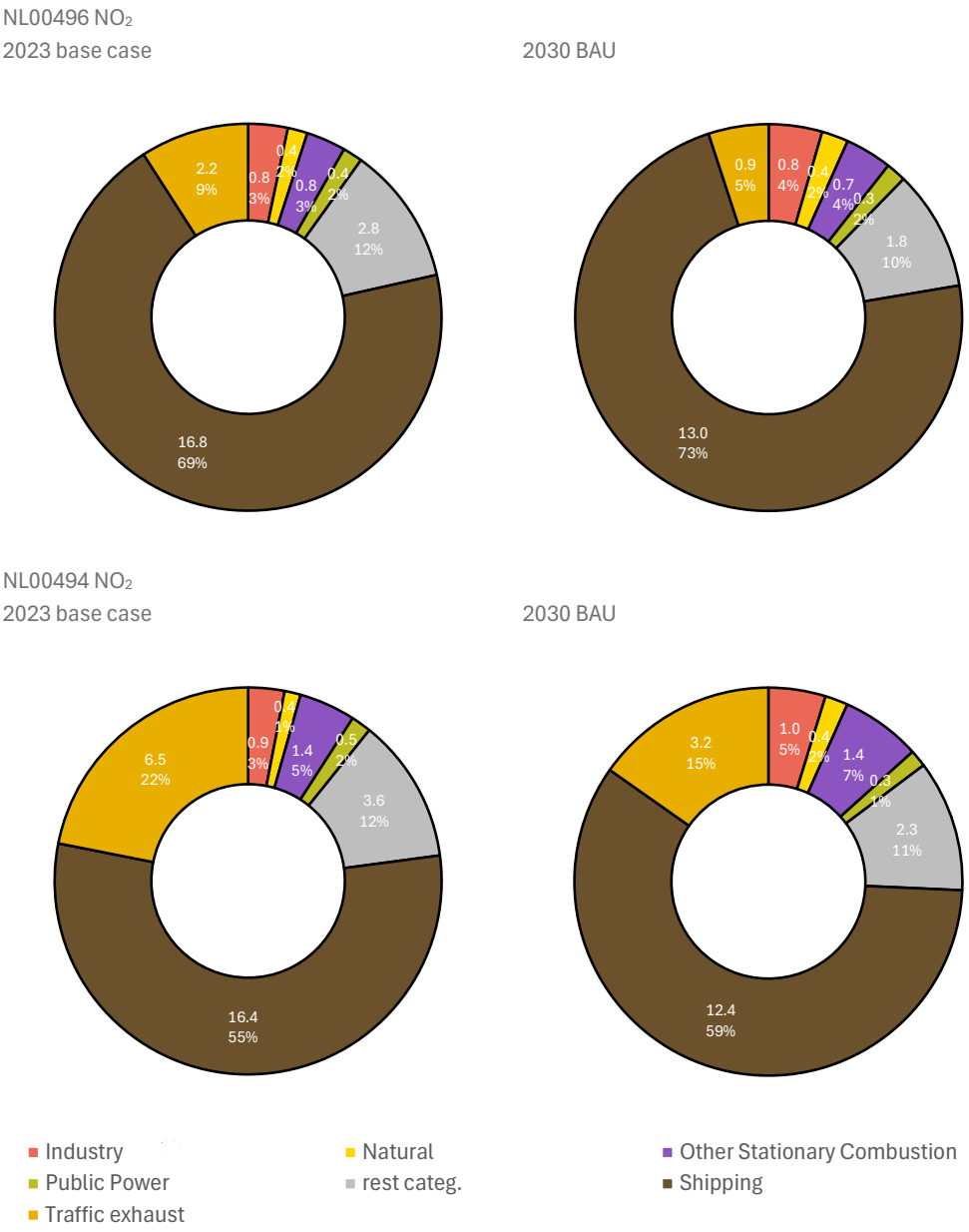

The main contributing sectors are shown here, whereas the remaining sectors are grouped in the "rest categories". The top labels are relative contribution and the lower labels are absolute contribution in $\mu g/m^3$.

Figure 35 shows the relative contribution of shipping and other sectors to daily surface NO_2 concentrations at the port (NL00496) and the city centre (NL00494) stations. In 2030, no daily NO_2 exceedances of the current EU daily (24-hour average) limit of 50 $\mu g/m^3$ are predicted in the city, with only one exceedance predicted in the port. However, when comparing to the WHO guideline of 25 $\mu g/m^3$ the port and city centre stations are predicted to have around three and four months of exceedances in 2030. Shipping still remains a dominant source of NO_2 concentrations in 2030 and therefore still at risk of contributing to an exceedance.

With respect to $PM_{2.5}$ (Appendix, section B2 Figure 48), the exceedances in the city centre and port are due to a mixed sector contribution. The relative differences between the assessed scenarios are limited and do not affect the number of exceedance days.

Figure 35 *Relative contribution to daily surface NO_2 concentrations at 0-25 µg/m³, 25-50 µg/m³, and exceeding 50 µg/m³ (2030 EU NO_2 daily limit) at stations NL00496 (port) and NL00494 (city)*

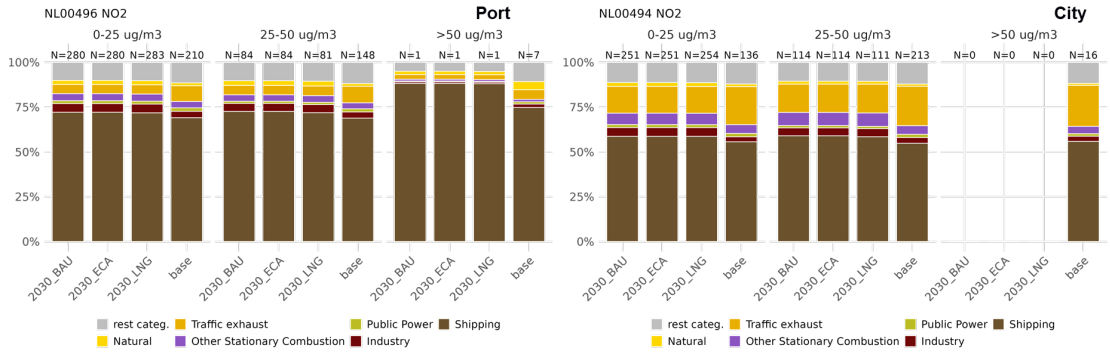

"N" represents the number of days in each scenario within each concentration range.

In summary, despite the predicted reduction in absolute concentrations of air pollutants attributed to shipping, the relative influence of shipping remains similar across the assessed scenarios in the port city of Rotterdam. Although the absolute levels of shipping-related NO_2 are projected to reduce significantly by 2030, its share of overall NO_2 rises. For $PM_{2.5}$, the relative contribution of shipping remains similar.

In terms of exceedances, the results indicate that NO_2 concentrations are unlikely to exceed the EU daily limit value of 50 µg/m³ in either the city or the port area (Figure 35). For $PM_{2.5}$, only a small number of exceedance days are predicted (Appendix, section B2 Figure 48). However, when assessed against the WHO air quality guidelines, substantially higher numbers of exceedances are predicted for both pollutants, particularly for daily NO_2 concentrations, with shipping identified as the dominant contributing source. All 2030 scenarios show only minor differences, and while daily NO_2 exceedances are unlikely in the city, they could still occur near the port.

3.4.4. Athens

Key highlights
• Shipping heavily influences air quality around Athens in 2023, contributing up to 80% of NO_2 near the port, up to 60% in the south and southwestern parts of the city, and reducing to less than 20% in the city centre where other sectors dominate, including road transport. • By 2030, shipping-related concentrations in Athens decrease, with average reductions of ~2.5 µg/m³ in NO_2 and 0.4–0.6 µg/m³ in $PM_{2.5}$ around the port and coastal areas. • Differences between the 2030 scenarios in Athens are small, with shipping contributing ~24% of NO_2 and ~4% of $PM_{2.5}$ in the city core. An increase of 7-8% shipping share of NO_2 is estimated in 2030 compared to 2023, and an insignificant reduction for $PM_{2.5}$ (less than 0.5%). • Shipping remains the dominant NO_2 source at the port (63% in 2030), while in the city centre road traffic is the primary contributor. • Seasonal variation in Athens remains consistent between 2023 and 2030, with the NO_2 shipping share being higher from March to November, and reducing in the winter period (December to February). • Both port and city stations are predicted to have exceedances of the EU NO_2 daily limit (50 µg/m³) in 2030, with most days of the year exceeding the WHO guideline (25 µg/m³). The main contributors to these are shipping at the port, and road traffic in the city.

Figure 36 shows the modelled NO_2 concentrations and the relevant shipping contribution in Athens in the 2023 base case simulation, together with the relevant results under the projected 2030 BAU scenario and associated differences. The city core (as defined in section 2.4.4 and marked with a white contour on the maps) is used for evaluating the shipping impact averaged across the city. Relevant observation station locations are used for validation and analysis with observed data, i.e. station GR0030A in the port and stations GR0003A in the city. Overall, the performance of the model for NO_2 and $PM_{2.5}$ is similar as for Antwerp (further details are presented in the Appendix, section B1 Figure 28 to Figure 31).

In the 2023 base case, the highest NO_2 concentrations are predicted in the city centre of Athens and the grid cell that includes the port. Shipping contributes up to 80% (~30 µg/m³) on NO_2 and up to 20% (~2 µg/m³) on $PM_{2.5}$ concentrations over the shipping lane in the Aegean Sea leading to the port. Moving towards inland, the shipping contribution attenuates from ~60% on NO_2 concentrations in the south-western part of the city and along the coastline, to less than 20% near the city centre. Respectively, for $PM_{2.5}$, the shipping share is predicted to reduce from 15% over the coastlines to less than 5% near the city centre.

The 2030 scenarios show reduced shipping NO_2 concentrations by ~2.5 µg/m³ (~12%) over the grid cells including the port and the adjacent grid cells over the sea. Differences related to shipping activity over the city centre are insignificant. $PM_{2.5}$ concentrations are predicted to reduce by ~0.6 µg/m³ over the port grid cell, the sea and the south-western coastline and by ~0.4 µg/m³ in the southern suburbs of the city. The 2030 LNG scenario shows slightly lower NO_2 shipping concentrations over the shipping lane leading to the port by ~0.8 µg/m³ (~5%) compared to the 2030 BAU and 2030 all-EU ECA scenarios. The latter two scenarios have insignificant differences between them.

The differences in $PM_{2.5}$ concentrations from the 2030 LNG compared to the 2030 BAU and 2030 all-EU ECA scenarios are negligible (less than 0.1 µg/m³) (Appendix, section B3 Table 31.

Figure 36 *Annual averaged total NO_2 surface concentrations [in µg/m^3] and shipping sector share [in %] within the Athens city core area (highlighted in white). Observation stations are marked as points*

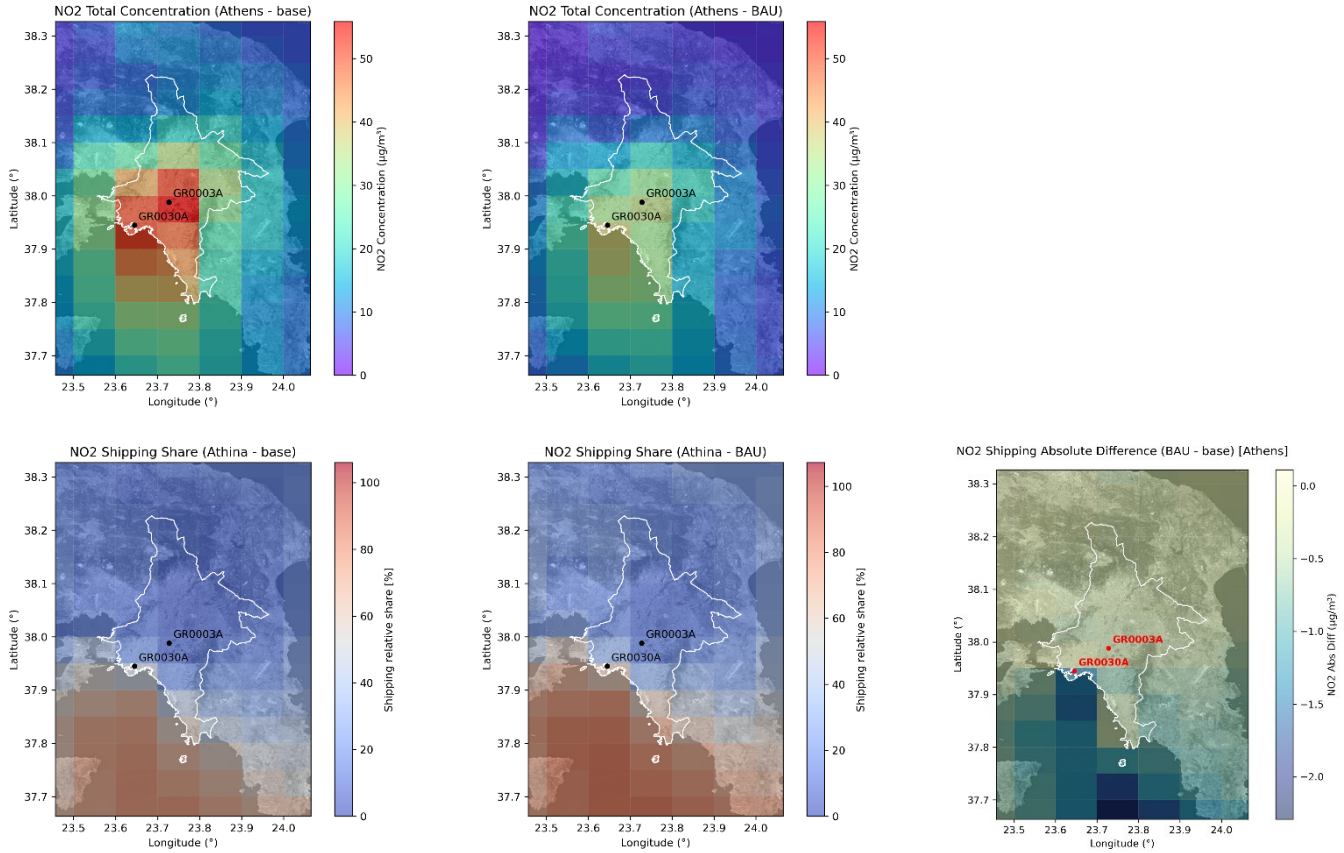

The top row shows the total modelled surface concentration in the 2023 base case (left) and 2030 BAU (right) scenarios. The bottom row shows the relative shipping share in the 2023 base case (left), and 2030 BAU (middle) scenarios, and the differences in the NO_2 concentrations attributed to shipping between the 2030 BAU and 2023 base case scenarios.

For the city-averaged concentrations in Athens, the predicted relative annual contribution of shipping to both NO_2 and $PM_{2.5}$ in 2030, shows only minor variation across the scenarios (Figure 37 and Appendix, section B3 Table 30 and Table 31). Although the LNG scenario yields slightly lower shipping-related contributions compared to the other scenarios, the differences are marginal (less than 0.2 µg/m^3 for NO_2). In relative terms for the city core, shipping contributes around 24% of NO_2 and 4% of $PM_{2.5}$ in the 2030 scenarios. An increase of 7-8% is estimated for NO_2 in 2030 compared to the 2023 base case. However, an insignificant reduction is estimated for $PM_{2.5}$ (less than 0.5%).

Figure 37 also shows the monthly relative contribution (right figure). A positive offset for NO_2 can be observed for all future scenarios (pink lines overlapping in the left figure) compared to the 2023 base case. The shipping share of NO_2 does not alter significantly from March until November, whereas in the winter period (December to February) the shipping share is lower. This reflects the increased importance of other sectors, such as residential combustion and road traffic during the winter months, when photolysis of NO_2 is weaker and concentrations accumulate over the city. $PM_{2.5}$ seasonal contributions are low and equivalent for the 2023 base case and the 2030 assessment scenarios, with higher contributions simulated in the months of April and October.

Figure 37 *Predicted annual NO_2 surface concentrations attributed to shipping (in µg/m^3, left) and predicted shipping contribution to monthly NO_2 surface concentrations (right) in Athens (Athina) city*

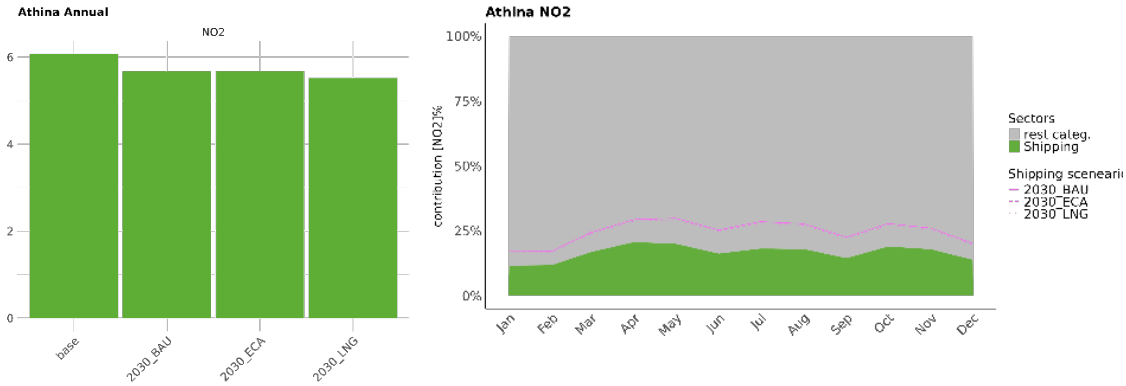

The pink lines are the three different 2030 scenarios of shipping contribution to surface concentration in µg/m^3.

The annual NO_2 source apportionment results for the two observation sites located in the port (GR0030A) and Athens city centre (GR0003A) are presented in Figure 38. The results show that shipping is the most dominant source at the port station, but not in the city centre of Athens. In the port station, shipping contributes ~50% of total NO_2 in 2023. In 2030, and despite that the NO_2 concentrations attributed to shipping are predicted to reduce by 1 µg/m^3, the relative share of shipping to total NO_2 concentrations is predicted to rise to 63% as a result of higher reductions to other sectors.

In 2023, in the Athens city centre, road traffic accounts for approximately 37.5 µg/m^3 (67%) of the total NO_2. In 2030, the NO_2 concentrations attributed to road traffic are predicted to reduce to 21 µg/m^3 (under the 2030 BAU scenario) in the city centre, however road traffic still remains the dominant sector (its relative share is predicted to be 60%). Shipping is predicted to be a considerable source in the city of Athens, however its relative share is predicted to be lower compared to

the port, with 16% of the total NO_2 concentrations in the city centre attributed to shipping in 2030 (under the 2030 BAU scenario). The shipping contribution to $PM_{2.5}$ is prevalent in the port area, increasing in all future scenarios and is minimised in the city centre (Appendix, section B2 Figure 51).

Figure 38 *Predicted NO_2 annual source apportionment results in Athens at observation sites GR0030A (port) and GR0003A (city centre)*

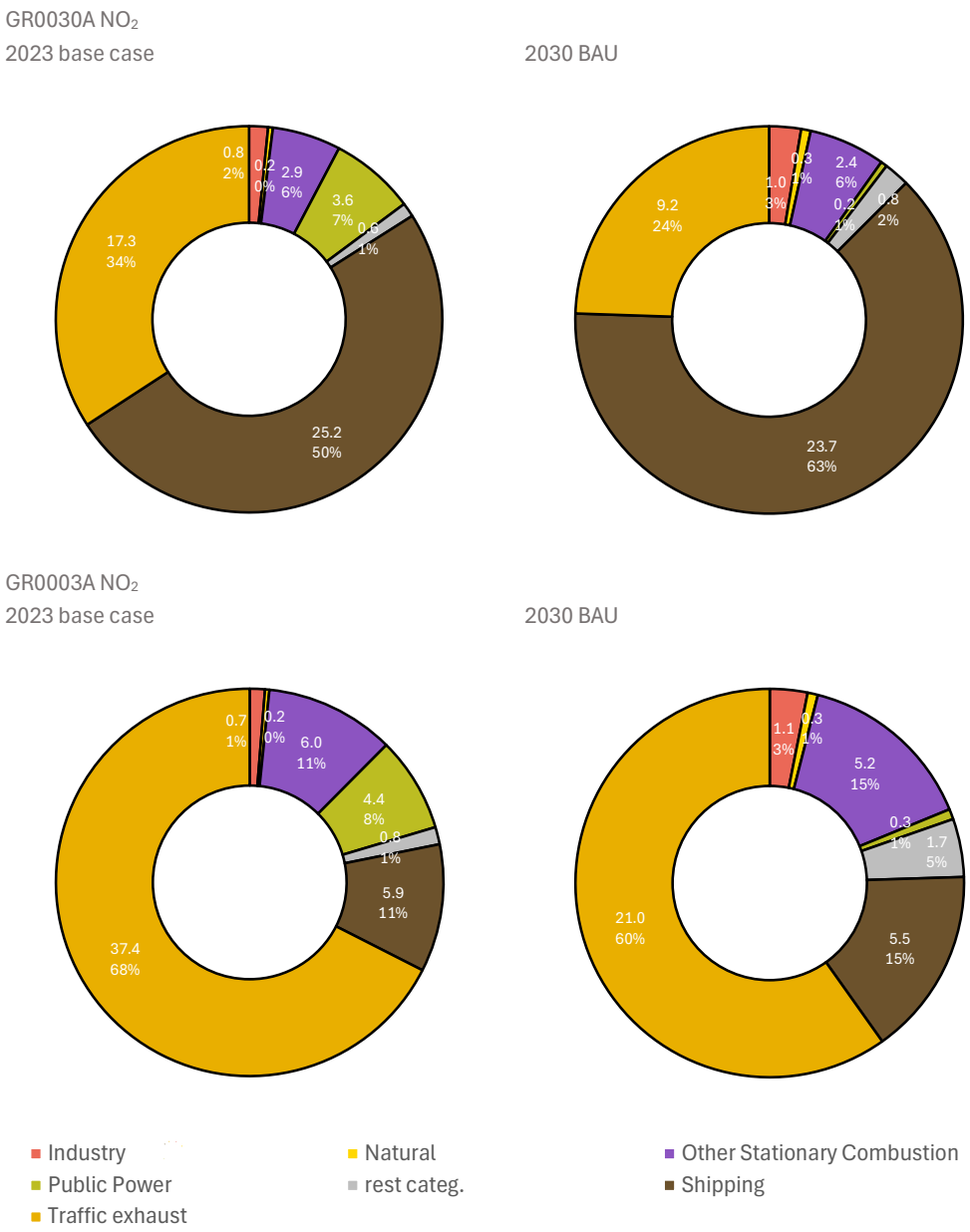

The main contributing sectors are shown here, whereas the remaining sectors are grouped in the "rest categories". The top labels are relative contribution and lower labels are absolute contribution in $\mu g/m^3$.

Figure 39 shows the relative contribution of shipping and other sectors to daily surface NO_2 concentrations at the port (GR0030A) and the city centre (GR0003A) stations. In 2030, exceedances of the current EU daily (24-hour average) limit of 50 $\mu g/m^3$ are predicted in both stations. When comparing to the WHO guideline of 25 $\mu g/m^3$, then the majority of days over the year would exceed the limit at both

station locations. Shipping is predicted to drive these exceedances in the port, but that is not the case for the city centre where road traffic exhaust is the dominant source of NO_2 concentrations.

In relation to $PM_{2.5}$ (Appendix, section B2 Figure 52), stationary combustion from the residential sector is the main contributor of the exceedances at both station locations in 2023. In 2030, natural sources dominate exceedances in the port when compared to the EU limit value, whereas in the city centre exceedances occur due a mixed sector contribution (stationary combustion, natural sources and road transport). When compared to the WHO air quality guideline, exceedances occur in both the port and city centre due a mixed sector contribution.

Figure 39 *Relative contribution to daily surface NO_2 concentrations at 0-25 µg/m^3, 25-50 µg/m^3, and exceeding 50 µg/m^3 (2030 EU NO_2 daily limit) at stations GR0030A (port) and GR0003A (city)*

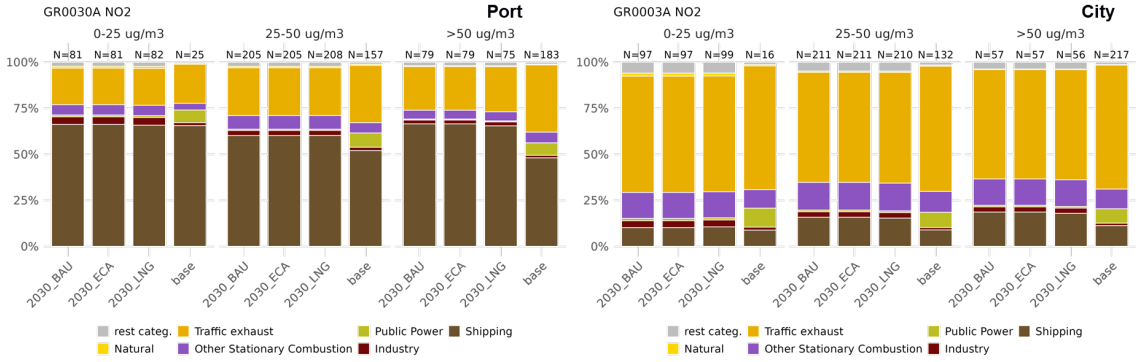

"N" represents the number of days in each scenario within each concentration range.

In summary, shipping will remain a dominant contributor to the air pollutant concentrations in the port of Athens, with considerable contributions to the city centre, where road traffic exhaust is the dominant source of NO_2 concentrations. The number of days exceeding air quality limits is also unlikely to be substantially altered by the assessed scenarios.

3.4.5. Marseille

Key highlights
• Shipping influences air quality around Marseille, with contributions of ~80% of NO_2 offshore, ~15% NO_2 in the city, and ~10% of $PM_{2.5}$ in the port. • By 2030, shipping-related concentrations in Marseille decrease, with average reductions of ~2 µg/m³ for NO_2 and ~0.2 µg/m³ for $PM_{2.5}$ in the port grid cells. • Differences between the 2030 scenarios in Marseille are small, with shipping contributing ~18-20% of NO_2 and ~3% of $PM_{2.5}$ in the city core. • Shipping is not the primary NO_2 source at either the port or city observation stations in Marseille, with industry dominating at the port (~50%) and road traffic dominating in the city centre (>50%); however, shipping's relative contribution increases by 2030, becoming the second-largest source at the port and the city. • Seasonal variation in Marseille remains consistent between 2023 and 2030, with the NO_2 shipping share being higher in spring and summer months, peaking in July. • While no exceedances of the EU NO_2 daily limit (50 µg/m³) are predicted in Marseille in 2030, when comparing to the WHO guideline (25 µg/m³) exceedances are predicted at both the port and city centre observation stations. The main contributors to these are road traffic and industry respectively.

Shipping emissions affect local air quality around Marseille, especially due to cruise ships and ferries operating near the city centre. Measured NOx and PM concentrations have been found to be twice as high in the port area compared to urban background areas (Le Berre et al., 2025), with simulated contributions from shipping being 6% in the city, and ~25% for $PM_{2.5}$ and up to 80% for NOx in the port area (Chevet et al., 2024).

Figure 40 shows the modelled NO_2 concentrations and the relevant shipping contribution in Marseille in the 2023 base case simulation, together with the relevant results under the projected 2030 BAU scenario and associated differences. The city core (as defined in section 2.4.4 and marked with a white contour on the maps) is used for evaluating the shipping impact averaged across the city. Relevant observation station locations are used for validation and analysis with observed data, i.e. station FR3043 near Port-de-Bouc and station FR02008 in the city.

In 2023, the highest NO_2 concentrations (~13 µg/m³) are predicted over the city and the port area (~20 µg/m³), as well as the Port-de-Bouc (~15 µg/m³), a smaller industrial port serving mainly for local and regional maritime needs and situated northwest of Marseille (port area west to the FR02008 observation site). Both Port-de-Bouc and Port of Marseille-Fos are part of the broader Marseille province maritime activities.

Shipping contribution to NO_2 concentrations is higher in the open-sea leading to both ports (up to ~80%) and ~15% over the city. For $PM_{2.5}$ the shipping share is much lower (~15%) over the sea and approximately 10% in the port areas. The impact of shipping is minimised further inland towards the city core, away from the port.

The 2030 BAU scenario shows an improvement of air quality in the greater port area of Marseille. NO_2 concentrations are predicted to decrease by 2 µg/m³ in the southern grid cell of the port (close to the FR03043 observation site) and by ~1.2 µg/m³ along the shipping lane leading to the port. $PM_{2.5}$ concentrations are also predicted to reduce, but the reduction does not exceed ~0.2 µg/m³ in the port grid cell and the surrounding shipping lanes (Appendix, section B2 Figure 53 and Figure 54).

Figure 40 *Annual averaged total NO_2 surface concentrations [in µg/m^3] and shipping sector share [in %] within the Marseille city core area (highlighted in white). Observation stations are marked as points*

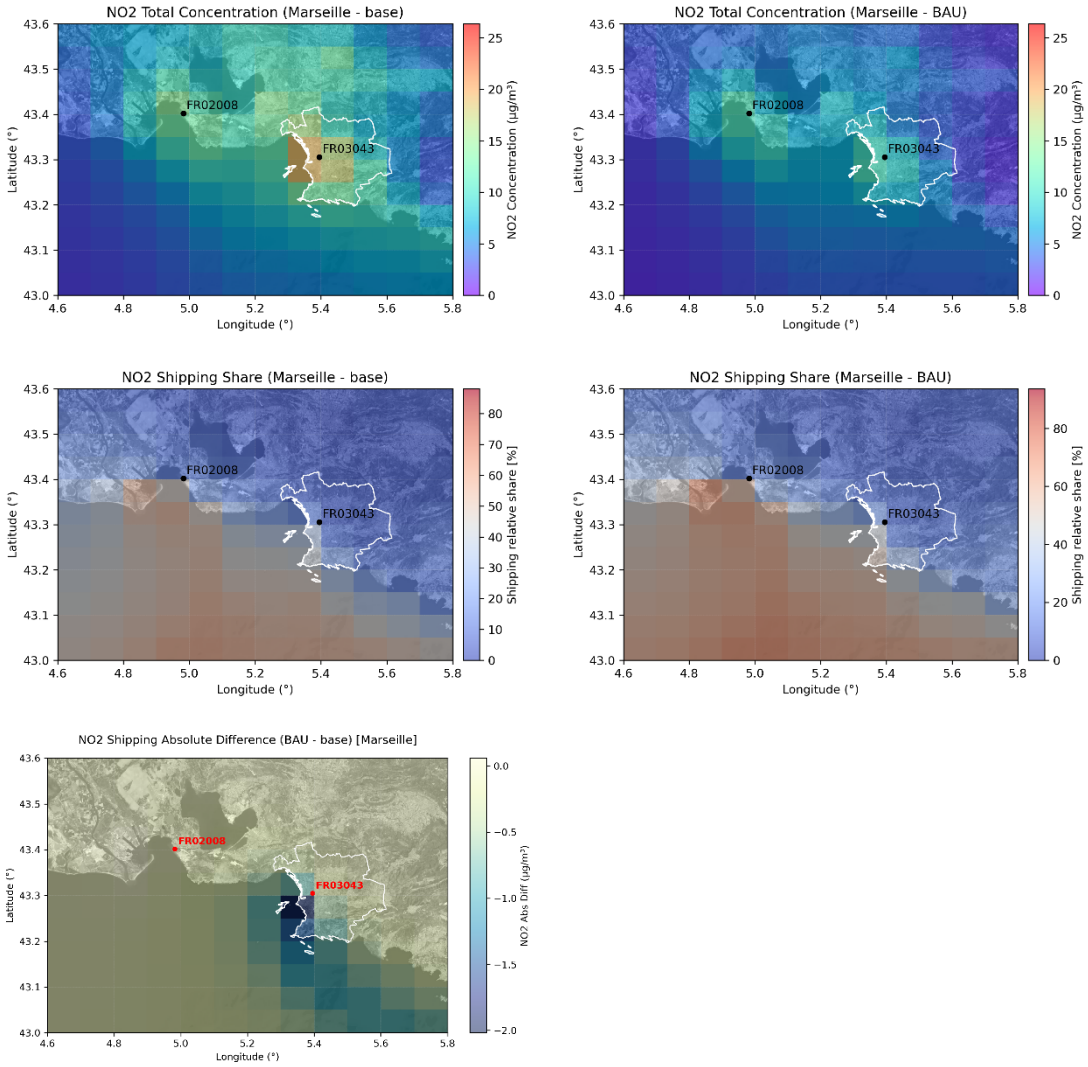

From top to bottom and left to right: 1) total modelled surface concentration in the 2023 base case and 2030 BAU scenarios; 2) relative shipping share in the 2023 base case and 2030 BAU scenarios; 3) differences in the NO_2 concentrations attributed to shipping between the 2030 BAU and 2023 base case scenarios.

For the averaged city core of Marseille, all three 2030 scenarios show limited differences, with the 2030 LNG scenario giving the lower shipping contribution to NO_2 concentrations (Figure 41). In relative terms for the city core, shipping contributes around 18-20% of NO_2 and 3% of $PM_{2.5}$ in the 2030 scenarios (Appendix, section B3). Compared to 2023, this corresponds to a 5-6% increase of the shipping share to NO_2 concentrations in 2030. In contrast, while a slight reduction is estimated for $PM_{2.5}$ (up to 1.5%).

Annual average NO_2 and $PM_{2.5}$ concentrations over the city of Marseille remain almost constant in all 2030 future scenarios with the 2030 LNG scenario showing slightly higher decreases for NO_2 (~0.1 µg/m^3) (Figure 41 and Appendix, section B3 Table 34). Differences for $PM_{2.5}$ between the 2030 scenarios over the city of

Marseille are statistically insignificant (<0.02 µg/m^3) (Appendix, section B3 Table 35).

Figure 41 also shows the monthly relative contribution (right figure). The 2030 scenarios exhibit a positive offset for NO_2 compared to the 2023 base case. The highest shipping contribution occurs during the spring and summer months, peaking in July (~22% in 2023), reflecting the increased shipping activities of passenger vessels in these months, and is lower during autumn and winter with a mean contribution of ~12%. All future scenarios, indicate an increased share of shipping activity to total NO_2 concentrations in 2030, accounting for more than 25% from April till August.

Figure 41 *Predicted annual NO_2 surface concentrations attributed to shipping (in µg/m^3, left) and predicted shipping contribution to monthly NO_2 surface concentrations (right) in Marseille city*

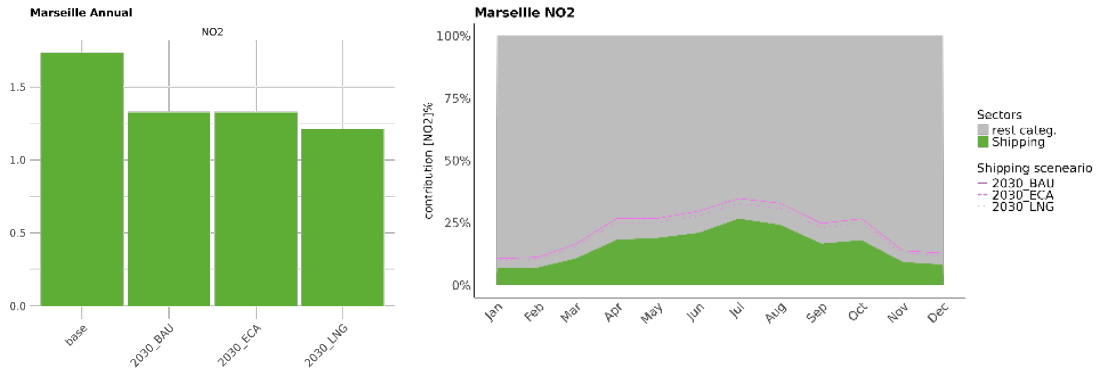

The pink lines are the three different 2030 scenarios of shipping contribution to surface concentration in µg/m^3.

The annual NO_2 source apportionment results for the two observation sites located near Port-de-Bouc (FR03043) and Marseille city centre (FR02008) are presented in Figure 42. The results predict that shipping is not the primary contributor to NO_2 concentrations at both station locations. In the city, the dominant source is predicted to be road traffic exhaust which accounts for almost half of NO_2 in 2023. However, in 2030 the shipping relative contribution is predicted to increase. At the port station, industry is the dominant source contributing about half of the total NO_2, followed by traffic (19%) and then shipping (14%). However, in 2030, the shipping source will replace road traffic as the second most important source for urban NO_2.

Figure 42 *Predicted NO_2 annual source apportionment results in Marseille at observation sites FR03043 (city centre) and FR02008 (port)*

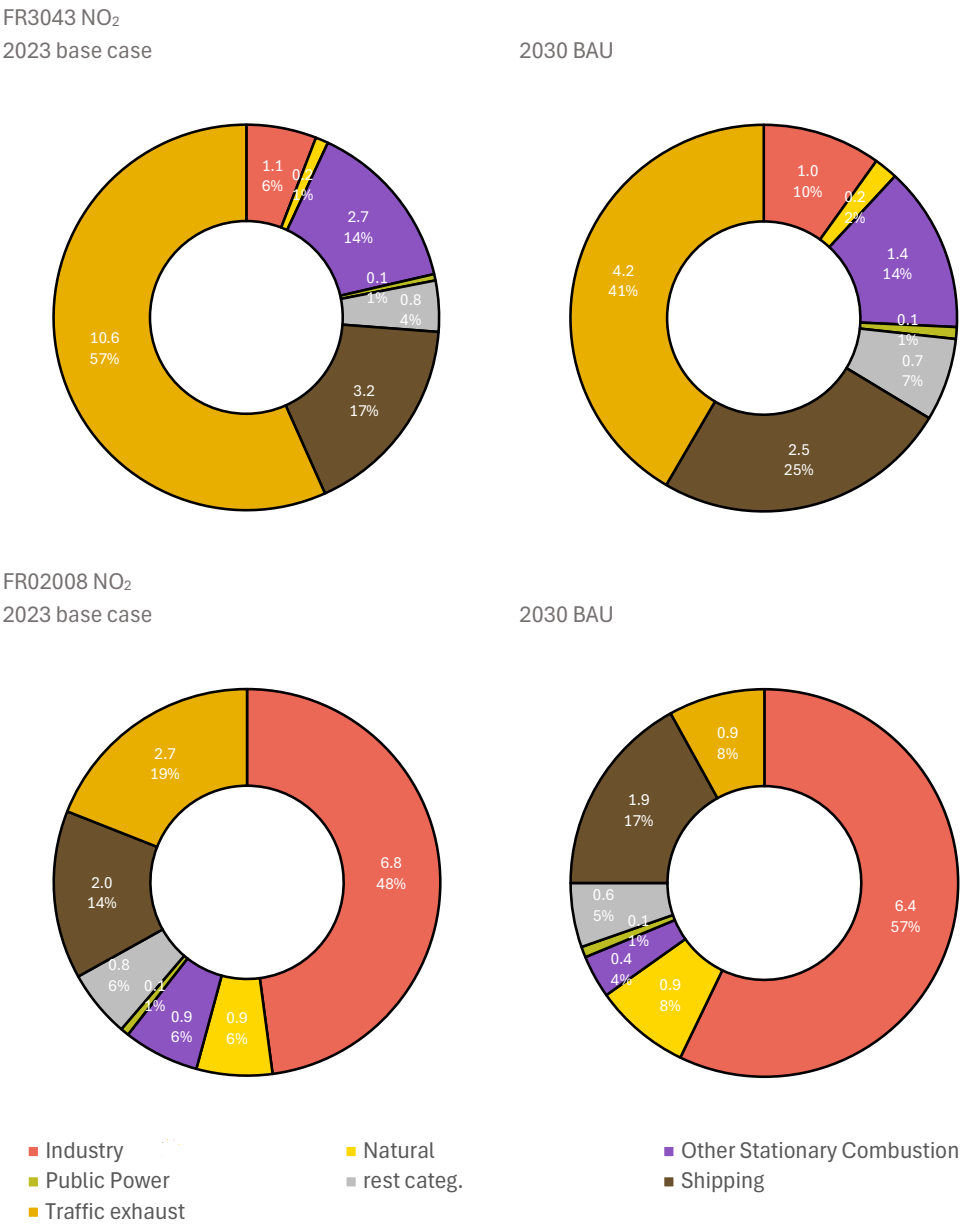

The main contributing sectors are shown here, whereas the remaining sectors are grouped in the "rest categories". The top labels are relative contribution and lower labels are absolute contribution in µg/m^3.

Figure 43 shows the relative contribution of shipping and other sectors to daily surface NO_2 concentrations at the port (FR3043) and the city centre (FR02008) stations. In 2030, no daily NO_2 exceedances are expected in either the port or city stations based on the current EU daily (24-hour average) limit of 50 µg/m^3. When comparing to the WHO guideline of 25 µg/m^3, exceedances are predicted at the port station for 2023 (more than 90 days), reducing to less than 10 days in 2030. Road traffic is predicted to be the main contributor. In the city station, NO_2 exceedances of the WHO guideline would also reduce from more than 1 month in 2023 to under 15 days in 2030, with industry being the main driver for the exceedances. The relative differences between the assessed scenarios are limited

and do not affect the number of exceedance days. Compared to the other three cities, Marseille has relatively less exceedance days for both the EU and WHO limits.

Figure 43 *Relative contribution to daily surface NO_2 concentrations at 0-25 µg/m^3, 25-50 µg/m^3, and exceeding 50 µg/m^3 (2030 EU NO_2 daily limit) at stations FR03043 (city) and FR02008 (port)*

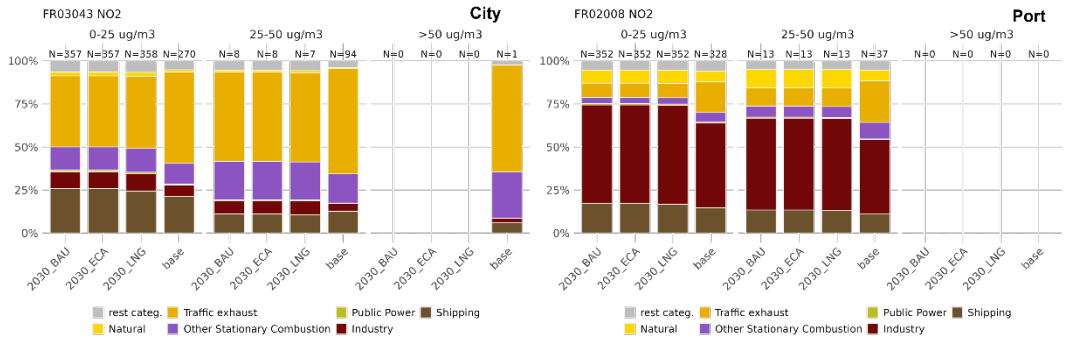

"N" represents the number of days in each scenario within each concentration range.

In summary, shipping is a strong contributor to air pollutant concentrations in the city and the ports of Marseille. The future assessment scenarios project an overall decline in concentrations and an increase of the shipping sector share, since other sectors, such as road traffic and combustion processes are expected to show higher reductions than the shipping sector.

4. CONCLUSION

This study examined the air quality impacts of sea shipping emissions across Europe under a 2023 base case and three hypothetical 2030 sensitivity scenarios, with particular focus on four major seaport cities: Rotterdam, Antwerp, Athens, and Marseille. Using the STEAM model combined with the CAMS-REG land-based emissions inventory and the LOTOS-EUROS chemistry transport model, the analysis provides a comparative picture of how shipping and other sectors are likely to shape European air quality by 2030.

Across all scenarios, absolute pollutant concentrations are projected to fall by 2030, with domain-wide reductions of ~22% (1.8 µg/m^3) for NO_2, ~14% (1.3 µg/m^3) for $PM_{2.5}$, and ~14% (0.4 µg/m^3) for SO_2 relative to 2023. These improvements are driven by reductions across both shipping and land-based sectors, with land-based emissions declining particularly sharply at around 40% for NOx (2,048 kton) and 35% for $PM_{2.5}$ (462 kton). However, because land-based sectors are reducing faster, shipping's relative contribution grows, with its NO_2 share across the European domain increasing by around 5% (despite a reduction in absolute terms). This pattern is especially pronounced at the seaport city level, where shipping's NO_2 share rises by up to 8% in Athens and 6% in Marseille by 2030.

The three 2030 scenarios yield distinct benefits depending on the pollutant and region considered. Along the EU waterways, the 2030 LNG scenario results in a larger reduction for NO_2 with 23% (0.51 µg/m^3), compared to 17% under the all-EU ECA scenario, whereas the latter is more efficient in reducing SO_2 concentrations with reductions of up to 60% (0.11 µg/m^3). For $PM_{2.5}$, both scenarios result in a similar reduction of ~32% (~0.11 µg/m^3). The expansion of emission control areas, particularly a Mediterranean SECA, produces significant SOx reductions of 44% to 56% and $PM_{2.5}$ reductions of 24% to 30% relative to 2023.

At the city level, the results highlight clear contrasts between port typologies. Shipping is the dominant NO_2 source in the BENELUX cities, contributing around 50% of urban NO_2, while road traffic drives exceedances in Athens and Marseille. NO_2 exceedances of the EU daily limit (50 µg/m^3) in 2030 are predicted only in Athens and Rotterdam ports, and exceedances against the non-binding WHO guideline (25 µg/m^3), used here for indicative purposes, are predicted at all four cities, underscoring the continued air quality challenge in major port areas.

These findings confirm that while progress across all sectors will bring measurable air quality improvements by 2030, sea shipping is set to become a proportionally more significant source of pollution as other sectors reduce faster.

5. GLOSSARY

AAQD	Ambient air quality directive
AIS	Automatic identification system
AQ	Air quality
Atmospheric concentration	The concentration of an atmospheric component in this report as mass per volume, in µg/m^3
Atmospheric surface concentration	The atmospheric concentration at 2.5 metres above ground level/earth surface.
BAU	Business as usual
BENELUX	Belgium, The Netherlands and Luxembourg
CAMS	Copernicus Atmospheric Monitoring Service
CAMS-REG	Copernicus Atmospheric Monitoring Service REGional emissions
CAPRI	Common Agricultural Policy Regionalised Impact
CEIP	Center on Emission Inventories and Projections
CLE	Current legislation
CLRTAP	Convention on Long-Range Transboundary Air Pollution
CO	Carbon monoxide
CTM	Chemical transport model
DEPAC	DEPosition of Acidifying Compounds
EAFO	European Alternative Fuels Observatory
EBAS	Environmental Database for Atmospheric Studies
EC	Elemental carbon
ECA	Emission control area
ECMWF	European Centre for Medium-Range Weather Forecasts
EEA	European Environment Agency
FMI	Finnish Meteorological Institute
GAINS	Greenhouse Gas - Air Pollution Interactions and Synergies
HPDF	High-pressure injection dual-fuel

IFS	Integrated Forecasting System
IMO	International Maritime Organization
Land-based emissions	Emissions from all sectors excluding sea shipping emissions (includes inland shipping)
LBSI	Lean burn spark ignited
LNG	Liquefied natural gas
LOTOS-EUROS	Long Term Ozone Simulation – EURopean Operational Smog model
LPDF	Low-pressure injection dual-fuel
MARPOL	International Convention for the Prevention of Pollution from Ships
MNB	Mean normalised bias
N_2O_5	Dinitrogen pentoxide
NECA	Nitrogen emission control area
NH_3	Ammonia
NH_4^+	Ammonium
NMVOC	Non-methane volatile organic compound
NO	Nitric oxide
NO_2	Nitrogen dioxide
NO_3^-	Nitrate
NOx	Nitrogen oxides (the total of nitric oxide and nitrogen dioxide)
O_3	Ozone
OC	Organic carbon
PM	Particulate matter
PM_{10}	Particulate matter with an aerodynamic diameter smaller than 10 micron meter
$PM_{2.5}$	Particulate matter with an aerodynamic diameter smaller than 2.5 micron meter
Pollutant	Atmospheric chemical species with known harmful effects to human health and/or the environment

POM	Primary organic matter
PRIMES	Price-Induced Market Equilibrium System
R^2	Coefficient of determination
RESTPPM	Rest of primary particulate matters
RMSE	Root mean square error
SA	Source apportionment
SCR	Selective catalytic reduction
SECA	Sulphur emission control area
SIA	Secondary inorganic aerosols
SO_2	Sulphur dioxide
SO_4^{2-}	Sulphate
SOx	Sulphur oxides
STEAM	Ship Traffic Emission Assessment Model
TEN-T	Trans-European transport network
TEU	Twenty-foot equivalent units
TNO	Netherlands organisation for applied scientific research (Nederlandse Organisatie voor Toegepast-Natuurwetenschappelijk Onderzoek)
Tracer	Model equivalent to a chemical species present in the atmosphere
UNFCCC	United Nations Framework Convention on Climate Change
VLSFO	Very low sulphur fuel oil
VOC	Volatile organic compound
WHO	World Health Organisation

6. REFERENCES

1. Banzhaf, S. (2013). Interaction of surface water and groundwater in the hyporheic zone – application of pharmaceuticals and temperature as indicators. https://depositonce.tu-berlin.de/items/urn:nbn:de:kobv:83-opus-38311

2. Banzhaf, S., Schaap, M., Kerschbaumer, A., Reimer, E., Stern, R., Van Der Swaluw, E., & Builtjes, P. (2012). Implementation and evaluation of pH-dependent cloud chemistry and wet deposition in the chemical transport model REM-Calgrid. Atmospheric Environment, 49, 378–390. https://doi.org/10.1016/j.atmosenv.2011.10.069

3. Beelen, R., Raaschou-Nielsen, O., Stafoggia, M., Andersen, Z. J., Weinmayr, G., Hoffmann, B., Wolf, K., Samoli, E., Fischer, P., Nieuwenhuijsen, M., Vineis, P., Xun, W. W., Katsouyanni, K., Dimakopoulou, K., Oudin, A., Forsberg, B., Modig, L., Havulinna, A. S., Lanki, T., … Hoek, G. (2014). Effects of long-term exposure to air pollution on natural-cause mortality: An analysis of 22 European cohorts within the multicentre ESCAPE project. The Lancet, 383(9919), 785–795. https://doi.org/10.1016/S0140-6736(13)62158-3

4. Curier, R. L., Kranenburg, R., Segers, A. J. S., Timmermans, R. M. A., & Schaap, M. (2014). Synergistic use of OMI NO2 tropospheric columns and LOTOS–EUROS to evaluate the NOx emission trends across Europe. Remote Sensing of Environment, 149, 58–69. https://doi.org/10.1016/j.rse.2014.03.032

5. Denier van der Gon, H., Kooter, I., Bronsveld, P., Hartendorf, F., Korstanje, T., Wijngaard, M., & Dortmans, A. (2022). Particulate matter: Standard achieved, problem unsolved. Better differentiation leads to more health benefits. https://www.tno.nl/en/newsroom/insights/2022/07-0/why-current-particulate-matter-standard/

6. DNV-GL. (2020). Maritime Forecast to 2050 (Energy Transition Outlook 2020).

7. EAFO. (2021). Ports and Infrastructure [Dataset]. https://alternative-fuels-observatory.ec.europa.eu/transport-mode/maritime-sea/ports-and-infrastructure

8. Escudero, M., Segers, A., Kranenburg, R., Querol, X., Alastuey, A., Borge, R., de la Paz, D., Gangoiti, G., & Schaap, M. (2019). Analysis of summer O3 in the Madrid air basin with the LOTOS-EUROS chemical transport model. Atmospheric Chemistry and Physics, 19(22), 14211–14232. https://doi.org/10.5194/acp-19-14211-2019

9. Eurostat. (2013). Land Use (Version 2009) [Dataset]. https://ec.europa.eu/eurostat/web/gisco/geodata/land-cover

10. Eurostat. (2021). Urban Audit [Dataset]. https://ec.europa.eu/eurostat/web/gisco/geodata/statistical-units/urban-audit

11. Fountoukis, C., & Nenes, A. (2007). ISORROPIA II: A computationally efficient thermodynamic equilibrium model for K+–Ca2+–Mg2+–NH4+–Na+–SO42−–NO3−–Cl−–H2O aerosols. Atmospheric Chemistry and Physics, 7(17), 4639–4659. https://doi.org/10.5194/acp-7-4639-2007

12. Fridell, E., Salberg, H., & Salo, K. (2021). Measurements of Emissions to Air from a Marine Engine Fueled by Methanol. Journal of Marine Science and Application, 20(1), 138–143. https://doi.org/10.1007/s11804-020-00150-6

13. Grigoriadis, A., Mamarikas, S., Ioannidis, I., Majamäki, E., Jalkanen, J.-P., & Ntziachristos, L. (2021). Development of exhaust emission factors for vessels: A review and meta-analysis of available data. Atmospheric Environment: X, 12, 100142. https://doi.org/10.1016/j.aeaoa.2021.100142

14. Guevara, M., Jorba, O., Tena, C., Denier Van Der Gon, H., Kuenen, J., Elguindi, N., Darras, S., Granier, C., & Pérez García-Pando, C. (2021). Copernicus Atmosphere Monitoring Service TEMPOral profiles (CAMS-TEMPO): Global and European emission temporal profile maps for atmospheric chemistry modelling. Earth System Science Data, 13(2), 367–404. https://doi.org/10.5194/ESSD-13-367-2021

15. Hooghiemstra, P. B. (2006). Towards advection on a full reduced grid for TM5 (No. TR-294). KNMI.

16. Jalkanen, J.-P., Brink, A., Kalli, J., Pettersson, H., Kukkonen, J., & Stipa, T. (2009). A modelling system for the exhaust emissions of marine traffic and its application in the Baltic Sea area. Atmospheric Chemistry and Physics, 9(23), 9209–9223. https://doi.org/10.5194/acp-9-9209-2009

17. Jalkanen, J.-P., Johansson, L., Kukkonen, J., Brink, A., Kalli, J., & Stipa, T. (2012). Extension of an assessment model of ship traffic exhaust emissions for particulate matter and carbon monoxide. Atmospheric Chemistry and Physics, 12(5), 2641–2659. https://doi.org/10.5194/acp-12-2641-2012

18. Jalkanen, J.-P., Johansson, L., Wilewska-Bien, M., Granhag, L., Ytreberg, E., Eriksson, K. M., Yngsell, D., Hassellöv, I.-M., Magnusson, K., Raudsepp, U., Maljutenko, I., Winnes, H., & Moldanova, J. (2021). Modelling of discharges from Baltic Sea shipping. Ocean Science, 17(3), 699–728. https://doi.org/10.5194/os-17-699-2021

19. Johansson, L., Jalkanen, J.-P., & Kukkonen, J. (2017). Global assessment of shipping emissions in 2015 on a high spatial and temporal resolution. Atmospheric Environment, 167, 403–415. https://doi.org/10.1016/j.atmosenv.2017.08.042

20. Jonson, J. E., Jalkanen, J. P., Johansson, L., Gauss, M., & Denier van der Gon, H. a. C. (2015). Model calculations of the effects of present and future emissions of air pollutants from shipping in the Baltic Sea and the North Sea. Atmospheric Chemistry and Physics, 15(2), 783–798. https://doi.org/10.5194/acp-15-783-2015

21. Kaiser, J. W., Heil, A., Andreae, M. O., Benedetti, A., Chubarova, N., Jones, L., Morcrette, J.-J., Razinger, M., Schultz, M. G., Suttie, M., & van der Werf, G. R. (2012). Biomass burning emissions estimated with a global fire assimilation system based on observed fire radiative power. Biogeosciences, 9(1), 527–554. https://doi.org/10.5194/bg-9-527-2012

22. Klimont, Z., Kiesewetter, G., Kaltenegger, K., Wagner, F., Kim, Y., Rafaj, P., Schindlbacher, S., Heyes, C., Denby, B., Holland, M., Borken-Kleefeld, J., Purohit, P., Fagerli, H., Vandyck, T., Warnecke, L., & Anderl, M. (2022). Support to the development of the third Clean Air Outlook. International Institute for Applied Systems Analysis (IIASA).

23. Köble, R., & Seufert, G. (2001). Novel Maps for Forest Tree Species in Europe. Proceedings of the 8th European Symposium on the Physico-Chemical Behaviour of Air Pollutants: “A Changing Atmosphere!”, 1–6.

24. Kranenburg, R., Segers, A. J., Hendriks, C., & Schaap, M. (2013). Source apportionment using LOTOS-EUROS: Module description and evaluation. Geoscientific Model Development, 6(3), 721–733. https://doi.org/10.5194/gmd-6-721-2013

25. Kuenen, J., Dellaert, S., Visschedijk, A., Jalkanen, J.-P., Super, I., & Denier van der Gon, H. (2022). CAMS-REG-v4: A state-of-the-art high-resolution European emission inventory for air quality modelling. Earth System Science Data, 14(2), 491–515. https://doi.org/10.5194/essd-14-491-2022

26. Majamäki, E., Johansson, L., Grönholm, T., & Jalkanen, J. P. (2025). Improving the global prediction of shipping emissions by modelling the effects of ambient conditions. Science of the Total Environment, 997(June), 180126. https://doi.org/10.1016/j.scitotenv.2025.180126

27. Manders, A. M. M., Builtjes, P. J. H., Curier, L., Denier van der Gon, H. A. C., Hendriks, C., Jonkers, S., Kranenburg, R., Kuenen, J. J. P., Segers, A. J., Timmermans, R. M. A., Visschedijk, A. J. H., Wichink Kruit, R. J., van Pul, W. A. J., Sauter, F. J., van der Swaluw, E., Swart, D. P. J., Douros, J., Eskes, H., van Meijgaard, E., … Schaap, M. (2017). Curriculum vitae of the LOTOS-EUROS (v2.0) chemistry transport model. Geoscientific Model Development, 10(11), 4145–4173. https://doi.org/10.5194/gmd-10-4145-2017

28. Mårtensson, E. M., Nilsson, E. D., de Leeuw, G., Cohen, L. H., & Hansson, H.-C. (2003). Laboratory simulations and parameterization of the primary marine aerosol production. Journal of Geophysical Research: Atmospheres, 108(D9). https://doi.org/10.1029/2002JD002263

29. Marticorena, B., & Bergametti, G. (1995). Modeling the atmospheric dust cycle: 1. Design of a soil-derived dust emission scheme. Journal of Geophysical Research: Atmospheres, 100(D8), 16415–16430. https://doi.org/10.1029/95JD00690

30. Mokhtari, M., Gomes, L., Tulet, P., & Rezoug, T. (2012). Importance of the surface size distribution of erodible material: An improvement on the Dust Entrainment And Deposition (DEAD) Model. Geoscientific Model Development, 5(3), 581–598. https://doi.org/10.5194/gmd-5-581-2012

31. Monahan, E. C., Spiel, D. E., & Davidson, K. L. (1986). A Model of Marine Aerosol Generation Via Whitecaps and Wave Disruption. In E. C. Monahan & G. M. Niocaill (Eds.), Oceanic Whitecaps: And Their Role in Air-Sea Exchange Processes (pp. 167–174). Springer Netherlands. https://doi.org/10.1007/978-94-009-4668-2_16

32. Pseftogkas, A., Koukouli, M.-E., Manders, A., Segers, A., Stavrakou, T., Tokaya, J., Meleti, C., & Balis, D. (2024). Maritime sector contributions on NO2 surface concentrations in major ports of the Mediterranean Basin. Atmospheric Pollution Research, 15(9), 102228. https://doi.org/10.1016/j.apr.2024.102228

33. Rémy, S., Veira, A., Paugam, R., Sofiev, M., Kaiser, J. W., Marenco, F., Burton, S. P., Benedetti, A., Engelen, R. J., Ferrare, R., & Hair, J. W. (2017). Two global data sets of daily fire emission injection heights since 2003. Atmospheric Chemistry and Physics, 17(4), 2921–2942. https://doi.org/10.5194/acp-17-2921-2017

34. Schaap, M., Apituley, A., Timmermans, R. M. A., Koelemeijer, R. B. A., & de Leeuw, G. (2009). Exploring the relation between aerosol optical depth and PM2.5

at Cabauw, the Netherlands. Atmospheric Chemistry and Physics, 9(3), 909–925. https://doi.org/10.5194/acp-9-909-2009

35. Schaap, M., Cuvelier, C., Hendriks, C., Bessagnet, B., Baldasano, J. M., Colette, A., Thunis, P., Karam, D., Fagerli, H., Graff, A., Kranenburg, R., Nyiri, A., Pay, M. T., Rouïl, L., Schulz, M., Simpson, D., Stern, R., Terrenoire, E., & Wind, P. (2015). Performance of European chemistry transport models as function of horizontal resolution. Atmospheric Environment, 112, 90–105. https://doi.org/10.1016/j.atmosenv.2015.04.003

36. Schaap, M., Timmermans, R. M. A., Roemer, M., Boersen, G. A. C., Builtjes, P. J. H., Sauter, F. J., Velders, G. J. M., & Beck, J. P. (2008). The LOTOS-EUROS model: Description, validation and latest developments. International Journal of Environment and Pollution, 32, 270–290.

37. Schaap, M., Van Loon, M., Ten Brink, H. M., Dentener, F. J., & Builtjes, P. J. H. (2004). Secondary inorganic aerosol simulations for Europe with special attention to nitrate. Atmospheric Chemistry and Physics, 4(3), 857–874. https://doi.org/10.5194/acp-4-857-2004

38. Skoulidou, I., Koukouli, M.-E., Manders, A., Segers, A., Karagkiozidis, D., Gratsea, M., Balis, D., Bais, A., Gerasopoulos, E., Stavrakou, T., van Geffen, J., Eskes, H., & Richter, A. (2021). Evaluation of the LOTOS-EUROS NO2 simulations using ground-based measurements and S5P/TROPOMI observations over Greece. Atmospheric Chemistry and Physics, 21(7), 5269–5288. https://doi.org/10.5194/acp-21-5269-2021

39. Steinbrecher, R., Smiatek, G., Köble, R., Seufert, G., Theloke, J., Hauff, K., Ciccioli, P., Vautard, R., & Curci, G. (2009). Intra- and inter-annual variability of VOC emissions from natural and semi-natural vegetation in Europe and neighbouring countries. Atmospheric Environment, 43(7), 1380–1391. https://doi.org/10.1016/j.atmosenv.2008.09.072

40. Stevens, C. J., David, T. I., & Storkey, J. (2018). Atmospheric nitrogen deposition in terrestrial ecosystems: Its impact on plant communities and consequences across trophic levels. Functional Ecology, 32(7), 1757–1769. https://doi.org/10.1111/1365-2435.13063

41. Takemura, T., Nozawa, T., Emori, S., Nakajima, T. Y., & Nakajima, T. (2005). Simulation of climate response to aerosol direct and indirect effects with aerosol transport-radiation model. Journal of Geophysical Research: Atmospheres, 110(D2). https://doi.org/10.1029/2004JD005029

42. Thürkow, M., Banzhaf, S., Butler, T., Pültz, J., & Schaap, M. (2023). Source attribution of nitrogen oxides across Germany: Comparing the labelling approach and brute force technique with LOTOS-EUROS. Atmospheric Environment, 292, 119412. https://doi.org/10.1016/j.atmosenv.2022.119412

43. Timmermans, R., Kranenburg, R., Manders, A., Hendriks, C., Segers, A., Dammers, E., Zhang, Q., Wang, L., Liu, Z., Zeng, L., Denier Van Der Gon, H., & Schaap, M. (2017). Source apportionment of PM2.5 across China using LOTOS-EUROS. Atmospheric Environment, 164, 370–386. https://doi.org/10.1016/j.atmosenv.2017.06.003

44. Timmermans, R., Van Pinxteren, D., Kranenburg, R., Hendriks, C., Fomba, K. W., Herrmann, H., & Schaap, M. (2022). Evaluation of modelled LOTOS-EUROS with

observational based PM10 source attribution. Atmospheric Environment: X, 14, 100173. https://doi.org/10.1016/j.aeaoa.2022.100173

45. van Zanten, M. C., Sauter, F. J., Wichink Kruit, R. J., van Jaarsveld, J. A., & van Pul, W. A. J. (2010). Description of the DEPAC module. Dry deposition modelling with DEPAC_GCN2010. RIVM. https://www.rivm.nl/bibliotheek/rapporten/680180001.pdf

46. Whitten, G. Z., Hogo, Henry., & Killus, J. P. (1980). The carbon-bond mechanism: A condensed kinetic mechanism for photochemical smog. Environmental Science & Technology, 14(6), 690–700. https://doi.org/10.1021/es60166a008

47. Wichink Kruit, R. J., Schaap, M., Sauter, F. J., Van Zanten, M. C., & Van Pul, W. A. J. (2012). Modeling the distribution of ammonia across Europe including bi-directional surface–atmosphere exchange. Biogeosciences, 9(12), 5261–5277. https://doi.org/10.5194/bg-9-5261-2012

48. World Shipping Council. (2023). The Top 50 Container Ports. World Shipping Council. https://www.worldshipping.org/top-50-ports

Concawe
Environmental Science for European Fuel Manufacturing

Concawe
Av. des Nerviens 85
1040, Brussels | Belgium

Tel: +32 2 566 91 60
e-mail: info@concawe.eu
http://www.concawe.eu

ISBN 978-2-87567-216-2